

Nuclear Spins in Quantum Dots

Nuclear Spins in Quantum Dots

Proefschrift

ter verkrijging van de graad van doctor
aan de Technische Universiteit Delft,
op gezag van de Rector Magnificus prof.dr.ir. J.T. Fokkema,
voorzitter van het College voor Promoties,
in het openbaar te verdedigen op dinsdag 16 september 2003 om 10.30 uur

door

Sigurdur Ingi ERLINGSSON

Meistarapróf í edlisfræði
Háskóli Íslands
geboren te Reykjavík, IJsland.

Dit proefschrift is goedgekeurd door de promotor:

Prof. dr. Yu. V. Nazarov

Samenstelling van de promotiecommissie:

Rector Magnificus,	voorzitter
Prof.dr. Yu. V. Nazarov	Technische Universiteit Delft, promotor
Prof.dr.ir. G. E. W. Bauer,	Technische Universiteit Delft
Prof.dr.ir. L. P. Kouwenhoven,	Technische Universiteit Delft
Prof.dr. D. Pfannkuche,	Universiteit Hamburg, Duitsland
Prof.dr. D. Loss,	Universiteit Basel, Zwitserland
Prof.dr. V. Gudmundsson,	Universiteit IJsland, IJsland
dr.ir. L. Vandersypen	Technische Universiteit Delft

Published and distributed by: DUP Science

DUP Science is an imprint of
Delft University Press

P.O. Box 98	Telephone: +31 15 27 85678
2600 MG Delft	Telefax: +31 15 27 85706
The Netherlands	E-mail: DUP@Library.TUdelft.NL
ISBN 90-407-2431-8	

Keywords: quantum dots, electron spin, hyperfine interaction

Copyright © 2003 by Sigurdur I. Erlingsson

All rights reserved. No part of the material protected by this copyright notice may be reproduced or utilized in any form or by any means, electronic or mechanical, including photocopying, recording or by any information storage and retrieval system, without permission from the publisher: Delft University Press.

Printed in the Netherlands

Preface

The work presented in this thesis is the result of four years of PhD research in the theoretical physics group in Delft. In the beginning of my PhD I knew that I wanted to work on electron spins and quantum dots but I only had vague ideas about what that entailed. With time these ideas became more clear, largely with the help of my supervisors, and I found myself working on the problem of quantum dots containing electron spins and how they interact with the surrounding nuclei. As it turned out this field was, and still is, a very active field of research. I feel privileged to have been able to do my research in Delft since it has allowed me to meet and interact with many great scientists, in Delft and elsewhere. It is a difficult task to adequately thank all the people who in one way or another contributed to my work, but in any case I will try.

Let me first thank my supervisors. During my first year in Delft I was supervised by Daniela Pfannkuche. Daniela taught me many things, especially the importance of many-body wave functions and being careful in using the single-particle picture. I would also like to thank her for helping me and Ragnhildur when we were settling in the Netherlands, and for her hospitality during my visit to Hamburg.

My main supervisor for the last three years, after Daniela moved to Hamburg for a professorship, was Yuli Nazarov. I have to admit that after my initial ‘encounters’ with Yuli I was rather intimidated by him. Well, as it turned out those fears were completely unfounded. I would like to thank Yuli for teaching me how to keep things simple, showing me the value of being honest in science, giving me invaluable ‘pep-talks’ when I felt stuck and simply exceeding his duties as a supervisor.

Although not being directly involved in my daily supervision, I learned a lot from Gerrit Bauer, especially concerning practical and political matters in the science business which, I was surprised to learn, are very important indeed. We also share a ‘passion’ for fantasy novels and Gerrit gave me quite a few hints concerning good books.

I have had the pleasure of working, and discussing, with very good people in our group, whether they are the ‘permanent’ staff, guests or postdocs. I would like to thank Yaroslav Blanter, Milena Grifoni, Joos Thijssen, Arkadi

Odintsov, Alexander Khaetskii, Mikeo Eto and Yasuhiro Tokura. The postdocs in our group have also taught me a great deal and we had some nice time over a few beers: thanks to Wolfgang Belzig, Mauro Ferreira, Takeshi Nakanishi, Dmitri Bagrets, Michael Thorwarts, Miriam Blaauboer, Wataru Izumida and Antonio DiLorenzo. I would especially like to thank our group secretary, Yvonne Zwang. She has always been very helpful, even though I failed her unofficial Dutch course.

When I began my studies, I joined the three PhD students who were already in the theory group: Maarten Wegewijs, Daniel Huertas-Hernandes and Freek Langeveld. I would like to thank them for our many interactions concerning physics related matters and all kinds of other stuff. Our reading group “The Physical Review” helped me understand many things, especially how difficult it is to keep a reading group going! I would also like to thank Malek Zareyan and Marcus Kinderman for many fruitful discussions. I have enjoyed many fun activities and discussions with the ‘younger generation’ of PhD students. Thank you guys: Joel Peguiron, Oleg Jouravlev, Jens Tobiska, Alexey Kovalev, Gabriele Campagnano, Sijmen Gerritsen, Omar Usmani and Wouter Wetzels.

Special thanks go to Leo Kouwenhoven for giving me the opportunity to participate in the qdot-group meetings and teaching me the difference between a theorist proposal and ‘reality’. I would also like to thank Silvano DeFrancenschi and Lieven Vandersypen for many enlightening discussions. Many thanks go to the PhD’s in Leo’s group, past and present: Wilfred van der Wiel, Jeroen Elzerman, Ronald Hanson and Laurens Willems van Beveren. They helped me understand “all I wanted to know about quantum dots, but was afraid to ask”.

I would also like to thank a few people which I have had the privilege of discussing with, listening to their talks or just playing football with (in some cases all of the above): Hannes Majer, Pablo Jarillo-Herrero, Sami Sapmaz, Alberto Morpurgo, Irinel Chiorescu, Eugen Onac, Kees Harmans, Vladimir Fal’ko, Daniel Loss, Hans-Andreas Engel, Michael Tews and Alexander Chudnovskii.

I want to thank my family for always supporting me and being there when I needed. Takk fyrir mamma, pabbi, Ella og Steindór. My early interest in science was sparked by all the books on physics, chemistry, electronics and engineering in my parents’ library. My current science ‘carrier’ can be traced directly to those humble beginnings, at least if a few year period where I wanted to be a film director is disregarded. Even though my brother Steindór and I disagree on many things, especially concerning science, he has helped me recognize that science, just like any other human endeavor, is no more infallible than the people who practice it. Finally I want to thank my fiancée Ragnhildur. She really helped me cope with my thesis and the accompanying stress. Elsku Ragnhildur, takk fyrir hjálpina.

Contents

1	Introduction	1
1.1	Quantum dots	1
1.2	Spin admixture	2
1.2.1	Spin-orbit interaction	3
1.2.2	The hyperfine interaction	4
1.3	Quantum dynamics and the reduced density matrix formalism . .	6
1.4	Spin-flip rates	7
1.5	Dynamics of electron spins	8
1.6	This thesis	9
	References	10
2	Nucleus-mediated spin-flip transitions in GaAs quantum dots	13
2.1	Introduction	14
2.2	Model and assumptions	15
2.3	Comparison and estimates	19
	References	22
3	Hyperfine-mediated transitions between a Zeeman split doublet in GaAs quantum dots: The role of the internal field	23
3.1	Introduction	24
3.2	Model and assumptions	25
3.3	Internal magnetic field	27
3.4	Transition rate	29
3.5	Discussion	34
	References	35
4	Nuclear spin induced coherent oscillations of transport current through a double quantum dot	37
4.1	Introduction	38
4.2	Model	39
4.3	Density matrix and average electron spin	43
4.4	Nuclear system dynamics	45

4.4.1	Integrals of motion	45
4.4.2	Numerical integration	54
4.5	Conclusions	55
	References	55
5	Time-evolution of the effective nuclear magnetic field due to a localized electron spin	57
5.1	Introduction	58
5.2	Hyperfine interaction in quantum dots	59
5.3	Semiclassical dynamics	60
5.4	Adiabatic approximation for the electron spin	64
5.5	Correlation functions	66
5.6	Nuclear subsystem dynamics	67
5.7	Conclusion	71
	References	71
A	Thermal average over nuclear spin pairs	73
B	Matrix elements for a parabolic quantum dot	75
	Summary	77
	Samenvatting	79
	Curriculum Vitae	83
	List of Publications	85

Chapter 1

Introduction

The continuing miniaturization of components used in integrated circuits are pushing devices ever closer to a regime where the expected classical behavior becomes strongly influenced by quantum effects [1]. From the point of view of those who would like to squeeze more and more ‘classical’ devices onto a chip this prospect is quite discouraging. The opposite viewpoint would be to come up with new devices which take advantage of these quantum effects. The operation of such devices would require coherent control of the quantum systems with precision which is quite difficult to achieve. There are both fundamental and practical obstacles that need to be overcome, if that is at all possible. The most ambitious of these proposed devices is the quantum bit, or qubit, which would form the building blocks of quantum computers [2–5].

There are many competing ideas on how to build qubits. The most mature systems are based on NMR techniques and manipulating trapped ions, but there are serious problems regarding scalability in those systems. On the contrary, solid state systems are more promising with respects to scalability but the problem of decoherence is much greater [6–8]. One proposed realization is based on localized electron spins in semiconductor quantum dots [9, 10]. The electron spin is a natural two level system and the electron spin should be less susceptible to environmental effects, e.g. relaxation and decoherence, than orbital degrees of freedom. It is also important that the technology to manufacture well controlled microstructures is well established and great technological advances have been made in the direction of controlling single spins in quantum dots. The question still remains what the detailed effects of the environment on the spin are.

1.1 Quantum dots

Quantum dots are micron-size, or smaller, structures which are manufactured using lithographic techniques or various so-called self-assembly methods. Irre-

spective of the method used to fabricate them, quantum dots are characterized by their localized wavefunctions and discrete energy spectrum [11]. Here the focus is on quantum dots in GaAs/AlGaAs heterostructures. This material is both technologically important and has peculiar material features which are important. GaAs is a polar semiconductor which is crucial in determining both the electron-phonon, and the spin-orbit interaction. Both Ga and As nuclei have nonzero nuclear spin which give rise to properties which are not present, or quite reduced, in other semiconductors, e.g. silicon.

Usually GaAs quantum dots are fabricated starting from a 2DEG at an AlGaAs/GaAs interface, or quantum well. The quantum dots are defined by etching through the 2DEG or by depositing gates on top of the heterostructure. Applying a negative voltage on these gates will deplete the 2DEG below them. Assuming a parabolic confinement in the 2DEG plane is in most cases a good approximation. The quantum dot Hamiltonian for a generic confining potential $V(z)$ in the z direction is

$$H_0 = \frac{(\mathbf{p} + e\mathbf{A}(\mathbf{r}))^2}{2m^*} + \frac{1}{2}m^*\Omega_0^2(x^2 + y^2) + V(z) + g\mu_B\mathbf{S} \cdot \mathbf{B}, \quad (1.1)$$

where \mathbf{A} is the gauge dependent vector potential which determines the magnetic field $\mathbf{B} = \nabla \times \mathbf{A}$. Knowing the potential $V(\mathbf{r})$ of the dot and the applied magnetic field \mathbf{B} the eigenstates are obtained by solving the stationary Schrödinger equation

$$H_0\langle\mathbf{r}|n, s\rangle = \hbar\omega_{n,s}\langle\mathbf{r}|n, s\rangle. \quad (1.2)$$

Here the eigenstates are labeled with the orbital index n which represents the relevant orbital quantum numbers and s indicates the spin state.

GaAs quantum dots come mainly in two flavors, so-called lateral and vertical quantum dots. Differences in fabrication of the dots is reflected in different choices of the confining potential $V(z)$. Initially, only the vertical dots allowed precise control of the number of electrons in the quantum dot, which could be tuned from 0 to few tens [12]. Recent experiments have also demonstrated this control in lateral quantum dots [13], and more importantly, the lateral dots allow greater control over the electron confinement potential in the dot. The results presented in this thesis apply equally well to vertical and lateral dots, the only difference being different numerical values due to the slightly different orbital wave functions.

1.2 Spin admixture

The Hamiltonian in Eq. (1.1) only takes into account the confining potential, the minimum coupling to the vector field \mathbf{A} . As a first approximation this

is a good starting point but more terms in the Hamiltonian are required for realistic modeling of the quantum dot. Let us assume for the moment that the coordinate system is chosen such that $[S_z, H_0] = 0$, thus the eigenstates of H_0 are also eigenstates of S_z ,

$$S_z|s\rangle = \hbar s|s\rangle, \quad s = \pm \frac{1}{2}. \quad (1.3)$$

Here the orbital indices are suppressed for the moment. When a small perturbing term H' , which contains spin operators such that $[S^z, H'] \neq 0$, is added to H_0 the eigenfunctions become

$$|''+\rangle \approx |+\rangle + \alpha|-\rangle \quad (1.4)$$

$$|''-\rangle \approx |-\rangle - \alpha^*|+\rangle, \quad (1.5)$$

where α is the strength of the perturbation. The admixture refers to the small component of the opposite spin, but the states still retain most of their spin ‘up’ and ‘down’ characteristics as long as $\alpha \ll 1$. The admixture terms in Eq. (1.5) include contributions from different orbitals, so any inter-orbital scattering mechanism will lead to scattering between spin states. The magnitude of the spin scattering is determined by α and the orbital scattering mechanism.

There are a number of possible admixture mechanisms in GaAs. The most important ones are due to hyperfine interaction and spin-orbit interaction. Although one could also include inelastic cotunneling in this list it is not an intrinsic mechanism of the dot since the cotunneling can be turned down to an arbitrarily small value by pinching of the quantum dot. No such ‘turning-off’ exists for the hyperfine or spin-orbit interaction although polarizing the nuclear system has been proposed as a means for reducing the effectiveness of the hyperfine scattering [14].

1.2.1 Spin-orbit interaction

The spin-orbit interaction is a relativistic correction to the Hamiltonian in Eq. (1.2). The textbook method of introducing the SO interaction is by considering the problem of an electron moving in a frame with a given stationary electric field $\mathbf{E} = -\nabla V(\mathbf{r})$ but zero magnetic field. In the reference frame moving with the electron the magnetic field is not zero since the Lorentz transformation of the electric field results in a small magnetic field [15]. This magnetic field couples to the electron spin giving rise to a Zeeman-like term. The Hamiltonian for the spin-orbit (SO) interaction (including the factor 1/2 due to the Thomas precession) is

$$H_{SO} = \frac{\hbar}{2m^2c^2}(\nabla V \times \mathbf{p}) \cdot \mathbf{S}, \quad (1.6)$$

where \mathbf{p} and \mathbf{S} are operators for momentum and spin, respectively. For any time reversal symmetric (no applied magnetic field) single particle Hamiltonian H_{sp} , Kramers theorem tells that all eigenstates of the total Hamiltonian $H = H_{\text{sp}} + H_{\text{SO}}$ are doubly degenerate [16, 17]. Non-zero transition amplitude between such doublet components is only possible in the presence of a magnetic field.

In bulk matter this Hamiltonian becomes modified due to details of the structure of the underlying material. Here symmetry of the crystal lattice plays an important role [18, 19]. The SO interaction Hamiltonian can be written quite generally as

$$H_{\text{SO}} = \hbar\boldsymbol{\Omega} \cdot \mathbf{S}, \quad (1.7)$$

where $\boldsymbol{\Omega}$ is some generalized precession frequency whose detailed form is determined by the structure of the crystal lattice. In GaAs, which has a zinc blende structure, the dominant SO coupling in the conduction band is due to the lack of inversion center in the crystal lattice. The resulting SO coupling, the so-called Dresselhaus term, may be written as

$$H_D = \hbar\boldsymbol{\Omega}_D \cdot \mathbf{S}, \quad (1.8)$$

where the SO precession frequency is defined as [20]

$$\Omega_{D,x} = \frac{\eta}{\hbar m^* \sqrt{2E_g m^*}} p_x (p_y^2 - p_z^2), \quad (1.9)$$

where η is a material dependent parameter (0.07 in GaAs), E_g is the gap energy and m^* is the effective electron mass. The other components of $\boldsymbol{\Omega}_D$ are obtained by cyclic permutation of the indices.

In addition to the intrinsic lack of an inversion center in GaAs, it is also possible to break the lattice symmetry at hetero-interfaces, e.g. at AlGaAs/GaAs interfaces. The spin orbit coupling arising from this effect is usually called the Rashba term

$$H_R = 2\alpha\hbar^{-1}(\mathbf{p} \times \mathbf{n}_{\text{het}}) \cdot \mathbf{S}, \quad (1.10)$$

where $\alpha \sim 10^{-11}$ eV m in GaAs determines the strength of the coupling and \mathbf{n}_{het} is a unit vector normal to the interface [21, 22]. In a recent paper the *in situ* control of the different SO couplings in a GaAs 2DEG was demonstrated [23].

1.2.2 The hyperfine interaction

Both Ga and As have a nuclear spin $I = 3/2$. This gives rise to the hyperfine interaction, i.e. conduction electrons interact with the magnetic moments of the

nuclei. The Hamiltonian of the hyperfine coupling of an electron spin to a single nucleus at position \mathbf{R} can be written as

$$H_{HF} = 2\mu_B\gamma_n\hbar \left(\frac{3(\mathbf{I} \cdot \mathbf{n})(\mathbf{S} \cdot \mathbf{n}) - \mathbf{I} \cdot \mathbf{S}}{|\mathbf{r} - \mathbf{R}|^3} + \frac{8\pi}{3} \mathbf{I} \cdot \mathbf{S} \delta(\mathbf{r} - \mathbf{R}) \right) \quad (1.11)$$

where $\mathbf{n} = (\mathbf{r} - \mathbf{R})/|\mathbf{r} - \mathbf{R}|$, γ_n is the nucleus magnetic moment. The former term in Eq. (1.11) is the usual coupling between magnetic dipoles of the electron and nuclei but the latter term, so-called contact term, is a correction due to the non-zero electron density at the nucleus [24].

In GaAs, and other materials with s -orbital conduction band, the dipole-dipole term is strongly suppressed, leaving the contact term as the dominant contribution. The contact term Hamiltonian become

$$H_{HF} = A \sum_k \hat{\mathbf{S}} \cdot \hat{\mathbf{I}}_k \delta(\mathbf{r} - \mathbf{R}_k), \quad (1.12)$$

where A is the (band renormalized) hyperfine constant and \mathbf{I}_k is the spin operator of nuclei at \mathbf{R}_k . The sum runs over all nuclei in the sample. Although Ga and As have different hyperfine coupling constants, or A 's in Eq. (1.12), we will consider only a single effective nuclear species characterized by a single A which is the weighted sum of the contributions from different isotopes of the Ga and As nuclei. The energy scales associated with this Hamiltonian can be extracted from A and the concentration of nuclear spins C_n . Assuming a completely polarized (in the z direction) nuclear state one can extract the Zeeman splitting of the spin doublet

$$E_n = AIC_n, \quad (1.13)$$

where I is the nuclear spin of the Ga and As nuclei. Note that this result does not depend on the form of the wavefunction. This spin splitting is a quantity that has been measured: $E_n = 0.135$ meV in GaAs samples [25, 26].

The form of the Hamiltonian is quite suggestive since it can be written on the form [27]

$$H_{HF} = \hat{\mathbf{S}} \cdot \hat{\mathbf{K}} \quad (1.14)$$

which is formally equivalent to the Zeeman term in Eq. (1.1) but the difference is that the field is now an operator

$$\hat{\mathbf{K}} = A \sum_k \hat{\mathbf{I}}_k \delta(\mathbf{r} - \mathbf{R}_k). \quad (1.15)$$

By introducing two identity operators $I = \sum_n |n\rangle\langle n|$ in the orbital Hilbert space the $\hat{\mathbf{K}}$ operator can be written as

$$\begin{aligned} \hat{\mathbf{K}} &= \sum_n |n\rangle\langle n| \hat{\mathbf{K}} \sum_m |m\rangle\langle m| \\ &= \sum_n |n\rangle\langle n| \hat{\mathbf{K}}_{n,n} + \sum_{n \neq m} |n\rangle\langle m| \hat{\mathbf{K}}_{n,m}, \end{aligned} \quad (1.16)$$

where we have defined

$$\hat{K}_{n,m} = A \sum_k \hat{I}_k \psi_n^*(\mathbf{R}_k) \psi_m(\mathbf{R}_k). \quad (1.17)$$

The former term acts as an effective magnetic field within a given orbital but the latter term gives rise to admixture of the opposite spin component in different orbital. The size of the admixture is determined by $K/\hbar(\omega_n - \omega_m) \ll 1$. The admixture has the same form as for spin-orbit coupling but there is an important difference that the transition amplitude due to the hyperfine interaction does not vanish at zero magnetic field, since Kramers theorem no longer applies.

In the same way as the electron spin is affected by the nuclei so are the nuclei influenced by the electron spin. The hyperfine coupling causes each nuclear spin to precess around the average electron spin. As long as the number of nuclei in the dot is much greater than one, this precession frequency is much smaller than for the electron. In addition to the hyperfine field due to the electron spin (and external magnetic field) each nuclei precesses in the dipolar field due to its nearest neighbor spins. Since the dipole-dipole interaction energy between different nuclei is $E_{\text{dip}} \approx 10^{-9}$ meV (corresponding to a local magnetic field $B_{\text{dip}} \approx 10^{-5}T$) disregarding direct nuclear spin interaction is a good approximation, at least up to times determined by E_{dip} . The complete dynamics of the electron plus nuclear spin system is quite complicated and not solvable except for simple cases. However, the very different timescales involved, i.e. electron spin motion is much faster than for the nuclear spin, help to solve the problem.

1.3 Quantum dynamics and the reduced density matrix formalism

Solving the dynamics of the isolated quantum dot is a trivial exercise once the eigenfunctions and eigenvalues of Eq. (1.1) are known. In order to describe a realistic system the environment of the system has to be taken into account. The term environment usually means all other degrees of freedom, e.g. phonons, magnetic and non-magnetic impurities and nuclear spins, to name a few [28–30]. For a bosonic environment (phonons) there exists a powerful method to extract the equation of motion of the reduced density matrix of the electron [28, 31–33]. The effects of the environment is included into an integral kernel K and the resulting equations of motion can be written as

$$\frac{d}{dt} \rho_{nn'} = -i(\omega_n - \omega_{n'}) \rho_{nn'} + \int_0^{t-t_0} d\tau \sum_{mm'} K_{nn',mm'}(\tau) \rho_{mm'}(t - \tau) \quad (1.18)$$

The integral kernel is related to the self-energy of the reduced density matrix propagator and it is thus quite convenient to include higher order contributions.

In many cases the Markov approximation is valid and the integral term reduces to

$$\sum_{mm'} \Gamma_{nn';mm'} \rho_{mm'}(t) \quad (1.19)$$

where the transition rate is

$$\Gamma_{nn';mm'} = \lim_{t_0 \rightarrow -\infty} \int_0^{t-t_0} d\tau K_{nn',mm'}(\tau) \quad (1.20)$$

The transition rate in Eq. (1.20), using the lowest order self-energy term, are equal to the Fermi Golden Rule result. Once these transition rates are known the equations of motion, including all non-diagonal density matrix terms has to be solved to describe coherent dynamics. Only including the diagonal elements gives the usual master-equation approach. The timescale of the decay of the diagonal elements is usually called T_1 and of the off-diagonal T_2 , these term being borrowed from the NMR community [34].

In most cases the dominant bosonic environment in semiconductors is the phonon bath, which can be thought of as quantized lattice vibrations. Besides the usual deformation potential electron phonon coupling the piezoelectric coupling in GaAs needs to be considered. In piezoelectric materials electric fields are induced if the lattice is distorted. The piezoelectric coupling to acoustic phonons can be written as [35]

$$H_{e-p} = \sum_{\nu, \mathbf{q}} \left(\frac{\hbar}{2\rho V c_\nu q} \right) e^{i\mathbf{r} \cdot \mathbf{q}} (b_{\nu, \mathbf{q}} + b_{\nu, -\mathbf{q}}^\dagger), \quad (1.21)$$

where \mathbf{q} is the wavevector, ρ is the mass density, c_ν is the sound velocity of branch ν and V is the normalization volume. Due to the different dependence on \mathbf{q} in the coupling constants for the deformation and piezoelectric phonons, the latter mechanism dominates at low energy. In GaAs it turns out that the piezoelectric interactions wins over the deformation potential coupling for phonon energies below ≈ 0.1 meV. This means that for electron spin dynamics, for which the natural energy scale is the Zeeman splitting, the piezoelectric phonon coupling should be used.

1.4 Spin-flip rates

In the previous section the general formalism for calculating transition rates was introduced. Applying it to transitions between states with different spin requires some mechanism that couples the spin components. Calculating transition rates between quantum dot states with different spin, so-called spin-flip rates, has been the subject of quite a few papers recently. The system of choice is GaAs quantum dots since they are technologically most relevant.

A very important feature of quantum dots, and other confined systems, is their discrete energy spectrum. In fact, the same applies to 2DEGs in magnetic fields where the spectrum is discrete which strongly suppresses the electron spin-flip rates. This feature has been studied, both in connection with hyperfine interaction [36] and spin-orbit interaction [37]. By comparing various spin-orbit related mechanisms in GaAs quantum dots it was shown that the most important mechanism is caused by the lack of inversion symmetry, as reflected in the Hamiltonian in Eq. (1.8) [38]. These calculations were done for a dot containing two electrons and the spin-flip transition was from a triplet to singlet so that the energy of the emitted phonon was in the meV range. Similar calculation were also done for transitions between doublet components [39]. Besides the difference in energy scales, i.e. phonon energies corresponding to the Zeeman splitting as opposed to much larger singlet-triplet splitting, the consequences of Kramers theorem show up in a vanishing transition amplitude at zero magnetic field, which strongly reduces the spin-flip rate. Other spin-orbit related spin-flip rates have also been proposed, e.g. based on motion of the interface of AlGaAs/GaAs heterostructures [40].

In the last few years quite ingenious ways of actually measuring singlet-triplet transition rates in GaAs quantum dot have been devised [41–43]. These measurements give a transition rate of $T_1 \approx 200 \mu\text{s}$. The resolving power of these experiments are limited by cotunneling so the intrinsic spin-flip rates could still be lower, giving rise to longer relaxation times [43]. Similar measurements for transitions between Zeeman split doublet levels of a single electron in a dot in high magnetic fields give a lower bound on the relaxation time $T_1 \gtrsim 50 \mu\text{s}$, the resolution again being limited by technical issues [44].

1.5 Dynamics of electron spins

The spin-flip rates in quantum dots are usually very small. At timescales much smaller than the inverse spin-flip rate the phonons should be frozen out. This has motivated researchers to calculate dynamics without the phonons. The environment which most strongly interacts with the electron spin in GaAs quantum dots are the nuclear spins, which couple to the electron via the hyperfine interaction. Calculating the dynamics of the electron spin in the presence of hyperfine coupling to many nuclei is quite a challenging task. Before attacking the whole problem of solving the exact electron spin dynamics some basic features of the dynamics can be identified. For short timescales the nuclear system is static and the electron spin experiences a fixed nuclear magnetic field. At times longer than $\sim 1 \mu\text{s}$ the nuclear system “starts” precessing around the average electron spin and finally at times $\gtrsim 1 \text{ms}$ the dipole-dipole interaction starts effecting the nuclear spin dynamics.

Quite a few papers have been written on the dynamics of the electron spin in the presence of hyperfine interaction [45–50]. Not all of these papers treat the nuclear system in the same way and the different approximations used can give quite different results.

The role of the position dependent hyperfine coupling was stressed in Ref. [46] where the authors calculated a certain electron spin correlation function which showed non-exponential decay. The same coupling was considered in Ref. [45] but there an ensemble of quantum dots was considered, resulting in very different behavior. An important point made in these two papers, and others, is the large difference of timescales of the electron and nuclear system, which can be utilized in solving the dynamic of the electron spin coupled to the nuclear spin system.

1.6 This thesis

In the second chapter of the thesis the spin-flip rate in a two electron quantum dot, mediated by hyperfine interaction with the nuclei, is estimated. The transition involves virtual transitions to higher energy states and the rate shows a divergence at magnetic field values at which special level crossings occur.

In chapter three a similar spin-flip rate is calculated for a single electron in a quantum dot. A semiclassical picture of the nuclear system is developed.

The subject of the fourth chapter is an application of the semiclassical description of the hyperfine interaction to explain intriguing current oscillations observed in transport through a double dot system [51]. We present a model for the transport cycle where the interplay of the electron spin and the nuclear system leads to an oscillating hyperfine coupling, and thus current.

The last chapter deals with the dynamics of a single electron spin in a quantum dot in the presence of the hyperfine interaction. We extend the semiclassical description to include non-homogeneous hyperfine coupling which results in complicated, but not chaotic motion of the electron spin.

References

- [1] *Mesoscopic Physics and Electronics*, edited by T. Ando *et al.* (Springer-Verlag, Berlin, 1998).
- [2] I. L. Chuang, R. Laflamme, P. W. Shor, and W. H. Zurek, *Science* **270**, 1633 (1995).
- [3] C. H. Bennet, *Physics Today* 24 (1995).
- [4] S. Lloyd, *Scientific American* 140 (1995).
- [5] D. P. DiVincenzo, *Science* **270**, 255 (1995).
- [6] Y. Nakamura, Y. A. Pashkin, and J. S. Tsai, *Nature* **398**, 786 (1999).
- [7] J. E. Mooij *et al.*, *Science* **285**, 1036 (1999).
- [8] B. E. Kane, *Nature* **393**, 133 (1998).
- [9] D. Loss and D. P. DiVincenzo, *Phys. Rev. A* **57**, 120 (1998).
- [10] L. M. K. Vandersypen *et al.*, [quant-ph/0207059](https://arxiv.org/abs/quant-ph/0207059).
- [11] L. P. Kouwenhoven, D. G. Austing, and S. Tarucha, *Rep. Prog. Phys.* **64**, 701 (2001).
- [12] S. Tarucha *et al.*, *Phys. Rev. Lett.* **77**, 3613 (1996).
- [13] J. M. Elzerman *et al.*, *Phys. Rev. B* **67**, 161308 (2003).
- [14] G. Burkard, D. Loss, and D. P. DiVincenzo, *Phys. Rev. B* **59**, 2070 (1999).
- [15] J. D. Jackson, *Classical Electrodynamics*, 2nd ed. (John Wiley & Sons, New York, 1975).
- [16] J. J. Sakurai, *Modern Quantum Mechanics* (Addison-Wesley, New York, 1985).
- [17] Y. Yafet, in *Solid State Physics*, edited by F. Seitz and F. Turnbull (Academic Press, New York, 1963).
- [18] G. Dresselhaus, *Phys. Rev.* **100**, 580 (1955).
- [19] C. Kittel, *Quantum Theory of Solids* (John Wiley & Sons, Inc., New York, 1963).
- [20] M. I. D'yakonov and V. Y. Kachorovskii, *Sov. Phys. Semicond.* **20**, 110 (1986).
- [21] Y. A. Bychkov and E. I. Rashba, *JETP Lett.* **79**, 78 (1984).
- [22] L. W. Molenkamp, G. Schmidt, and G. E. W. Bauer, *Phys. Rev. B* **64**, 121202(R) (2001).
- [23] J. B. Miller *et al.*, *Phys. Rev. Lett.* **90**, 076807 (2003).

-
- [24] C. Cohen-Tannoudji, B. Diu, and F. Laloë, *Quantum Mechanics* (Wiley, New York, 1977).
- [25] D. Paget, G. Lampel, B. Sapoval, and V. I. Safarov, Phys. Rev. B **15**, 5780 (1977).
- [26] M. Dobers *et al.*, Phys. Rev. Lett. **61**, 1650 (1988).
- [27] M. I. D'yakonov and V. I. Perel, Sov. Phys. JETP **38**, 177 (1974).
- [28] R. P. Feynman and F. L. Vernon, Ann. Phys. **24**, 118 (1963).
- [29] A. J. Legget *et al.*, Rev. Mod. Phys. **59**, 1 (1987).
- [30] N. V. Prokof'ev and P. C. E. Stamp, Rep. Prog. Phys. **63**, 669 (2000).
- [31] J. Rammer, Rev. Mod. Phys. **63**, 781 (1991).
- [32] H. Schoeller and G. Schoen, Phys. Rev. B **50**, 18436 (1994).
- [33] J. König, J. Schmid, H. Schoeller, and G. Schön, Phys. Rev. B **54**, 16820 (1996).
- [34] C. P. Slichter, *Principles of Magnetic Resonance*, 3rd ed. (Springer-Verlag, Berlin, 1990).
- [35] P. J. Price, Ann. Phys. **133**, 217 (1981).
- [36] J. H. Kim, I. D. Vagner, and L. Xing, Phys. Rev. B **49**, 16777 (1994).
- [37] D. M. Frenkel, Phys. Rev. B **43**, 14228 (1991).
- [38] A. V. Khaetskii and Y. V. Nazarov, Phys. Rev. B **61**, 12639 (2000).
- [39] A. V. Khaetskii and Y. V. Nazarov, Phys. Rev. B **64**, 125316 (2001).
- [40] L. M. Woods, T. L. Reinecke, and Y. Lyanda-Geller, Phys. Rev. B **66**, 161318(R) (2002).
- [41] T. Fujisawa, Y. Tokura, and Y. Hirayama, Phys. Rev. B **63**, R81304 (2001).
- [42] T. Fujisawa, Y. Tokura, and Y. Hirayama, Physica B **298**, 573 (2001).
- [43] T. Fujisawa *et al.*, Nature **419**, 278 (2002).
- [44] R. Hanson *et al.*, cond-mat/0303139 (unpublished).
- [45] I. A. Merkulov, A. L. Efros, and M. Rosen, Phys. Rev. B **65**, 205309 (2002).
- [46] A. V. Khaetskii, D. Loss, and L. Glazman, Phys. Rev. Lett. **88**, 186802 (2002).
- [47] J. Schliemann, A. V. Khaetskii, and D. Loss, Phys. Rev. B **66**, 245303 (2002).
- [48] S. Saykin and V. Privman, Nano Lett. **2**, 651 (2002).
- [49] R. de Sousa and S. Das Sarma, Phys. Rev. B **67**, 033301 (2003).
- [50] Y. G. Seminov and K. W. Kim, Phys. Rev. B **67**, 73301 (2003).
- [51] K. Ono and S. Tarucha, (unpublished).

Chapter 2

Nucleus-mediated spin-flip transitions in GaAs quantum dots

Sigurdur I. Erlingsson, Yuli V. Nazarov, and Vladimir I. Fal'ko

Spin-flip rates in GaAs quantum dots can be quite slow, thus opening up the possibilities to manipulate spin states in the dots. We present here estimations of inelastic spin-flip rates, between triplet and singlet states, mediated by hyperfine interaction with nuclei. Under general assumptions the nucleus-mediated rate is proportional to the phonon relaxation rate for the corresponding non-spin-flip transitions. The rate can be accelerated in the vicinity of a singlet-triplet excited state crossing. The small proportionality coefficient depends inversely on the number of nuclei in the quantum dot. We compare our results with known mechanisms of spin-flip in GaAs quantum dot.

2.1 Introduction

The electron spin states in bulk semiconductor and heterostructures have attracted much attention in recent years. Experiments indicate very long spin decoherence times and small transition rates between states of different spin [1–3]. These promising results have motivated proposals for information processing based on electron spins in quantum dots, which might lead to a realization of a quantum computer [4, 5].

A quantum dot is a region where electrons are confined. The energy spectrum is discrete, due to the small size, and can display atomic-like properties [6, 7]. Here we will consider quantum dots in GaAs-AlGaAs heterostructures. The main reasons for studying them are that relevant quantum dots are fabricated in such structures and GaAs has peculiar electron and phonon properties which are of interest. There are two main types of gate controlled dots in these systems, so-called vertical and lateral dots [8]. They are characterized by different transverse confinement, which is approximately a triangular well and a square well for the lateral and vertical dots, respectively.

Manipulation of the electron spin in a coherent way requires that it should be relatively well isolated from the surrounding environment. Coupling a quantum dot, or any closed quantum system, to its environment can cause decoherence and dissipation. One measure of the strength of the coupling to the environment is the transition rates, or inverse lifetimes, of the quantum dot states. Calculations of transition rates between different spin states due to phonon-assisted spin-flip process mediated by spin-orbit coupling, which is one possibility for spin relaxation, have given surprisingly low rates in quantum dots [9–11]. For these calculations it is very important that the electron states are discrete, and the result differs strongly from that obtained in application to two dimensional (2D) extended electron states in GaAs. The same argument applies to the phonon-scattering mechanisms, since certain phonon processes possible in 2D and 3D electron systems are not effective in scattering the electron in 0D. An alternative mechanism of spin relaxation in quantum dots is caused by hyperfine coupling of nuclear spins to those of electrons. Although the hyperfine interaction mediated spin relaxation in donors was considered a long time ago [12], no analysis has been made yet, to our knowledge, of the hyperfine interaction mediated spin flip processes in quantum dots.

The present paper offers an estimation of the scale of hyperfine interaction induced spin relaxation rates in GaAs quantum dots and its magnetic field dependence. The transition is from a triplet state to a ground state singlet. The main result is presented by the expression in Eq. (2.12). Since the parameters of hyperfine interaction between conduction band electrons and underlying nuclei in GaAs have been extensively investigated [13, 14], including the Overhauser effect and spin-relaxation in GaAs/AlGaAs heterostructures [15–19], we are able

now to predict the typical time scale for this process in particular quantum dot geometries. The rate that we find depends inversely on the number of nuclei in the dot (which can be manipulated by changing the gate voltage) and is proportional to the inverse squared exchange splitting in the dot (which can be varied by application of an external magnetic field with orientation within the 2D plane). The following text is organized in two sections: section 2.2, where the transition rates in systems with discrete spectra are analyzed and section 2.3 where the obtained result is compared to transition rates provided by the spin-orbit coupling mechanism.

2.2 Model and assumptions

The ground state of the quantum dot is a many electron singlet $|S_g\rangle$, for sufficiently low magnetic fields. This can change at higher magnetic fields. We assume that the system is in a regime of magnetic field so that the lowest lying states are ordered as shown in Fig. 2.1. The relevant energy scales used in the following analysis are given by the energy difference between the triplet state (we assume small Zeeman splitting) and the ground state $\varepsilon = E_{T'} - E_g$, and exchange splitting $\delta_{ST} = E_{S'} - E_{T'}$ between the first excited singlet and the triplet. It is possible to inject an electron into an excited state of the dot. If this excited state is a triplet, the system may get stuck there since a spin-flip is required to cause transitions to the ground state.

The Γ -point of the conduction band in GaAs is mainly composed of s orbitals, so that the hyperfine interaction can be described by the contact interaction Hamiltonian [20]

$$H_{\text{HF}} = A \sum_{i,k} \mathbf{S}_i \cdot \mathbf{I}_k \delta(\mathbf{r}_i - \mathbf{R}_k) \quad (2.1)$$

where \mathbf{S}_i (\mathbf{I}_k) and \mathbf{r}_i (\mathbf{R}_k) denote the spin and position the i th electron (k th nuclei). This coupling flips the electron spin and simultaneously lowers/raises the z -component of a nuclear spin, which mixes spin states and provides the possibility for relaxation.

But the hyperfine interaction alone does not guarantee that transitions between the above-described states occur, since the nuclear spin flip cannot relax the excessive initial-state energy. (The energy associated with a nuclear spin is the nuclear Zeeman, $\hbar\omega_n$, energy which is three orders of magnitude smaller than the electron Zeeman energy and the energies related to the orbital degree of freedom.) For free electrons, the change in energy accompanying a spin flip caused by the hyperfine scattering is compensated by an appropriate change in its kinetic energy. In the case of a quantum dot, or any system with discrete a energy spectrum, this mechanism is not available and no hyperfine induced

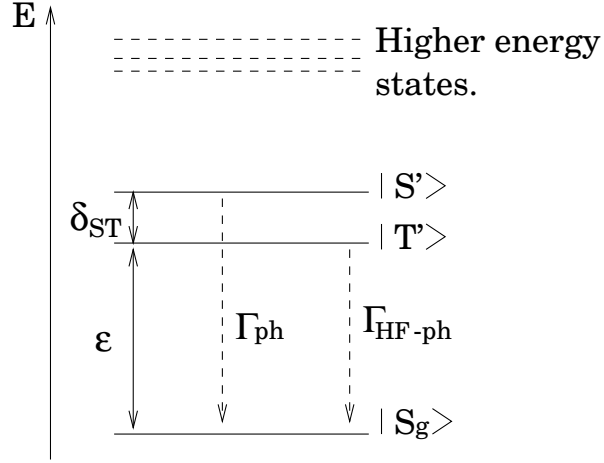


Figure 2.1: The lowest lying states of the quantum dot. The energy separation of the ground state singlet and the first triplet is denoted by ε and the exchange splitting by δ_{ST} . The two rates indicated are the phonon rate Γ_{ph} and the combined hyperfine and phonon rate $\Gamma_{\text{HF-ph}}$

transitions will occur because the energy released by the quantum dot cannot be absorbed. Therefore the spin relaxation process in a dot also requires taking into account the electron coupling to the lattice vibrations. The excess energy from the quantum dot can be emitted in the form of a phonon. Since the ‘bare’ electron-phonon interaction, H_{ph} does not contain any spin operators and thus does not couple directly different spin states, one has to employ second-order perturbation theory which results in transitions via virtual states. The amplitude of such a transition between the triplet state $|T'\rangle$ and the ground state $|S_g\rangle$ is

$$\begin{aligned} \langle T'|S_g\rangle &= \sum_t \frac{\langle T'|H_{\text{ph}}|t\rangle \langle t|H_{\text{HF}}|S_g\rangle}{E_{T'} - (E_t + \hbar\omega_{\mathbf{q}})} \\ &+ \sum_s \frac{\langle T'|H_{\text{HF}}|s\rangle \langle s|H_{\text{ph}}|S_g\rangle}{E_{T'} - (E_s + \hbar\omega_n)} \end{aligned} \quad (2.2)$$

where $\hbar\omega_{\mathbf{q}}$ is the energy of the emitted phonon and $\hbar\omega_n \approx 0$ is the energy changed by raising/lowering a nuclear spin.

It is natural to assume that the exchange splitting is smaller than the single-particle level splitting, so that the dominating contribution to the amplitude $\langle T'|S_g\rangle$ comes from the term describing the virtual state $|s\rangle = |S'\rangle$, due to a small denominator. All other terms can be ignored and the approximate

amplitude takes the form

$$\langle T' | S_g \rangle \approx \frac{\langle T' | H_{\text{HF}} | S' \rangle \langle S' | H_{\text{ph}} | S_g \rangle}{E_{T'} - E_{S'}}. \quad (2.3)$$

The justification for this assumption is that we aim at obtaining estimates of the rates, and including higher states would not affect the order of magnitude, even if the exchange splitting is substantial. Note that the phonon and nuclear state are not explicitly written in Eq. (2.3).

The transition rate from $|T'\rangle$ to $|S_g\rangle$ is given by Fermi's golden rule,

$$\tilde{\Gamma}_{\text{HF-ph}} = \frac{2\pi}{\hbar} \sum_{N'_q, \mu'} |\langle T' | S_g \rangle|^2 \delta(E_i - E_f), \quad (2.4)$$

where N'_q and μ' are the final phonon and nuclear states respectively and E_i and E_f stand for the initial and final energies. Inserting Eq. (2.3) into Eq. (2.4) and averaging over initial nuclear states with probability $P(\mu)$, we obtain an approximate equation for the nucleus mediated transition rate

$$\begin{aligned} \Gamma_{\text{HF-ph}} &= \frac{2\pi}{\hbar} \sum_{N'_q} |\langle S'; N'_q | H_{\text{ph}} | S_g; N_q \rangle|^2 \delta(E_i - E_f) \\ &\times \sum_{\mu', \mu} \frac{P(\mu) |\langle T'; \mu' | H_{\text{HF}} | S'; \mu \rangle|^2}{(E_{T'} - E_{S'})^2} \end{aligned} \quad (2.5)$$

$$= \Gamma_{\text{ph}}(\varepsilon) \sum_{\mu', \mu} \frac{P(\mu) |\langle T'; \mu' | H_{\text{HF}} | S'; \mu \rangle|^2}{(E_{T'} - E_{S'})^2}, \quad (2.6)$$

where Γ_{ph} is the non-spin-flip phonon rate as a function of the relaxed energy $\varepsilon = E_{T'} - E_{S_g}$.

We will approximate the many-body orbital wave functions by symmetric, $|\Psi_S\rangle$, and antisymmetric, $|\Psi_T\rangle$, Slater determinants corresponding to the singlet and triplet states respectively. It is not obvious *a priori* why this approximation is applicable, since the Coulomb interaction in few electron quantum dots can be quite strong [21]. The exact energy levels are very different from those obtained by simply adding the single particle energies. However the wave function will not drastically change and especially the matrix elements calculated using Slater determinants are comparable to the ones obtained by using exact ones. The singlet and triplet wave functions can be decomposed into orbital and spin parts: $|T'\rangle = |\Psi_T\rangle|T\rangle$ and $|S\rangle = |\Psi_S\rangle|S\rangle$, where

$$|T\rangle = -\frac{\nu_x - i\nu_y}{\sqrt{2}} |1, +1\rangle + \frac{\nu_x + i\nu_y}{\sqrt{2}} |1, -1\rangle + \nu_z |1, 0\rangle, \quad (2.7)$$

Using the above discussed wave functions in Eq. (2.6) we obtain the following

$$\sum_{\boldsymbol{\mu}'\boldsymbol{\mu}} P(\boldsymbol{\mu}) |\langle T'; \boldsymbol{\mu} | H_{\text{HF}} | S'; \boldsymbol{\mu}' \rangle|^2 = \frac{A^2}{4} G_{\text{corr}} \sum_k (|\Psi_1(\mathbf{R}_k)|^2 - |\Psi_2(\mathbf{R}_k)|^2)^2, \quad (2.8)$$

where $\Psi_{1,2}$ are the wave functions of the lowest energy states. The factor G_{corr} contains the nuclear correlation functions

$$G_{\text{corr}} = \sum_{\eta, \gamma=x,y,z} \nu_\eta \nu_\gamma^* \left(\bar{G}_{\eta\gamma} + \frac{1}{2} i \sum_\kappa \epsilon_{\gamma\eta\kappa} \langle I_\kappa \rangle \right). \quad (2.9)$$

Here we have introduced symmetric part of the nuclear correlation tensor $\bar{G}_{\eta\gamma} = \langle \delta I_\eta \delta I_\gamma + \delta I_\gamma \delta I_\eta \rangle / 2$, where $\delta I_\eta = I_\eta - \langle I_\eta \rangle$. The ν_η 's are the coefficients in the triplet state expansion in Eq. (2.7) and $\epsilon_{\gamma\eta\kappa}$ is the totally anti-symmetric tensor. We assume that nuclei are identical and non-interacting (thus we can drop the k subscript), which gives for an isotropic system $G_{\text{corr}} = I(I+1)/3 = 1.25$ since Ga and As both have nuclear spin $I = 3/2$.

Let us now introduce the length scales ℓ and z_0 which are the spatial extent of the electron wave function in the lateral direction and the dot thickness respectively. Let C_n denote concentration of nuclei with non-zero spin. The effective number of nuclei contained within the quantum dot is

$$N_{\text{eff}} = C_n \ell^2 z_0. \quad (2.10)$$

In GaAs $N_{\text{eff}} \gg 1$ and the sum over the nuclei in Eq. (2.8) can be replaced by $C_n \int d^3 \mathbf{R}_k$ and we define the dimensionless quantity

$$\gamma_{\text{int}} = \ell^2 z_0 \int d^3 \mathbf{R}_k (|\Psi_1(\mathbf{R}_k)|^2 - |\Psi_2(\mathbf{R}_k)|^2)^2. \quad (2.11)$$

To relate the hyperfine constant A (which has dimension energy \times volume) to a more convenient parameter we note that the splitting of spin up and spin down states at maximum nuclear polarization is $E_n = AC_n I$, where $I = 3/2$ is the nuclear spin. Thus, the hyperfine mediated transition rate is

$$\Gamma_{\text{HF-ph}} = \Gamma_{\text{ph}}(\varepsilon) \left(\frac{E_n}{\delta_{ST}} \right)^2 \frac{G_{\text{corr}} \gamma_{\text{int}}}{(2I)^2 N_{\text{eff}}} \quad (2.12)$$

Note that the rate is inversely proportional to the number of nuclei N_{eff} in the quantum dot and depends on the inverse square of δ_{ST} , which are both possible to vary in experiments [22, 23]. In particular, the singlet-triplet splitting of excited states of a dot can be brought down to zero value using magnetic field parallel to the 2D plane of the heterostructure, which would accelerate the relaxation process. The nuclear correlation functions in G_{corr} may also be manipulated by optical orientation of the nuclear system [13, 14].

2.3 Comparison and estimates

We now consider Eq. (2.12) for a specific quantum dot structure. It is assumed that the lateral confinement is parabolic and that the total potential can be split into a lateral and transverse part. For vertical dots the approximate transverse wave function is

$$\chi^{\text{ver}}(z) = \left(\frac{2}{z_0}\right)^{1/2} \sin\left(\frac{\pi z}{z_0}\right), \quad (2.13)$$

where z_0 is the thickness of the quantum well, i.e. the dot thickness. The wave functions in the lateral direction are the Darwin-Fock solutions $\phi_{n,l}(x,y)$ with radial quantum number n and angular momentum l . The single particle states corresponding to $(n,l) = (0,0)$ and $(0,\pm 1)$ are used to construct the Slater determinant for a two-electron quantum dot. In the case of these states the factor γ_{int} in Eq. (2.11) is then $\gamma_{\text{int}} = 0.12$ for a vertical dot and $\gamma_{\text{int}} = 0.045$ for a lateral one.

One property of the Darwin-Fock solution is the relation $\ell^{-2} = \hbar\omega m^*/\hbar^2$ where $\omega = \sqrt{\Omega_0^2 + \omega_c^2}/4$ is the effective confining frequency and $\omega_c = eB/m^*$ the cyclotron frequency. Inserting this and Eq. (2.10) into Eq. (2.12) the rate for parabolic quantum dots becomes

$$\Gamma_{\text{HF-ph}} = \Gamma_{\text{ph}}(\varepsilon)\hbar\omega \left(\frac{E_n}{\delta_{ST}}\right)^2 \frac{G_{\text{corr}}\gamma_{\text{int}}}{(2I)^2} \left(\frac{m^*}{\hbar^2 C_n z_0}\right). \quad (2.14)$$

Spin relaxation due to spin orbit related mechanisms in GaAs quantum dots were investigated by Khaetskii and Nazarov in Refs. [10] and [9]. We will summarize their results here for comparison with our hyperfine-phonon mechanism. In Ref. [10], it has been found that the dominating scattering mechanism is due to the absence of inversion symmetry. There are three rates related to this mechanism,

$$\Gamma_1 = \Gamma_{\text{ph}}(\varepsilon) \frac{8}{3} \left(\frac{m^*\beta^2}{\hbar\omega}\right)^3, \quad (2.15)$$

$$\Gamma_2 = \Gamma_{\text{ph}}(\varepsilon) \frac{7}{24} \frac{(m^*\beta^2)(\hbar\omega)}{E_z^2}, \quad (2.16)$$

$$\Gamma_5 = \Gamma_{\text{ph}}(\varepsilon) 6(m^*\beta^2)(g^*\mu_B B)^2 \frac{\hbar\omega}{(\hbar\Omega_0)^4}. \quad (2.17)$$

The Hamiltonian representing the absence of inversion symmetry has two distinct contribution which behave differently under a certain unitary transformation [10]. This behavior results in the two different rates in Eqs. (2.15) and (2.16). The inclusion of Zeeman splitting gives the rate in Eq. (2.17). Here, $m^*\beta^2$ is determined by the transverse confinement and band structure parameters and $E_z = \langle p_z^2 \rangle / (2m^*)$. For vertical dots of thickness $z_0 = 15$ nm, then

$m^*\beta^2 \approx 4 \times 10^{-3}$ meV, but one should be cautious when considering a different thickness, since $m^*\beta^2 \propto z_0^{-4}$, so the rates are sensitive to variations in z_0 . The transition rates in Eqs. (2.12), (2.15) and (2.16) are all proportional to the phonon rate Γ_{ph} evaluated for the same energy difference ε . It is thus sufficient to compare the only the proportionality coefficients.

Let us now consider for which confining energies the different rates are comparable. At zero magnetic field $\Gamma_1 = \Gamma_2$ at $\hbar\Omega_0 \approx 0.8$ meV. The estimated confining energies of vertical quantum dots used in experiment are in the range 2 – 5.5 meV [7, 23, 24]. For those dots $\Gamma_2 \gg \Gamma_1$ due to the very different dependence on the confinement, $\Gamma_1 \propto (\hbar\Omega_0)^{-3}$ and $\Gamma_2 \propto \hbar\Omega_0$. Doing the same for Γ_1 and $\Gamma_{\text{HF-ph}}$ we obtain that those rates are equal at $\hbar\Omega_0 \approx 4.4$ meV. The numerical values used for the hyperfine rate in Eq. (2.12) are the following: $E_n = 0.13$ meV [15], $\delta_{ST} = 2.3$ meV [25] and a $z_0 = 15$ nm. Thus, for $B = 0$ T and the previously cited experimental values for the confining energy the dominant transition rate is Eq. (2.16).

For clarity we will give the values of the rates. The non-spin-flip rate $\Gamma_{\text{ph}}(\varepsilon)$ is given in Ref. [10] and using the values $\hbar\Omega_0 = 5.5$ meV and $B = 0$ T we get

$$\Gamma_{\text{ph}} \approx 3.6 \times 10^7 \text{ s}^{-1}, \quad (2.18)$$

$$\Gamma_{\text{HF-ph}} \approx 2 \times 10^{-2} \text{ s}^{-1}, \quad (2.19)$$

$$\Gamma_2 \approx 1 \times 10^2 \text{ s}^{-1}. \quad (2.20)$$

The values of level separations $\varepsilon = 2.7$ meV and $\delta_{ST} = 2.84$ meV are taken from Ref. [23].

An application of a magnetic field to the dot may result in two effects. The rate Γ_5 becomes larger than Γ_2 for magnetic fields around $B = 1$ T ($\hbar\Omega_0 = 3$ meV) to $B \approx 5.4$ T ($\hbar\Omega_0 = 5.5$ meV). More importantly, the exchange splitting δ_{ST} can vanish in some cases and the hyperfine rate in Eq. (2.12) will dominate. It is also worth noting that in this limit the approximation used in obtaining Eq. (2.3) becomes very good. Since the rates considered here are all linear in the phonon rate the divergence of Γ_{ph} at the singlet-triplet transition does not affect the ratio of the rates. The above estimates were focused on vertical dots. To obtain the corresponding results for lateral dots the value of γ_{int} in Eq. (2.14) should be used.

In summary, we have calculated the nucleus mediated spin-flip transition rate in GaAs quantum dots. The comparison of our results to those previously obtained for the spin-orbit scattering mechanism indicates that the rates we obtained here are relatively low, due to the discrete spectrum, so we believe that hyperfine interaction would not cause problems for spin-coherent manipulation with GaAs quantum dots. Nevertheless, the hyperfine rate, which was found to be lower than the spin-orbit rates at small magnetic field, may diverge and become dominant at certain values of magnetic field corresponding to the

resonance between triplet and singlet excited states in the dot.

This work is a part of the research program of the “Stichting voor Fundamenteel Onderzoek der Materie (FOM)”, EPSRC and INTAS. One of authors (VF) acknowledges support from NATO CLG and thanks R. Haug and I. Aleiner for discussions.

References

- [1] J. M. Kikkawa and D. D. Awschalom, *Phys. Rev. Lett.* **80**, 4313 (1997).
- [2] Y. Ohno *et al.*, *Physica E* **6**, 817 (2000).
- [3] T. Fujisawa, Y. Tokura, and Y. Hirayama, *Phys. Rev. B* **63**, R81304 (2001).
- [4] D. Loss and D. P. DiVincenzo, *Phys. Rev. A* **57**, 120 (1998).
- [5] G. Burkard, D. Loss, and D. P. DiVincenzo, *Phys. Rev. B* **59**, 2070 (1999).
- [6] R. C. Ashoori, *Nature* **379**, 413 (1996).
- [7] S. Tarucha *et al.*, *Phys. Rev. Lett.* **77**, 3613 (1996).
- [8] L. P. Kouwenhoven *et al.*, in *Mesoscopic Electron Transport, NATO Series*, edited by L. L. Sohn, L. P. Kouwenhoven, and G. Schoen (Kluwer, Dordrecht, 1997), Chap. Electron transport in quantum dots, p. 105.
- [9] A. V. Khaetskii and Y. V. Nazarov, *Physica E* **6**, 470 (2000).
- [10] A. V. Khaetskii and Y. V. Nazarov, *Phys. Rev. B* **61**, 12639 (2000).
- [11] D. M. Frenkel, *Phys. Rev. B* **43**, 14228 (1991).
- [12] D. Pines, J. Bardeen, and C. P. Slichter, *Phys. Rev.* **106**, 489 (1957).
- [13] D. Paget, G. Lampel, B. Sapoval, and V. I. Safarov, *Phys. Rev. B* **15**, 5780 (1977).
- [14] D. Paget and V. L. Berkovits, in *Optical Orientation*, edited by F. Meier and B. P. Zakharchenya (North-Holland, Amsterdam, 1984).
- [15] M. Dobers *et al.*, *Phys. Rev. Lett.* **61**, 1650 (1988).
- [16] A. Berg, M. Dobers, R. R. Gerhardts, and K. v. Klitzing, *Phys. Rev. Lett.* **64**, 2563 (1990).
- [17] I. D. Vagner, T. Maniv, and E. Ehrenfreund, *Solid State Comm.* **44**, 635 (1982).
- [18] S. E. Barrett *et al.*, *Phys. Rev. Lett.* **74**, 5112 (1995).
- [19] R. Tycko *et al.*, *Science* **268**, 1460 (1995).
- [20] S. W. Brown, T. A. Kennedy, and D. Gammon, *Solid State Nucl. Magn. Reson.* **11**, 49 (1998).
- [21] D. Pfannkuche, Ph.D. thesis, Universität Karlsruhe, 1998.
- [22] W. G. van der Wiel *et al.*, *Physica B* **256-258**, 173 (1998).
- [23] S. Tarucha *et al.*, *Physica E* **3**, 112 (1998).
- [24] L. P. Kouwenhoven *et al.*, *Science* **278**, 1788 (1997).
- [25] F. Bolton, *Phys. Rev. B* **54**, 4780 (1996).

Chapter 3

Hyperfine-mediated transitions between a Zeeman split doublet in GaAs quantum dots: The role of the internal field

Sigurdur I. Erlingsson, Yuli V. Nazarov

We consider the hyperfine-mediated transition rate between Zeeman split states of the lowest orbital level in a GaAs quantum dot. We separate the hyperfine Hamiltonian into a part which is diagonal in the orbital states and another one which mixes different orbitals. The diagonal part gives rise to an effective (internal) magnetic field which, in addition to an external magnetic field, determines the Zeeman splitting. Spin-flip transitions in the dots are induced by the orbital mixing part accompanied by an emission of a phonon. We evaluate the rate for different regimes of applied magnetic field and temperature. The rates we find are bigger than the spin-orbit related rates provided the external magnetic field is sufficiently low.

3.1 Introduction

Manipulation of an individual quantum state in a solid state system is currently the focus of an intense research effort. There are various schemes which have been proposed and they are in various stages of development. [1–4] Many proposals concentrate on the spin degree of freedom of an electron in a quantum dot. Recent experiments indicate very long spin decoherence times and small transition rates between states of different spin [5–7] in some semiconductor heterostructures.

A characteristic feature of a quantum dot is its discrete energy spectrum. Depending on the strength of the confinement, both potential and magnetic, an orbital level energy separation of a few meV is possible. [8] This large energy separation strongly affects inelastic transition rates in the dot. The nuclei in GaAs have a substantial hyperfine interactions with the conduction electrons. This makes it relevant to investigate hyperfine related effects in quantum dots in GaAs-AlGaAs heterostructures.

Manipulating the electron spin while maintaining phase coherence requires that it should be relatively well isolated from the environment. Coupling a quantum dot, or any closed quantum system, to its environment can cause decoherence and dissipation. One of the measures of the strength of the coupling to the environment are the transition rates, or inverse lifetimes, between the quantum dot states. In GaAs there are two main mechanisms that can cause finite lifetimes of the spin states. These are the spin-orbit interaction and the hyperfine interaction with the surrounding nuclei. If a magnetic field is applied the change in Zeeman energy due to a spin-flip has to be accompanied by phonon emission. For two electron quantum dots, where the transitions are between triplet and singlet spin states, both spin-orbit [9, 10] and hyperfine [11] mediated transitions have been studied. In both cases the transition rates are much smaller than the usual phonon rates, the spin-orbit rate being the higher except when the excited singlet and triplet states cross. [11] For low magnetic fields, i.e. away from the singlet-triplet transition, the energy of the emitted phonon can be quite large and the transitions involve deformation phonons rather than piezoelectric ones.

If there are an odd number of electrons in the dot the ground state is usually a spin doublet so that energy change associated with the spin-flip is the electron Zeeman energy. Owing to the small g -factor in GaAs this energy is rather small compared to the orbital level spacing and the dominating phonon mechanism is due to piezoelectric phonons. Recently spin-orbit mediated spin-flip transitions between Zeeman levels were investigated [12]. Due to Kramer's degeneracy the transition amplitude for the spin-flip is proportional to the Zeeman splitting. This results in a spin-orbit spin-flip rate proportional to the fifth power of the Zeeman splitting.

In this paper we consider hyperfine mediated transitions between Zeeman split levels in a quantum dot. The transition amplitude remains finite at zero external magnetic field, resulting in a spin-flip rate [Eq. (3.27)] that is proportional to the cube of the Zeeman splitting. The cause of this is an internal magnetic field due to the hyperfine interaction. We consider the important concept of internal magnetic field in some detail. Since the parameters of hyperfine interaction between conduction band electrons and underlying nuclei in GaAs have been extensively investigated [13, 14], including the Overhauser effect and spin-relaxation in GaAs/AlGaAs heterostructures [15–19], we are able to calculate the hyperfine-mediated spin-flip transition rate for quantum dots in such structures.

Upon completion of this work we learned about recent results of Khaetskii, Loss and Glazman [20]. They consider essentially the same situation and model and obtain *electron spin decoherence* without considering any mechanism of dissipation. This is in clear distinction from the present result for the *spin-flip rate* that requires a mechanism of dissipation, i.e. phonons.

The rest of the paper is organized as follows: in section 3.2 the model used is introduced in addition to the basic assumptions and approximations used, section 3.3 deals with the internal magnetic field due to the hyperfine interaction and section 3.4 contains the derivation of the transition rates. Finally, in section 3.5 the results are discussed.

3.2 Model and assumptions

We consider a quantum dot embedded in a AlGaAs/GaAs heterostructure. Since the details of the quantum dot eigenstates are not important for now, it suffices to say that the energy spectrum is discrete and the wave functions are localized in space. The spatial extension of the wave function in the lateral and transverse direction (growth direction) are denoted with ℓ and z_0 , respectively. Quantum dots in these heterostructures are formed at a GaAs/AlGaAs interface, where the confining potential is very strong so that $\ell \gg z_0$. We define the volume occupied by an electron as $V_{\text{QD}} = \pi\ell^2 z_0$. The Hamiltonian of the quantum dot can be written in the form

$$H_0 = \sum_l \left(\varepsilon_l + g\mu_B \mathbf{B} \cdot \hat{\mathbf{S}} \right) |l\rangle\langle l|, \quad (3.1)$$

where ε_l are the eigenenergies which depend on the structure of the confining potential and the applied magnetic field \mathbf{B} . The magnetic field also couples to the electron spin via the Zeeman term, where g is the conduction band g-factor and μ_B is the Bohr magneton.

Since the Γ point of the conduction band in GaAs is mainly composed of s

orbitals the dipole interaction with the nuclei vanishes and the hyperfine interaction can be described by the usual contact term

$$H_{\text{HF}} = A\hat{\mathbf{S}} \cdot \sum_k \hat{\mathbf{I}}_k \delta(\mathbf{r} - \mathbf{R}_k), \quad (3.2)$$

where $\hat{\mathbf{S}}$ ($\hat{\mathbf{I}}_k$) and \mathbf{r} (\mathbf{R}_k) denote, respectively, the spin and position of the electron (k th nuclei). The delta function indicates that the point-like nature of the contact interaction will result in a position dependent coupling. The coupling constant A has the dimension volume \times energy. To get a notion of the related energy scale, it is straightforward to relate A to the energy splitting of the doublet for a fully polarized nuclear system,

$$E_n = AC_n I, \quad (3.3)$$

C_n being density of nuclei and I the spin of a nucleus. In GaAs this energy is $E_n \approx 0.135$ meV, which corresponds to a magnetic field of about 5 T. [15] For a given quantum dot geometry the number of nuclei occupying the dot is defined as $N_{\text{QD}} = C_n V_{\text{QD}}$. Since the Ga and As nuclei have the same spin and their coupling constants are comparable, we will assume that all the nuclear sites are characterized by the same hyperfine coupling A , and $C_n \approx a_0^{-3}$ where a_0 is the lattice spacing. For realistic quantum dots $N_{\text{QD}} \approx 10^4 - 10^6$, and it is therefore an important big parameter in the problem.

The coupling between the electron and the phonon bath is represented with

$$H_{\text{ph}} = \sum_{\mathbf{q}, \nu} \alpha_\nu(\mathbf{q}) (b_{\mathbf{q}, \nu} e^{i\mathbf{q} \cdot \mathbf{r}} + b_{\mathbf{q}, \nu}^\dagger e^{-i\mathbf{q} \cdot \mathbf{r}}), \quad (3.4)$$

where $b_{\mathbf{q}, \nu}^\dagger$ and $b_{\mathbf{q}, \nu}$ are creation and annihilation operators for the phonon mode with wave-vector \mathbf{q} on branch ν . In GaAs there are two different coupling mechanisms, deformation ones and piezoelectric ones. For transitions between Zeeman split levels in GaAs, i.e. low energy emission, the most effective phonon mechanism is due to piezoelectric phonons. We will assume that the heterostructure is grown in the [100] direction. This is the case for almost all dots and it imposes important symmetry relations on the coupling coefficient. The square of the coupling coefficient for the piezoelectric phonons is then given by (see Ref. [21])

$$\alpha_\nu^2(\mathbf{q}) = \frac{(eh_{14})^2 \hbar}{2\rho c_\nu V q} A_\nu(\theta) \quad (3.5)$$

where (eh_{14}) is the piezoelectric coefficient, ρ is the mass density, c_ν is the speed of sound of branch ν , V is normalization volume, we have defined $\mathbf{q} = q(\cos \phi \sin \theta, \sin \phi \sin \theta, \cos \theta)$ and the A_ν 's are the so-called anisotropy functions, see Appendix B.

3.3 Internal magnetic field

In this section we will introduce the concept of the effective magnetic field, the *internal field*, acting on the electron due to the hyperfine interaction. This internal field is a semiclassical approximation to the nuclear system, this approximation being valid in the limit of a large number of nuclei, $N_{\text{QD}} \gg 1$. If the nuclei are noticeably polarized, this field coincides with the Overhauser field that represents the average nuclear polarization. It is important that the internal field persists even at zero polarization giving rise to Zeeman splitting of the order $E_n N_{\text{QD}}^{-1/2}$.

First we write the Hamiltonian in Eq. (3.2) in the basis of the electron orbital states and present it as a sum of two terms

$$H_{\text{HF}} = H_{\text{HF}}^0 + V_{\text{HF}}, \quad (3.6)$$

where the terms are defined as

$$H_{\text{HF}}^0 = A \sum_l |l\rangle \langle l| \hat{\mathbf{S}} \cdot \sum_k |\langle \mathbf{R}_k | l \rangle|^2 \hat{\mathbf{I}}_k \quad (3.7)$$

$$V_{\text{HF}} = A \sum_{l \neq l'} |l\rangle \langle l'| \hat{\mathbf{S}} \cdot \sum_k \langle l | \mathbf{R}_k \rangle \langle \mathbf{R}_k | l' \rangle \hat{\mathbf{I}}_k. \quad (3.8)$$

By definition H_{HF}^0 does not couple different orbital levels. By combining Eqs. (3.1) and (3.7) one obtains the following Hamiltonian

$$H_0 = \sum_l \left(\varepsilon_l + g\mu_B \hat{\mathbf{B}}_l \cdot \hat{\mathbf{S}} \right) |l\rangle \langle l|. \quad (3.9)$$

We will regard the mixing term V_{HF} as a perturbation to H_0 . The justification for this is that the typical fluctuations of the electron energy due to the hyperfine interaction are much smaller than the orbital energy separation.

We now concentrate on H_0 and formulate a semiclassical description of it. For this we consider the operator of the orbitally dependent effective magnetic field,

$$\hat{\mathbf{B}}_l = \mathbf{B} + \frac{1}{g\mu_B} \hat{\mathbf{K}}_l, \quad (3.10)$$

where

$$\hat{\mathbf{K}}_l = \frac{E_n}{IC_n} \sum_k |\langle \mathbf{R}_k | l \rangle|^2 \hat{\mathbf{I}}_k. \quad (3.11)$$

Our goal is to replace the operator $\hat{\mathbf{K}}_l$ with a classical field. To prove the replacement is reasonable we calculate the average of the square for a given unpolarized nuclear state $|\boldsymbol{\mu}\rangle$

$$\mathbf{K}_l^2 = \langle \boldsymbol{\mu} | \hat{\mathbf{K}}_l^2 | \boldsymbol{\mu} \rangle \approx \frac{E_n^2}{N_{\text{QD}}}. \quad (3.12)$$

We cannot simply replace $\hat{\mathbf{K}}_l$ by its eigenvalues: as in the case of the usual spin algebra, different components of $\hat{\mathbf{K}}_l$ do not commute. In addition its square does not commute with individual components, $[\hat{\mathbf{K}}_l^2, \hat{K}_l^\alpha] \neq 0$. To estimate fluctuations of $\hat{\mathbf{K}}_l$ we calculate the uncertainty relations between its components

$$\Delta K_l^\alpha \Delta K_l^\beta \geq \frac{\alpha_l E_n^2}{N_{\text{QD}}^{3/2}} \approx \mathbf{K}_l^2 \frac{1}{N_{\text{QD}}^{1/2}}, \quad (3.13)$$

where α_l is a numerical constant $o(1)$ which depends on the details of the orbital wave functions. Since $N_{\text{QD}}^{-1/2} \ll 1$ we have proved that the quantum fluctuations in $\hat{\mathbf{K}}_l$ are much smaller than its typical amplitude. The semiclassical picture introduced above is only valid for high temperatures, $kT \gg E_n N_{\text{QD}}^{-1}$, where there are many states available to the nuclear system and the typical amplitude of \mathbf{K}_l is proportional to $E_n N_{\text{QD}}^{-1/2}$. For temperatures below $E_n N_{\text{QD}}^{-1}$ the nuclear system will predominantly be in the ground state and the classical picture breaks down. This is similar to the quantum mechanical description of a particle moving in a potential. At zero temperature it will be localized in some potential minimum and quantum mechanics will dominate. At sufficiently high temperatures the particle occupies higher energy states and its motion is well described by classical mechanics. Having established this we can replace the average over the density matrix of the nuclei by the average over a classical field \mathbf{K}_l , and note that it has no ‘hat’, whose values are Gaussian distributed

$$P(\mathbf{K}_l) = \left(\frac{1}{2\pi\sigma_l^2} \right)^{3/2} \exp \left(-\frac{(\mathbf{K}_l - \mathbf{K}_l^{(0)})^2}{2\sigma_l^2} \right), \quad (3.14)$$

where $\sigma_l^2 = \frac{1}{3}(\langle \mathbf{K}_l^2 \rangle - \langle \mathbf{K}_l \rangle^2)$ is the variance and $\mathbf{K}_l^{(0)}$ is the average, or Overhauser, field. In the case of a polarized nuclear system the variance decreases and the distribution becomes sharper around the Overhauser field, eventually becoming $P(\mathbf{K}_l) = \delta(\mathbf{K}_l - \mathbf{K}_l^{(0)})$ as $\sigma_l^2 \rightarrow 0$. The effective magnetic field acting on the electron is $\mathbf{B}_l = \mathcal{B}_l \mathbf{n}$ where \mathbf{n} is the unit vector along the total field for a given \mathbf{K}_l , see Fig. 3.1. For this configuration the spin eigenfunctions are $|\mathbf{n}_\pm\rangle$, corresponding to eigenvalues

$$\mathbf{n} \cdot \hat{\mathbf{S}} |\mathbf{n}_\pm\rangle = \pm \frac{1}{2} |\mathbf{n}_\pm\rangle. \quad (3.15)$$

The effective Zeeman Hamiltonian is then

$$H_Z = g\mu_B \mathbf{B}_l \cdot \hat{\mathbf{S}} \quad (3.16)$$

in this given internal field configuration. The spectrum of H_0 thus consists of many doublets distinguished by the value of \mathbf{B}_l . The magnitude of the effective field \mathcal{B}_l determines the Zeeman splitting of each doublet,

$$\begin{aligned} \Delta_l &= g\mu_B \mathcal{B}_l \\ &= (E_B^2 + K_l^2 + 2E_B K_l \cos \theta)^{1/2} \end{aligned} \quad (3.17)$$

where $E_B = g\mu_B B$ is the external field Zeeman energy.

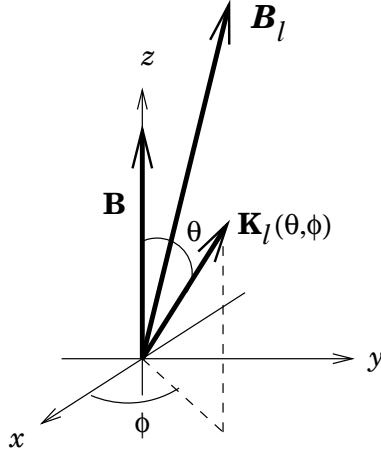


Figure 3.1: The internal field coordinate system is set by the external magnetic field \mathbf{B} , i.e. $e_z \parallel \mathbf{B}$. The combination of the external and the internal field \mathbf{K}_l results in an effective field \mathbf{B}_l .

We conclude this section with two remarks concerning time and energy scales. First, since the dynamics of \mathbf{K}_l is due to the precession around the average electron spin, and the time scale for a full rotation is proportional to $N_{\text{QD}}\hbar/E_n$. [22] For electron processes taking place on shorter time scales \mathbf{K}_l plays the role of a ‘frozen disorder’. At longer timescales self-averaging over all values of \mathbf{K}_l takes place. Second, the typical length of \mathbf{K}_l is approximately 5×10^{-4} meV (for a value $N_{\text{QD}} \approx 10^5$) which corresponds to a 100 Gauss magnetic field.

3.4 Transition rate

We concentrate on the transitions between the doublet components in Eq. (3.15). Assuming that the higher energy doublet state is initially occupied, we will calculate the transition rate to the lower one. The transition must be accompanied by energy dissipation equal to Δ_0 . This energy cannot be absorbed by the nuclear system. [11, 23] So an external mechanism of energy dissipation is required. The most effective one in quantum dots is known to be phonons. However the phonons alone cannot change the electron spin so we need a mechanism which mixes spin and orbital degrees of freedom, that is V_{HF} from Eq. (3.8). Thus the transition amplitude is proportional to both V_{HF} and the electron phonon coupling H_{ph} .

Here we assume that the electron is in the lowest orbital state $|0\rangle$ since the phonon mechanism will bring the electron to this state from any higher orbital on timescales much smaller than those related to transitions between the doublet components. Thus we consider an initial state of the entire system $|i\rangle = |0, \mathbf{n}_-; \boldsymbol{\mu}; \mathbf{N}\rangle$ which is a product state of the electron, nuclear $|\boldsymbol{\mu}\rangle$ and phonon $|\mathbf{N}\rangle$ systems and the final state $|f\rangle = |0, \mathbf{n}_+; \boldsymbol{\mu}'; \mathbf{N}'\rangle$. Note that to a given state of the nuclear system $|\boldsymbol{\mu}\rangle$, which is a product state of all individual nuclei, there is an associated value of the classical field \mathbf{K}_l . The transition amplitude between $|i\rangle$ and $|f\rangle$, in second order perturbation theory, reads

$$\begin{aligned} \mathcal{T} = \sum_{l \neq 0} & \left(\frac{\langle 0, \mathbf{n}_+; \boldsymbol{\mu}' | V_{\text{HF}} | l, \mathbf{n}_-; \boldsymbol{\mu} \rangle \langle l; \mathbf{N}' | H_{\text{ph}} | 0; \mathbf{N} \rangle}{(\varepsilon_0 - \varepsilon_l) + E_B} \right. \\ & \left. + \frac{\langle 0; \mathbf{N}' | H_{\text{ph}} | l; \mathbf{N} \rangle \langle l, \mathbf{n}_+; \boldsymbol{\mu}' | V_{\text{HF}} | 0, \mathbf{n}_-; \boldsymbol{\mu} \rangle}{(\varepsilon_0 - \varepsilon_l) - E_B} \right). \end{aligned} \quad (3.18)$$

The summation is over virtual states involving higher orbitals and the denominators in Eq. (3.18) contains the energy differences between different orbital states. The internal field depends on the orbital state, resulting in a rather complicated expression. Albeit the energy related to the internal field is much smaller than the orbital separation so we can safely replace the Zeeman splitting with E_B . The reason for that is that only at high external fields where $\Delta_0 \approx E_B$ will the effects of the Zeeman splitting be appreciable in the denominator. The internal field also appears in the phonon rate since it determines the electron energy difference between the initial and final states. Since H_{ph} does not connect different nuclear states and conversely V_{HF} does not mix different phonon states the sums over intermediate phonon and nuclear states reduce to a single term. From this transition amplitude the transition rate is obtained via Fermi's golden rule

$$\Gamma_{\text{sf}} = \frac{2\pi}{\hbar} \sum_{\mathbf{N}'} \sum_{\boldsymbol{\mu}'} |\mathcal{T}|^2 \delta(E_i - E_f), \quad (3.19)$$

where $E_i - E_f$ is the energy difference between the initial and final states of the combined systems. Substituting Eq. (3.18) into Eq. (3.19) we get the following

relation for the spin-flip rate

$$\begin{aligned}
\Gamma_{\text{sf}} = & \sum_{l,l' \neq 0} \left(\frac{\langle l, \mathbf{n}_-; \boldsymbol{\mu} | V_{\text{HF}} | 0, \mathbf{n}_+ \rangle \langle 0, \mathbf{n}_+ | V_{\text{HF}} | l', \mathbf{n}_-; \boldsymbol{\mu} \rangle}{((\varepsilon_0 - \varepsilon_l) + E_B)((\varepsilon_0 - \varepsilon_{l'}) + E_B)} \right. \\
& \times \frac{2\pi}{\hbar} \sum_{\mathbf{N}'} \langle 0; \mathbf{N} | H_{\text{ph}} | l; \mathbf{N}' \rangle \langle l'; \mathbf{N}' | H_{\text{ph}} | 0; \mathbf{N} \rangle \delta(E_i - E_f) \\
& + \frac{\langle l, \mathbf{n}_-; \boldsymbol{\mu} | V_{\text{HF}} | 0, \mathbf{n}_+ \rangle \langle l', \mathbf{n}_+ | V_{\text{HF}} | 0, \mathbf{n}_-; \boldsymbol{\mu} \rangle}{((\varepsilon_0 - \varepsilon_l) + E_B)((\varepsilon_0 - \varepsilon_{l'}) - E_B)} \\
& \times \frac{2\pi}{\hbar} \sum_{\mathbf{N}'} \langle 0; \mathbf{N} | H_{\text{ph}} | l; \mathbf{N}' \rangle \langle 0; \mathbf{N}' | H_{\text{ph}} | l'; \mathbf{N} \rangle \delta(E_i - E_f) \\
& + \frac{\langle 0, \mathbf{n}_-; \boldsymbol{\mu} | V_{\text{HF}} | l, \mathbf{n}_+ \rangle \langle 0, \mathbf{n}_+ | V_{\text{HF}} | l', \mathbf{n}_-; \boldsymbol{\mu} \rangle}{((\varepsilon_0 - \varepsilon_l) - E_B)((\varepsilon_0 - \varepsilon_{l'}) + E_B)} \\
& \times \frac{2\pi}{\hbar} \sum_{\mathbf{N}'} \langle l; \mathbf{N} | H_{\text{ph}} | 0; \mathbf{N}' \rangle \langle l'; \mathbf{N}' | H_{\text{ph}} | 0; \mathbf{N} \rangle \delta(E_i - E_f) \\
& + \frac{\langle 0, \mathbf{n}_-; \boldsymbol{\mu} | V_{\text{HF}} | l, \mathbf{n}_+ \rangle \langle l', \mathbf{n}_+ | V_{\text{HF}} | 0, \mathbf{n}_-; \boldsymbol{\mu} \rangle}{((\varepsilon_0 - \varepsilon_l) - E_B)((\varepsilon_0 - \varepsilon_{l'}) - E_B)} \\
& \left. \times \frac{2\pi}{\hbar} \sum_{\mathbf{N}'} \langle l; \mathbf{N} | H_{\text{ph}} | 0; \mathbf{N}' \rangle \langle 0; \mathbf{N}' | H_{\text{ph}} | l'; \mathbf{N} \rangle \delta(E_i - E_f) \right). \tag{3.20}
\end{aligned}$$

The spin-flip rate depends on the initial state of the nuclear system $|\boldsymbol{\mu}\rangle$. This poses the problem of how to deal with the nuclear state $|\boldsymbol{\mu}\rangle$, since we already demoted all the spin operators to a collective classical variable. A conceptually simple solution lies in the fact that when Eqs. (3.20) and (3.8) are considered together one sees that the rate is a sum over all pairs of nuclei in the system. Focusing on a given pair of nuclei k and k' , all the other nuclei are unchanged when the electron spin is ‘scattered’ on by this pair. By simply redefining the classical field such that it is composed of all nuclei except this given pair we can circumvent the problem. This procedure will not change our previous result regarding the properties of \mathbf{K}_l and by defining $|\boldsymbol{\mu}\rangle = |\mu_k\rangle|\mu_{k'}\rangle$ makes it straightforward to work with the nuclear states in Eq. (3.20).

Although the transition rate can be very slow, the typical duration of a transition event is set by energy uncertainty, \hbar/Δ_0 . This is much shorter than the typical time for nuclear system dynamics so that the nuclear system is frozen in a given value of \mathbf{K}_0 during the transition. In this case taking an average over \mathbf{K}_0 , using the probability distribution in Eq. (3.14), is not well motivated. For now we will postpone the averaging over the classical field. Expanding the energy denominators to second order in the Zeeman splitting and performing the thermal average over nuclei spin pairs (see Appendix A) we obtain the

following equation for the transition rate

$$\begin{aligned} \Gamma_{\text{sf}} = & G_{\text{corr}} \left(\sum_{l \neq 0} \left\{ \frac{2a_{ll}\gamma_{ll}}{\delta\varepsilon_l^2} \left(1 + 3\frac{E_B^2}{\delta\varepsilon_l^2} \right) + \frac{2\Re\{\tilde{a}_{ll}\tilde{\gamma}_{ll}\}}{\delta\varepsilon_l^2} \left(1 + \frac{E_B^2}{\delta\varepsilon_l^2} \right) \right\} \right. \\ & + \sum_{l < l' \neq 0} \frac{4\Re\{a_{ll'}\gamma_{ll'}\}}{\delta\varepsilon_l\delta\varepsilon_{l'}} \left(1 + \left(\frac{(\delta\varepsilon_l + \delta\varepsilon_{l'})^2}{\delta\varepsilon_l\delta\varepsilon_{l'}} - 1 \right) \frac{E_B^2}{\delta\varepsilon_l\delta\varepsilon_{l'}} \right) \\ & \left. + \sum_{l < l' \neq 0} \frac{4\Re\{\tilde{a}_{ll'}\tilde{\gamma}_{ll'}\}}{\delta\varepsilon_l\delta\varepsilon_{l'}} \left(1 + \left(\frac{(\delta\varepsilon_l - \delta\varepsilon_{l'})^2}{\delta\varepsilon_l\delta\varepsilon_{l'}} + 1 \right) \frac{E_B^2}{\delta\varepsilon_l\delta\varepsilon_{l'}} \right) \right) \end{aligned} \quad (3.21)$$

where $\delta\varepsilon_l = \varepsilon_0 - \varepsilon_l$. The parameters $a_{ll'}, \tilde{a}_{ll'}$ are related to the V_{HF} matrix elements

$$a_{ll'} = A^2 C_n \int d^3 \mathbf{R}_k \Psi_l^*(\mathbf{R}_k) |\Psi_0(\mathbf{R}_k)|^2 \Psi_{l'}(\mathbf{R}_k) \quad (3.22)$$

$$\tilde{a}_{ll'} = A^2 C_n \int d^3 \mathbf{R}_k \Psi_l^*(\mathbf{R}_k) \Psi_{l'}^*(\mathbf{R}_k) \Psi_0(\mathbf{R}_k)^2, \quad (3.23)$$

and $\gamma_{ll'}, \tilde{\gamma}_{ll'}$ are generalized phonon transition rates

$$\gamma_{ll'} = \frac{2\pi}{\hbar} \sum_{\mathbf{q}\nu} \frac{\alpha_\nu^2(\mathbf{q}) [e^{-i\mathbf{q}\cdot\mathbf{r}}]_{0,l} [e^{i\mathbf{q}\cdot\mathbf{r}}]_{l',0}}{1 - e^{-\beta\hbar\omega_{\mathbf{q},\nu}}} \delta(\hbar\omega_{\mathbf{q}\nu} - \Delta_0) \quad (3.24)$$

$$\tilde{\gamma}_{ll'} = \frac{2\pi}{\hbar} \sum_{\mathbf{q}\nu} \frac{\alpha_\nu^2(\mathbf{q}) [e^{-i\mathbf{q}\cdot\mathbf{r}}]_{0,l} [e^{i\mathbf{q}\cdot\mathbf{r}}]_{0,l'}}{1 - e^{-\beta\hbar\omega_{\mathbf{q},\nu}}} \delta(\hbar\omega_{\mathbf{q}\nu} - \Delta_0). \quad (3.25)$$

Here we have only included the emission process since we assume that the spin is initially in the higher energy doublet state.

Until now we have considered a general quantum dot and the rate in Eq. (3.21) is valid for any quantum dot. To proceed further we will specify the confining potential to be parabolic in the lateral direction and in the transverse one a triangular well potential is chosen. The wave function is $\langle \mathbf{r} | l \rangle \equiv \chi_0(z) \psi_{n,M}(r, \theta)$ where n, M denote the orbital and angular momentum quantum numbers respectively of the Darwin-Fock solution and $\chi_0(z)$ is the wave function in the transverse direction. The generic quantum number thus becomes $l = (n, M)$. The square of the lateral confining length is $\ell^2 = \hbar^2 / m^* \hbar \Omega$, where m^* is the electron effective mass and $\Omega = (\Omega_0^2 + (\omega_c/2)^2)^{1/2}$ is the effective confining frequency, with $\hbar\Omega_0$ being the confining energy and $\omega_c = eB/m^*$ the cyclotron frequency. What remains is to calculate the a 's and γ 's in Eqs. (3.22)-(3.25). The result of these calculations are presented Appendix B.

In principle it is possible to obtain the rate for all parameter values but to make the discussion more transparent we will consider two regimes of applied magnetic field (i) $E_B \approx E_n N_{\text{QD}}^{-1/2}$ and (ii) $E_B \gg E_n N_{\text{QD}}^{-1/2}$. In regime (i) both $\Delta_0 \ll \hbar c_\nu \ell^{-1}$ and $\Delta_0 \ll kT$ (for experimentally relevant temperatures)

and only the lowest order terms in $\Delta_0/\hbar c_\nu \ell^{-1}$ need to be considered. In GaAs $\hbar c_l \ell^{-1} = 3.3 \ell^{-1} \text{ nm} \times \text{meV}$ and $\hbar c_t \ell^{-1} = 2.0 \ell^{-1} \text{ nm} \times \text{meV}$ for the longitudinal and transverse branches respectively. In the other regime the applied field dominates and the internal field may be ignored, but no additional assumptions are made in this case. The resulting hyperfine-mediated spin-flip rates are

$$\Gamma_{\text{HF}} = 0.34 \frac{G_{\text{corr}}}{I^2} \frac{E_n^2}{N_{\text{QD}}(\hbar\Omega)^2} \frac{(eh_{14}\ell)^2 kT}{8\pi\rho c^5 \hbar^4} (E_B^2 + K_0^2 + 2E_B K_0 \cos\theta) \quad \text{for } E_B \approx E_n N_{\text{QD}}^{-1/2} \quad (3.26)$$

$$\Gamma_{\text{HF}} = \frac{G_{\text{corr}}}{I^2} \frac{E_n^2 (n(E_B) + 1)}{N_{\text{QD}}(\hbar\Omega)^2} \frac{(eh_{14}\ell)^2 E_B^3}{8\pi\rho c^5 \hbar^4} \left(C_0(E_B) + \left(\frac{E_B}{\hbar\Omega} \right)^2 C_2(E_B) \right) \quad \text{for } E_B \gg E_n N_{\text{QD}}^{-1/2} \quad (3.27)$$

Note that the rates have different dependencies on the emitted energy Δ_0 . In Eq. (3.27) we introduce the functions C_0 and C_2 which contain the details of the higher orbitals and the anisotropy integrals. For low fields $\Delta_0 \ll \hbar c_\nu \ell^{-1}$ these functions are constant. The saturation value of the spin-flip rate in Eq. (3.26), for some typical value of $K_0 = 5 \times 10^{-4} \text{ meV}$, is very low $\Gamma_{\text{HF}} < 10^{-6} \text{ s}$. This results in a lifetime of days, which will be extremely difficult to measure. For

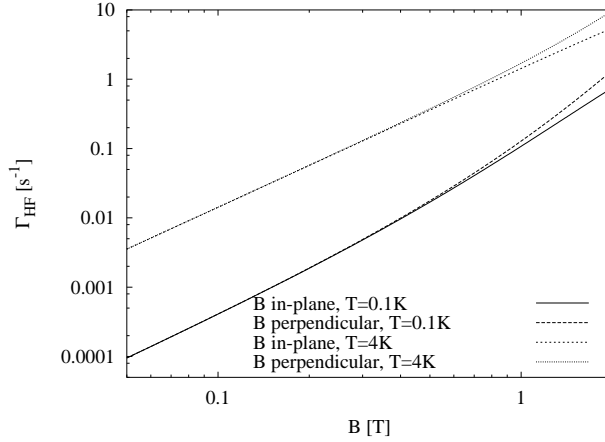


Figure 3.2: The hyperfine-mediated spin-flip rate for a quantum dot with $z_0 = 10 \text{ nm}$ and $\hbar\Omega_0 = 2 \text{ meV}$, plotted as a function of external magnetic field for two different temperatures $T = 0.1 \text{ K}$ and 4 K .

regime (ii) we have plotted the general spin-flip rate in Eq. (3.27) for different confining energies and temperatures in Figs. 3.2 and 3.3, for both in-plane and perpendicular applied magnetic field. Due to the Bose distribution function factor $(n(E_B) + 1)$, there is a crossover from $\Gamma_{\text{HF}} \propto kTE_B^2$ to $\Gamma_{\text{HF}} \propto E_B^3$ that

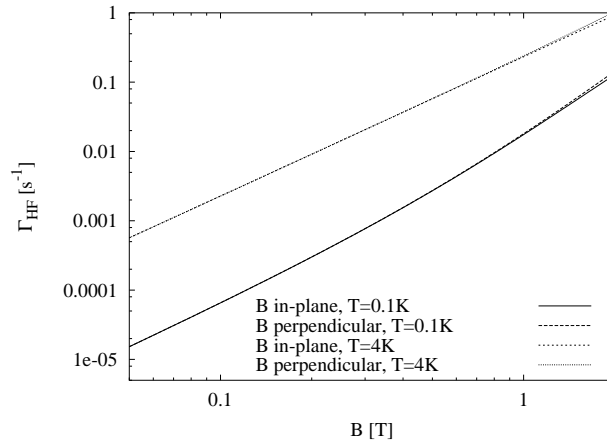


Figure 3.3: The hyperfine-mediated spin-flip rate for a quantum dot with $z_0 = 10$ nm and $\hbar\Omega_0 = 5$ meV, plotted as a function of external magnetic field for two different temperatures $T = 0.1$ K and 4 K.

occurs around $E_B \approx kT$. In both Figs. 3.2 and 3.3 this crossover is observed for the $T = 0.1$ K curves around $B = 0.34$ T. For the $T = 1$ K curves the crossover occurs around 12 T. In the case of the higher confining energy there is small difference between the in-plane and perpendicular direction of the external magnetic field. For the lower confining energy there is a substantial difference between the two directions of magnetic field. In this case the approximation $\Delta_0 \ll \hbar c_\nu \ell^{-1}$ is no longer good and the Δ_0 dependence of the rate is changed by the C -functions. The values of the rates are quite small, depending on the applied field, being ~ 1 s $^{-1}$ for $T = 4$ K at $B \approx 0.5$ T for a confining frequency of $\hbar\Omega_0 = 2$ meV.

3.5 Discussion

Generally speaking, inelastic spin-flip rates require an external source of dissipation to facilitate the transitions. This is why at small Zeeman splittings they will contain small factor reflecting the vanishing phonon density of states. For a spin-orbit rate [12], the Kramer's degeneracy results in this small factor being proportional to E_B^5 . The presence of nuclear spins violates Kramer's theorem. Thus, the hyperfine rate discussed in the present paper is proportional to E_B^3 and will dominate at sufficiently low fields.

Comparing the hyperfine rate in Eq. (3.27) to spin-orbit related rates [12] and requiring that the rates are equal we obtain $(E_B/\hbar\Omega)^2 \epsilon_\beta^2 \approx E_n^2 N_{\text{QD}}^{-1}$, where ϵ_β determines the spin-orbit admixture strength. The extra factor $(E_B/\hbar\Omega)^2$ is

due to Kramers degeneracy which suppresses the spin-orbit rate compared to hyperfine one at low fields. The crossover occurs at $E_B \approx \hbar\Omega(E_n N_{\text{QD}}^{-1/2}/\epsilon_\beta)$, which correspond to magnetic field $B \approx 0.3$ T, assuming typical quantum dot parameters $z_0 = 10$ nm and $\hbar\Omega_0 = 4$ meV.

The role of the internal field produced by the nuclei is that the spin-flip rate does not vanish even for in the absence of external magnetic field. We show that the minimum rate is rather small, corresponding to a relaxation time of the order of days. We believe that the internal field will play an important role when the full dynamics of the electron spin in the presence of the nuclear system is considered. Our model should also be applicable to other polar semiconductors which have non-zero nuclear spin, e.g. InAs where the g -factor is much larger.

One author (SIE) would like to thank Daniela Pfannkuche, Alexander Chudnovskii for fruitful discussions. We also acknowledge discussions with Daniel Loss and Alexander V. Khaetskii. This work is a part of the research program of the ‘‘Stichting voor Fundamenteel Onderzoek der Materie (FOM)’’

References

- [1] Y. Nakamura, Y. A. Pashkin, and J. S. Tsai, *Nature* **398**, 786 (1999).
- [2] J. E. Mooij *et al.*, *Science* **285**, 1036 (1999).
- [3] B. E. Kane, *Nature* **393**, 133 (1998).
- [4] D. Loss and D. P. DiVincenzo, *Phys. Rev. A* **57**, 120 (1998).
- [5] J. M. Kikkawa and D. D. Awschalom, *Phys. Rev. Lett.* **80**, 4313 (1997).
- [6] Y. Ohno *et al.*, *Physica E* **6**, 817 (2000).
- [7] T. Fujisawa, Y. Tokura, and Y. Hirayama, *Phys. Rev. B* **63**, R81304 (2001).
- [8] L. P. Kouwenhoven *et al.*, in *Mesoscopic Electron Transport, NATO Series*, edited by L. L. Sohn, L. P. Kouwenhoven, and G. Schoen (Kluwer, Dordrecht, 1997), Chap. Electron transport in quantum dots, p. 105.
- [9] A. V. Khaetskii and Y. V. Nazarov, *Phys. Rev. B* **61**, 12639 (2000).
- [10] A. V. Khaetskii and Y. V. Nazarov, *Physica E* **6**, 470 (2000).
- [11] S. I. Erlingsson, Y. V. Nazarov, and V. I. Fal’ko, *Phys. Rev. B* **64**, 195306 (2001).
- [12] A. V. Khaetskii and Y. V. Nazarov, *Phys. Rev. B* **64**, 125316 (2001).
- [13] D. Paget, G. Lampel, B. Sapoval, and V. I. Safarov, *Phys. Rev. B* **15**, 5780 (1977).

Using the notation in Ref. [12] the spin-orbit admixture constant is $\epsilon_\beta = \beta\hbar/a$, where a is the lateral quantum dot size, corresponding to ℓ in the present paper.

- [14] D. Paget and V. L. Berkovits, in *Optical Orientation*, edited by F. Meier and B. P. Zakharchenya (North-Holland, Amsterdam, 1984).
- [15] M. Dobers *et al.*, Phys. Rev. Lett. **61**, 1650 (1988).
- [16] A. Berg, M. Dobers, R. R. Gerhardts, and K. v. Klitzing, Phys. Rev. Lett. **64**, 2563 (1990).
- [17] I. D. Vagner, T. Maniv, and E. Ehrenfreund, Solid State Comm. **44**, 635 (1982).
- [18] S. E. Barrett *et al.*, Phys. Rev. Lett. **74**, 5112 (1995).
- [19] R. Tycko *et al.*, Science **268**, 1460 (1995).
- [20] A. V. Khaetskii, D. Loss, and L. Glazman, Phys. Rev. Lett. **88**, 186802 (2002).
- [21] P. J. Price, Ann. Phys. **133**, 217 (1981).
- [22] I. A. Merkulov, A. L. Efros, and M. Rosen, Phys. Rev. B **65**, 205309 (2002).
- [23] J. H. Kim, I. D. Vagner, and L. Xing, Phys. Rev. B **49**, 16777 (1994).

Chapter 4

Nuclear spin induced coherent oscillations of transport current through a double quantum dot

Sigurdur I. Erlingsson, Oleg N. Jouravlev and Yuli V. Nazarov

We propose a mechanism for coherent oscillations of transport current through a double quantum dot. It is based on coupling of the states of different spin due to hyperfine interaction with nuclei. We study the dependence of the current oscillations on various system parameters and external magnetic field. Our results may qualitatively explain recent experimental observations.

4.1 Introduction

Motivated by possible device applications which utilize both the spin and charge of electrons there has been a great effort to come up with means of manipulating the electron spin and even the nuclear spin of the host material. In GaAs the dominant coupling mechanism between electron and nuclear spins is the hyperfine interaction. Furthermore, the nuclear spin relaxation times are much longer than other timescales related to electron dynamics [1]. This difference of timescales has facilitated many experiments where a quasi-stationary polarization of the nuclear system is achieved and its effect on the electronic behavior can be observed [2–5]. Many recent experiments have involved novel ways of controlling the coupling of the electron and nuclear spin [6, 7], and even coherent oscillations between 'up' and 'down' polarized nuclear system have been reported [8].

Transport experiments have proven to be a very good tool to probe nanostructures. This is especially true in quantum dots where the control of the dot energetics allows for a detailed study of the quantum dot spectrum, both in the linear regime and in excitation spectroscopy [9, 10]. In between the conduction peaks, i.e. in the Coulomb blockade regime, there still flows a small current due to cotunneling [11]. This cotunneling current, sometimes referred to as leakage current, has been discussed in connection with limitations of operating SET devices [12].

Unexpected oscillations of the leakage current through a double quantum dot in a spin blockade regime have been observed in transport experiments [13]. The system is the same as used in a recent experiment where current rectification was observed in the transport characteristics [14]. The origin of this rectification was explained in terms of spin blockade, i.e. interdot transitions between states with different spins are blocked. The inclusion of a spin-flip mechanism lifts the spin blockade, giving rise to a small leakage current in a similar way cotunneling lifts the Coulomb blockade. Related ideas of spin blockade based on certain selection rules have previously were proposed in [15]. More recently, spin blockade was observed in transport through quantum dot systems that was attributed to spin polarized leads [16]. The timescale of the leakage current oscillations, which is much larger than the usual timescale related to electronic transport, and the fact that the oscillation period and amplitude were modified by resonant excitation of the nuclei indicates that the origin of the oscillations may be traced to the hyperfine interaction [13].

Here we propose a novel transport mechanism based on the hyperfine interaction which leads to an oscillating leakage current in the spin blockade regime. This mechanism may, in a qualitative way, shed light on some of the experimental results observed in Ref. [13]. The key steps in formulating a solution of the problem are (*i*) calculating the stationary solution of the density matrix

for the double dot system assuming a fixed nuclear system and (ii) using that stationary solution to determine the average electrons spins in the dots which are then used to calculate the dynamics of the nuclear system. This approach is only valid if the transport timescales are much shorter than the dynamical timescales associated with the nuclear system. We assume that this is the case in the system studied here. The relevant transport processes may be characterized by 4 rates, the left (right) barrier tunnel rate Γ_L (Γ_R), the inelastic interdot tunnel rate Γ_i and the transport rate in the spin blockade regime $\propto (K_A/\Delta_{ST})^2\Gamma_i$, where K_A and Δ_{ST} respectively characterize the coupling and energy separation of the blocked and non-blocked spin states. The factor $(K_A/\Delta_{ST}) \ll 1$ is responsible for suppressing the current in the spin blockade regime in comparison with non-blocked current $\propto \Gamma_i$. The fastest nuclear spin process which enters the density matrix is the precession frequency γ of the nuclear system in the hyperfine field of the average electron spins [17]. This results in the condition $\Gamma_i \gg (\Delta_{ST}/K_A)^2\gamma$ for the validity of our approach. The timescale of the oscillation is determined by the factor $\gamma^{-1}(\Delta_{ST}/K_A)$, which can be quite long approaching tenths of seconds.

4.2 Model

For details of the setup we refer the reader to Ref. [14]. Each charge configuration of the double dot system can be characterized by (N_L, N_R) where $N_L(N_R)$ is the number of charges of the left (right) dot, see Fig. 4.1. The multiplicity of the (0,1) configuration is 2 since it is a spin doublet, denoted by $|\pm\rangle$. The (1,1) configuration has a multiplicity of 4, one singlet $|S_0\rangle$ and 3 triplets $|T_i\rangle$, $i = 1, 2, 3$. At low magnetic fields the total spin of the configuration (0,2) is a singlet [14], the state being denoted by $|S_g\rangle$.

It is instructive to look more closely at the eigenstates of the double dot system since they are instrumental in determining the transport characteristics. Also, the spin structure of the eigenstates becomes clear after diagonalizing the Hamiltonian of the double dot system. The Hamiltonian for the isolated double dot system is

$$H_{DD} = H_0 + H_T + H_C \quad (4.1)$$

where H_0 is the Hamiltonian of each dot

$$H_0 = \sum_{\eta} (\epsilon_{L\eta} d_{L\eta}^{\dagger} d_{L\eta} + (\epsilon_{R\eta} + e\Delta V) d_{R\eta}^{\dagger} d_{R\eta}) \quad (4.2)$$

where $d_{\alpha\eta}^{\dagger}$ creates a particle in state $\alpha = L, R$ with spin $\eta = \uparrow, \downarrow$ and $e\Delta V$ is determined by the voltage drop over the central barrier. Using the above assumptions about the possible charge configurations, only one orbital level on

each is dot is relevant. The quantization axis of the electron spin is along the external magnetic field that is applied parallel to the 2DEG plane. The orbitals are not affected by the field and thus the sole effect of magnetic field is through the Zeeman energy

$$\epsilon_{\alpha\eta} = \hbar\Omega_{\alpha} \pm \Delta/2, \quad (4.3)$$

where $\hbar\Omega_{\alpha}$ is the ground state orbital energy of the $\alpha = L, R$ dot and $\Delta = g\mu_B B$ is the Zeeman splitting. The second term in Eq. (4.1) is the tunneling Hamiltonian describing interdot tunneling between the L and R orbital, assuming spin conservation,

$$H_t = \sum_{\eta} (V_{\tau} d_{L\eta}^{\dagger} d_{R\eta} + V_{\tau}^* d_{R\eta}^{\dagger} d_{L\eta}), \quad (4.4)$$

where V_{τ} is the tunneling amplitude. The Coulomb interaction is approximated by the following expression

$$H_C = U_L n_{L\uparrow} n_{L\downarrow} + U_R n_{R\uparrow} n_{R\downarrow} + \sum_{\eta\eta'} U_{LR} n_{L\eta} n_{R\eta'}. \quad (4.5)$$

where $n_{\alpha\eta} = d_{\alpha\eta}^{\dagger} d_{\alpha\eta}$, U_L and U_R are the charging energies for the on-site charging and U_{LR} is the interdot charging energy.

Once a suitable basis has been chosen, the double dot Hamiltonian can be diagonalized. It is convenient to introduce the following basis states

$$\begin{aligned} |0; \eta\rangle &= d_{R\eta}^{\dagger} | \rangle \\ |\eta; \eta'\rangle &= d_{L\eta}^{\dagger} d_{R\eta'}^{\dagger} | \rangle \\ |0; \uparrow\downarrow\rangle &= d_{R\uparrow}^{\dagger} d_{R\downarrow}^{\dagger} | \rangle. \end{aligned}$$

These states are eigenstates of H_0 and H_C but not H_T . It is easy to establish that only three (of seven possible) states are coupled by H_T . By diagonalizing the submatrix of these three states, the resulting eigenstates and eigenenergies are

$$|T_2\rangle = \frac{1}{\sqrt{2}}(|\uparrow; \downarrow\rangle + |\downarrow; \uparrow\rangle), \quad E_{T_2} = \hbar\Omega_L + \hbar\Omega_R + U_{LR} \quad (4.6)$$

$$|S_0\rangle \approx \frac{1}{\sqrt{2}}(|\uparrow; \downarrow\rangle - |\downarrow; \uparrow\rangle), \quad E_{S_0} \approx E_{T_2} + \frac{|V_{\tau}|^2}{e\Delta V - \delta U} \quad (4.7)$$

$$|S_g\rangle \approx |0; \uparrow\downarrow\rangle, \quad E_{S_g} \approx E_{T_2} - e\delta V + \delta U - \frac{|V_{\tau}|^2}{e\delta V - \delta U}, \quad (4.8)$$

where $\delta U = U_R - U_{LR}$. These equations were obtained assuming $V_{\tau} \ll (e\Delta V - \delta U)$, which is a good approximation for the system in question. The other four

eigenstates are simply

$$|T_1\rangle = |\uparrow; \uparrow\rangle, \quad E_{T_1} = E_{T_2} - \Delta \quad (4.9)$$

$$|T_3\rangle = |\downarrow; \downarrow\rangle, \quad E_{T_3} = E_{T_2} + \Delta \quad (4.10)$$

$$|\pm\rangle = |0; \uparrow/\downarrow\rangle, \quad E_{\pm} = \hbar\Omega_R \pm \Delta/2. \quad (4.11)$$

The triplet states are degenerate at $B = 0$ and otherwise they are separated by the Zeeman splitting Δ . The (1, 1) singlet has a higher energy at zero field than the triplet states. The $|S_0\rangle$ and $|T_3\rangle$ states cross at a magnetic field

$$B^* = \frac{1}{g\mu_B} \frac{|V_\tau|^2}{e\Delta V - \delta U}. \quad (4.12)$$

The hyperfine interaction induces mixing of the singlet and triplets in the (1, 1) configuration which lift the spin blockade. Since we are interested in the leakage current *oscillations*, other spin-flip mechanisms that only give rise to a dc current will not be considered. Our starting point is to introduce a semiclassical picture of the hyperfine interaction. This approximation [17–19] is valid when the number of nuclei in the quantum dot $N_{\text{QD}} \gg 1$. The part of the total Hamiltonian which explicitly contains the electron spin operators \hat{S}_L and \hat{S}_R is

$$\begin{aligned} H_s &= \mathbf{K}_L \cdot \hat{S}_L + \mathbf{K}_R \cdot \hat{S}_R + g\mu_B \mathbf{B}_{\text{ext}} \cdot (\hat{S}_L + \hat{S}_R) \\ &= \frac{1}{2} (\mathbf{K}_L + \mathbf{K}_R) \cdot (\hat{S}_L + \hat{S}_R) + \frac{1}{2} (\mathbf{K}_L - \mathbf{K}_R) \cdot (\hat{S}_L - \hat{S}_R) \\ &\quad + g\mu_B \mathbf{B}_{\text{ext}} \cdot (\hat{S}_L + \hat{S}_R) \\ &= g\mu_B B \hat{S}_z + \frac{1}{2} \mathbf{K}_A \cdot (\hat{S}_L - \hat{S}_R) \end{aligned} \quad (4.13)$$

where g is the g -factor, μ_B is the Bohr magneton and \mathbf{K}_L (\mathbf{K}_R) is the semiclassical effective nuclear magnetic field acting on the electron spin localized in the left (right) dot. In Eq. (4.13) the quantization axis has been set along the total magnetic field

$$\mathbf{B} = \mathbf{B}_{\text{ext}} + \frac{1}{2g\mu_B} (\mathbf{K}_L + \mathbf{K}_R) \quad (4.14)$$

and \hat{S}_z is the z -component of the total spin operator. The latter term in Eq. (4.14) does not couple the singlet and triplets, it only changes the Zeeman splitting of the triplet states. The second term in Eq. (4.13) mixes the (1, 1) singlet and triplet states, i.e. the mixing is proportional to the asymmetry in the two effective nuclear magnetic fields

$$\mathbf{K}_A = \mathbf{K}_L - \mathbf{K}_R. \quad (4.15)$$

The spin operator is $\hat{S}_\alpha = \sum_{\eta, \gamma} \hat{\sigma}_{\eta\gamma} d_{\alpha\eta}^\dagger d_{\alpha\eta}$ where $\hat{\sigma} = (\hat{\sigma}_x, \hat{\sigma}_y, \hat{\sigma}_z)$ are the Pauli matrices and $d_{L\eta}^\dagger$ creates an electron with spin η in dot α .

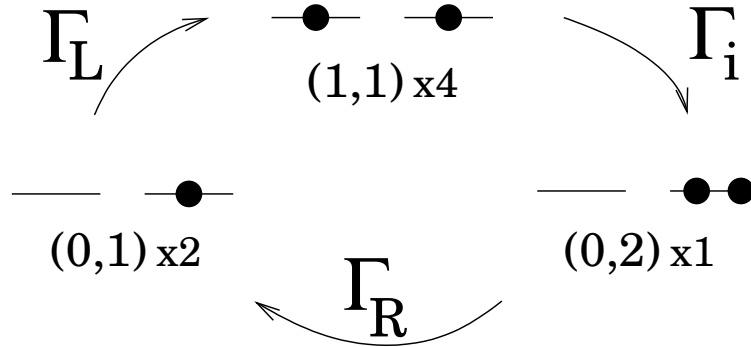


Figure 4.1: The three possible charge configurations of the double dot system. Each charge configuration is characterized by (N_L, N_R) and there can be many quantum mechanical states corresponding to a given configuration. See text for discussion on the Γ 's.

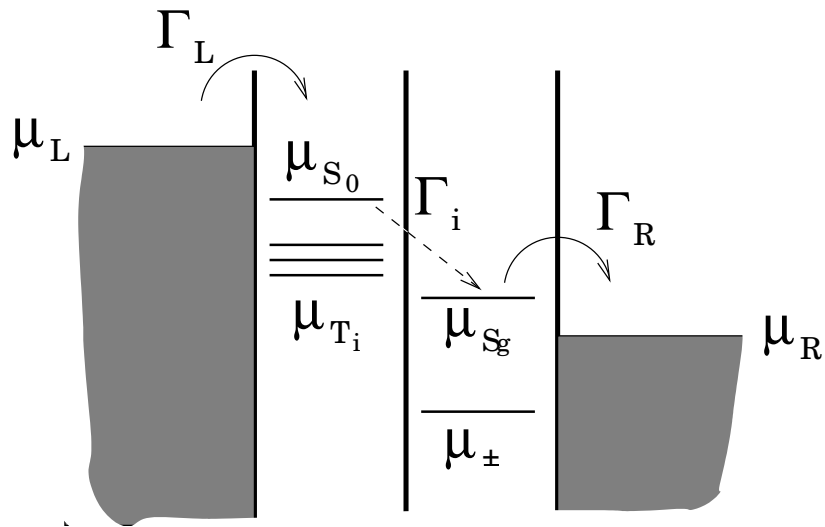


Figure 4.2: The energy diagram of the double dot system.

This is quite reasonable since the singlet and triplet states are not eigenstates when the magnetic field is inhomogeneous [20]. The matrix elements of Eq.

(4.13) between the singlet and triplet states are

$$[H_s]_{S_0T_1} = -[H_s]_{T_3S_0} = \frac{(K_{Ax} + iK_{Ay})}{2\sqrt{2}}, \quad [H_s]_{S_0T_0} = \frac{K_{Az}}{2} \quad (4.16)$$

and the matrix element between different triplet states are zero. The magnitude of the semiclassical fields is determined by $K_{L/R} \propto E_n N_{\text{QD}}^{-1/2}$ where $E_n \approx 0.135$ meV in GaAs and $N_{\text{QD}} \approx 10^6$ for the quantum dots in question [19].

4.3 Density matrix and average electron spin

In addition to the hyperfine coupling to nuclei the double dot system is coupled to a left and right lead, and also to a phonon bath. The coupling to the leads is represented by tunneling rates Γ_L and Γ_R , which are determined by the barrier transparency and the density of states at the Fermi energy in the leads. Since the energies of the two singlet states are not equal, some mechanism for inelastic scattering is required to facilitate the current. The most probable inelastic scattering mechanism is the phonon scattering. The inelastic scattering is taken into account by introducing the rate Γ_i that couples the (1, 1) and (0, 2) charge configuration states. At this point the spin structure of these states comes into play. Eqs. (4.7) and (4.8) represent only the leading contribution to the singlet eigenstates. In fact both states contain an additional admixture of each other, e.g. the (1, 1) singlet is

$$|\tilde{S}_0\rangle = |S_0\rangle + \frac{\sqrt{2}V_\tau}{E_{S_0} - E_{S_g}} |0; \uparrow\downarrow\rangle, \quad (4.17)$$

and the other singlet has a similar structure (the magnitude of the admixture is just the perturbation theory result, which is the ratio of the coupling strength and the energy separation). In other words, the (0, 2) singlet is only coupled to the (1, 1) singlet and none of the triplets. Thus any orbital scattering mechanism, e.g. phonons, will only couple the singlet states. The transport cycle is shown in Fig. 4.1. In this scenario a blocking of the current occurs as soon as one of the triplets is occupied, which occurs on a timescale $\propto \Gamma_L^{-1}$.

The density matrix approach is a very powerful method of describing the evolution of the double dot system. The full density matrix for the whole system is 49×49 which can be reduced to 19×19 by disregarding off-diagonal elements involving states $|S_g\rangle$ and $|\pm\rangle$. The justification for this is that the matrix elements between these state and the (1, 1) states involve exchanging electrons with the leads and thus all coherence is lost on a timescale $\propto \Gamma_R^{-1}$. Instead of writing the whole set of equations, it is more instructive to write a

few representative equations indicating the role of the off-diagonal elements

$$\frac{d\rho_{11}}{dt} = \frac{\Gamma_L}{2}\rho_{++} + \Im\{K_A^+\rho_{10}\} \quad (4.18a)$$

$$\begin{aligned} \frac{d\rho_{00}}{dt} &= -\Gamma_i\rho_{00} + \frac{\Gamma_L}{4}(\rho_{++} + \rho_{--}) \\ &\quad + \Im\{-K_A^+\rho_{10} + K_{Az}\rho_{20} + K_A^-\rho_{30}\} \end{aligned} \quad (4.18b)$$

$$\begin{aligned} \frac{d\rho_{10}}{dt} &= -i(w_{10} + i\frac{\Gamma_i}{2})\rho_{10} + \frac{1}{2}(-iK_A^-(\rho_{11}-\rho_{00}) \\ &\quad + iK_{Az}\rho_{12} + iK_A^+\rho_{13}), \end{aligned} \quad (4.18c)$$

where $w_{10} = \hbar^{-1}(E_1 - E_0)$ and the complex variable

$$K_A^+ = \frac{1}{\sqrt{2}}(K_{Ax} + iK_{Ay}) \quad (4.19)$$

has been introduced. The rates and the chemical potentials of the dot states and the leads are shown in Fig. 4.2. Note that the inelastic rate Γ_i does not appear in Eq. (4.18a), the same is true for the other triplets, but it is present in Eq. (4.18b) for the singlet. The inclusion of the off-diagonal term goes beyond the standard master-equation approach and will give rise to average electron spin not only in the z -direction but also the xy -plane. The set of equations in Eq. (4.18) are sometimes referred to as Bloch equations. The stationary solution $\hat{\rho}_{\text{St}}$ of Eq. (4.18) is obtained by ignoring the time dependence of \mathbf{K}_A . This is equivalent to treating the semiclassical field in the adiabatic approximation. The average electron spin in each dot is thus $\langle \hat{\mathbf{S}}_{L/R} \rangle = \text{Tr}\{\hat{\rho}_{\text{St}}\hat{\mathbf{S}}_{L/R}\}$. The energy scales that determine the stationary solution are the (1,1) singlet-triplet splitting $\Delta_{ST} = E_2 - E_0$ and the Zeeman splitting of the triplets $\Delta = E_3 - E_2$. The exact solutions for the average spin are too large to present here, so instead we present the leading order in K_A/Δ_{ST} which is the relevant expansion parameter

$$\langle S_{L/Rx} \rangle = \frac{\pm \frac{K_{Ax}}{2\Delta_{ST}}}{2(1+x_B^2) + |K_A^+|^2/(K_{Az})^2} \quad (4.20a)$$

$$\langle S_{L/Ry} \rangle = \frac{\pm \frac{K_{Ay}}{2\Delta_{ST}}}{2(1+x_B^2) + |K_A^+|^2/(K_{Az})^2} \quad (4.20b)$$

$$\langle S_{L/Rz} \rangle = \frac{-2x_B \pm \frac{K_{Az}}{2\Delta_{ST}} \frac{|K_A^+|^2}{(K_{Az})^2}}{2(1+x_B^2) + |K_A^+|^2/(K_{Az})^2}, \quad (4.20c)$$

where $x_B = \Delta/\Delta_{ST}$ and the current is given by

$$\frac{I}{e} = \frac{4\Gamma_i}{\left(1 + \frac{\Gamma_i^2}{\Delta_{ST}^2}\right) \left(\frac{\Delta_{ST}^2}{(K_{Az})^2} + \frac{2\Delta_{ST}^2}{|K_A^+|^2}\right) + x_B^2 \frac{2\Delta_{ST}^2}{|K_A^+|^2}}. \quad (4.21)$$

Note that the term proportional to x_B in the z -component of the spins is the dominant term, i.e. on average the electron spins point mainly in the direction of the applied field.

4.4 Nuclear system dynamics

Knowing the average electron spin in both the left and right dots allows us to write down the equation of motion of the effective nuclear magnetic field

$$\frac{d}{dt}\mathbf{K}_\alpha = \gamma_\alpha \langle \mathbf{S}_\alpha \rangle \times \mathbf{K}_\alpha + \gamma_{\text{GaAs}} \mathbf{B} \times \mathbf{K}_\alpha \quad (4.22)$$

where γ_{GaAs} is the effective gyromagnetic ratio of nuclei in GaAs and γ_α is determined by the hyperfine coupling and the quantum dot wave functions [17, 21]. The hyperfine coupling is assumed to be constant for all nuclei within a given dot. The details of the dynamics change when the coupling is made inhomogeneous but the timescale of the oscillations remains the same, see Chap. 5. The effect of introducing an inhomogeneous hyperfine coupling will be discussed later in the paper.

There are 6 equations of motion and at least 2 integrals of motion, i.e. the square moduli \mathbf{K}_α^2 and in the following discussion we try to identify more to simplify the dynamics. Since the average spins are known functions of \mathbf{K}_α then Eq. (4.22) constitutes a set of autonomous differential equation whose solution will determine the time dependence of the coupling strength \mathbf{K}_A . We will proceed along two parallel paths in solving these equations of motion. Firstly we will use the approximate expressions for the electron spin in Eq. (4.20) which allow us to express the period of the motion as a single integral which we solve numerically. The other approach is to use the full solution for the average spin and use a numerical method to obtain an approximate solution of the equations of motion in Eqs. (4.22).

4.4.1 Integrals of motion

It is possible to simplify the equations of motion in Eq. (4.22) using the approximate solution for the average electron spin. As a first step new variables are introduced, in a similar fashion as in Eq. (4.19), for each $\alpha = L, R$

$$K_\alpha^+ \equiv \frac{K_{\alpha x} + iK_{\alpha y}}{\sqrt{2}} \quad (4.23)$$

and subsequently the equations of motion in Eq. (4.22) become

$$\frac{dK_\alpha^+}{dt} = i\gamma_\alpha \langle S_{\alpha z} \rangle K_\alpha^+ - i\gamma_\alpha \langle S_\alpha^+ \rangle K_{\alpha z} + i\gamma_{\text{GaAs}} B K_\alpha^+ \quad (4.24)$$

$$\frac{dK_{\alpha z}}{dt} = i\gamma_\alpha (\langle S_\alpha^- \rangle K_\alpha^+ - \langle S_\alpha^+ \rangle K_\alpha^-) \quad (4.25)$$

Note that the x and y components of the original equations have been incorporated into a single equation, Eq. (4.23), for a complex variable. It is also convenient to introduce a parameterization of K_α^+ and $K_{\alpha z}$ which explicitly

incorporate the known integrals of motion. One choice would be to write \mathbf{K}_α in spherical coordinates but it turns out that cylindrical coordinates are better suited since retaining the z components will turn out to be useful later on. The xy components of the semiclassical fields are written in polar coordinates

$$K_{\alpha x} = \sqrt{K_\alpha^2 - K_{\alpha z}^2} \cos \phi_\alpha \quad (4.26)$$

$$K_{\alpha y} = \sqrt{K_\alpha^2 - K_{\alpha z}^2} \sin \phi_\alpha. \quad (4.27)$$

Note that this parameterization ensures a constant K_α^2 , and the number of dynamical variables is 4. Writing the variables in Eq. (4.23) in terms of the polar coordinates gives

$$K_\alpha^+ = \frac{1}{\sqrt{2}} \sqrt{K_\alpha^2 - K_{\alpha z}^2} e^{i\phi_\alpha} \quad (4.28)$$

and its time derivative is

$$\frac{dK_\alpha^+}{dt} = iK_\alpha^+ \frac{d\phi_\alpha}{dt} + \frac{K_{\alpha z} K_\alpha^+}{K_\alpha^2 - K_{\alpha z}^2} \frac{dK_{\alpha z}}{dt}. \quad (4.29)$$

Using Eqs. (4.24) and (4.28) to get rid of K_α^\pm we get, after some manipulation, the following equations of motion

$$\frac{d\phi_L}{dt} = \gamma_L \frac{-2x_B + \frac{K_{Az}}{2\Delta_{ST}} \frac{|K_A^+|^2}{K_{Az}^2} - \frac{K_{Lz}}{\Delta_{ST}} \left(1 + \frac{\sqrt{K_R^2 - K_{Rz}^2}}{\sqrt{K_L^2 - K_{Lz}^2}} \cos(\phi) \right)}{2(1+x_B^2) + |K_A^+|^2/K_{Az}^2} + \gamma_{\text{GaAs}} B \quad (4.30)$$

$$\frac{dK_{Lz}}{dt} = -\frac{\gamma_L}{2} \frac{\sqrt{K_R^2 - K_{Rz}^2} \sqrt{K_L^2 - K_{Lz}^2}}{2(1+x_B^2) + |K_A^+|^2/K_{Az}^2} \sin \phi \quad (4.31)$$

$$\frac{d\phi_R}{dt} = \gamma_R \frac{-2x_B - \frac{K_{Az}}{2\Delta_{ST}} \frac{|K_A^+|^2}{K_{Az}^2} - \frac{K_{Rz}}{\Delta_{ST}} \left(1 + \frac{\sqrt{K_L^2 - K_{Lz}^2}}{\sqrt{K_R^2 - K_{Rz}^2}} \cos(\phi) \right)}{2(1+x_B^2) + |K_A^+|^2/K_{Az}^2} + \gamma_{\text{GaAs}} B \quad (4.32)$$

$$\frac{dK_{Rz}}{dt} = \frac{\gamma_R}{2} \frac{\sqrt{K_R^2 - K_{Rz}^2} \sqrt{K_L^2 - K_{Lz}^2}}{2(1+x_B^2) + |K_A^+|^2/K_{Az}^2} \sin \phi. \quad (4.33)$$

where the polar angle difference

$$\phi = \phi_L - \phi_R \quad (4.34)$$

has been introduced. The right hand sides of the preceding equations contain term $|K_A^+|^2$, which in terms of the new cylindrical variables is

$$|K_A^+|^2 = \frac{1}{2} \left(K_L^2 - K_{Lz}^2 + K_R^2 - K_{Rz}^2 - 2\sqrt{K_L^2 - K_{Lz}^2} \sqrt{K_R^2 - K_{Rz}^2} \cos(\phi) \right).$$

$$(4.35)$$

Note that $|K_A^+|$ only depends on ϕ_L and ϕ_R through their difference ϕ . On inspection it is apparent from Eqs. (4.31) and (4.33) that

$$\frac{d}{dt} \left(\frac{K_{Lz}}{\gamma_L} + \frac{K_{Rz}}{\gamma_R} \right) = 0 \quad (4.36)$$

from which a third integral of motion can be defined as

$$K_{S_z} = \frac{\gamma_L \gamma_R}{\gamma_L + \gamma_R} \left(\frac{K_{Lz}}{\gamma_L} + \frac{K_{Rz}}{\gamma_R} \right). \quad (4.37)$$

To reduce the number of dynamical variables further it is necessary to separate fast term from slow ones. To this end the sum of the polar angles is introduced

$$\Phi = \phi_L + \phi_R. \quad (4.38)$$

In the right hand side of Eqs. (4.30) and (4.32) the precession rate due to the external field γ_{GaAs} is much larger than the terms proportional to $\gamma_{L/R}$, for the magnetic fields used in the experiment. Thus, the equation of motion may be approximated as

$$\frac{d\Phi}{dt} \approx \gamma_{\text{GaAs}} B \quad (4.39)$$

and thus Φ has effectively been decoupled from the other equations of motion since it does not appear in anywhere on the right hand side of Eqs. (4.30)-(4.33). Finally, the terms that depend on K_{Lz} and K_{Rz} can be rewritten in term of the integral of motion in Eq. (4.37) and K_{Az}

$$K_{Lz} = K_{S_z} + \frac{\gamma_L}{\gamma_L + \gamma_R} K_{Az} \quad (4.40)$$

$$K_{Rz} = K_{S_z} - \frac{\gamma_R}{\gamma_L + \gamma_R} K_{Az}. \quad (4.41)$$

At this point is worthwhile to summarize the the results from the above manipulations. Initially there were 6 equations of motion with 2 known integrals of motion. These integrals of motion were incorporated into the parameterization in Eq. (4.28). The number of variables was further reduced by identifying a new integral of motion K_{S_z} and assuming a fast rotation in Eq. (4.38). This leaves us with only two independent variables K_{Az} and ϕ . It is also important that the current depends on these variables only. This means that determining the dynamics of K_{Az} and ϕ will give the time dependence of the current.

Let us now write the equation of motion for the two remaining variables in the form

$$\frac{dK_{Az}}{dt} = \frac{a(K_{Az}) \sin \phi}{b(K_{Az}) - \cos \phi} \quad (4.42)$$

$$\frac{d\phi}{dt} = \frac{c(K_{Az}) - f(K_{Az}) \cos \phi}{b(K_{Az}) - \cos \phi} \quad (4.43)$$

where the functions a, b, c and f are determined by straightforward manipulation of Eqs. (4.30)-(4.33), resulting in

$$a(K_{Az}) = -\frac{(\gamma_L + \gamma_R)K_{Az}^2}{2\Delta_{ST}} \quad (4.44)$$

$$b(K_{Az}) = \frac{2(x_B + 1)K_{Az}^2}{\sqrt{K_L^2 - K_{Lz}^2}\sqrt{K_R^2 - K_{Rz}^2}} + \frac{1}{2} \left(\frac{\sqrt{K_R^2 - K_{Rz}^2}}{\sqrt{K_L^2 - K_{Lz}^2}} + \frac{\sqrt{K_L^2 - K_{Lz}^2}}{\sqrt{K_R^2 - K_{Rz}^2}} \right) \quad (4.45)$$

$$c(K_{Az}) = -\left((\gamma_L - \gamma_R)2x_B + \frac{\gamma_L K_{Lz}}{\Delta_{ST}} - \frac{\gamma_R K_{Rz}}{\Delta_{ST}} \right) \frac{K_{Az}^2}{\sqrt{K_L^2 - K_{Lz}^2}\sqrt{K_R^2 - K_{Rz}^2}} + \frac{(\gamma_L + \gamma_R)K_{Az}}{4\Delta_{ST}} \left(\frac{\sqrt{K_R^2 - K_{Rz}^2}}{\sqrt{K_L^2 - K_{Lz}^2}} + \frac{\sqrt{K_L^2 - K_{Lz}^2}}{\sqrt{K_R^2 - K_{Rz}^2}} \right) \quad (4.46)$$

$$f(K_{Az}) = \frac{(\gamma_L + \gamma_R)K_{Az}}{2\Delta_{ST}} + \frac{K_{Az}^2}{2\Delta_{ST}} \left(\frac{\gamma_L K_{Lz}}{K_L^2 - K_{Lz}^2} + \frac{\gamma_R K_{Rz}}{K_R^2 - K_{Rz}^2} \right), \quad (4.47)$$

where $K_{L/Rz}$ depends on K_{Az} through Eqs. (4.40) and (4.41).

The asymmetry in the precession frequencies $\Delta\gamma = \gamma_L - \gamma_R$ only appears in the function $c(K_{Az})$. Even if $\Delta\gamma/\gamma_\alpha \ll 1$ it can still be large compared to the other important scale K_L/Δ_{ST} . To emphasize this a dimensionless measure of the asymmetry is defined as

$$\epsilon = \frac{\gamma_L - \gamma_R}{2\gamma} \frac{\Delta_{ST}}{K_L}, \quad (4.48)$$

where $2\gamma = (\gamma_L + \gamma_R)$. The ϵ parameter is important since depending on whether it is larger, or smaller, than 1 strongly affects the dynamics and the period of the resulting solution.

The form of Eqs. (4.42) and (4.43) suggest that it is possible to further reduce the problem. To proceed we introduce the function

$$\mathcal{L}(K_{Az}, \phi) = X(K_{Az}) + Y(K_{Az}) \cos \phi. \quad (4.49)$$

The function \mathcal{L} can be made an integral of motion by requiring that its time derivative vanishes

$$\frac{d\mathcal{L}}{dt} = \frac{dX}{dK_{Az}} \frac{dK_{Az}}{dt} + \frac{dY}{dK_{Az}} \frac{dK_{Az}}{dt} \cos \phi - Y \frac{d\phi}{dt} \sin \phi \quad (4.50)$$

$$= \left(a(K_{Az}) \frac{dX}{dK_{Az}} - c(K_{Az})Y \right) \cos \phi + \left(a(K_{Az}) \frac{dY}{dK_{Az}} - f(K_{Az})Y \right) \cos \phi \sin \phi = 0. \quad (4.51)$$

The quantities in both the parentheses need to vanish which results in the

following equations for X and Y

$$Y(x) = \exp\left(\int^x du \frac{f(u)}{a(u)}\right) \quad (4.52)$$

$$X(x) = \int^x du Y(u) \frac{c(u)}{a(u)}. \quad (4.53)$$

It turns out that these integrals can be solved analytically using Eqs. (4.44), (4.46) and (4.47). The resulting functions are

$$X(k_z) = -\frac{1^2 + k_R^2 - 2k_{S_z}^2}{2} k_z + 2\epsilon x_B k_z^2 + \frac{1}{4} \left(1 + \left(\frac{\Delta\gamma}{2\gamma}\right)^2\right) k_z^3 \quad (4.54)$$

$$Y(k_z) = k_z \sqrt{1 - \left(k_{S_z} + \frac{\gamma_L}{2\gamma} k_z\right)} \sqrt{k_R^2 - \left(k_{S_z} - \frac{\gamma_R}{2\gamma} k_z\right)} \quad (4.55)$$

where $k_z = K_{Az}/K_L$ and other small caps k -variables are measured in units of K_L .

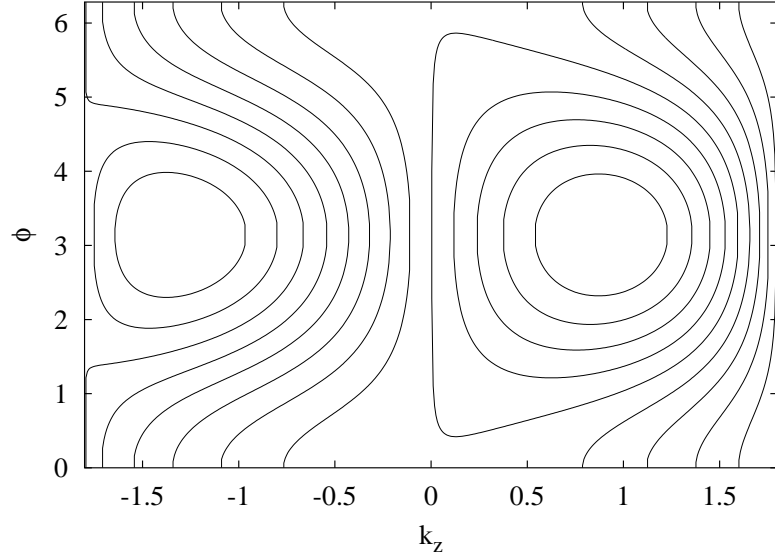


Figure 4.3: The phase space plot for different values of the integral of motion L , with $\epsilon=0.1$, $x_B = 1.2$ and $k_{S_z} = 0$.

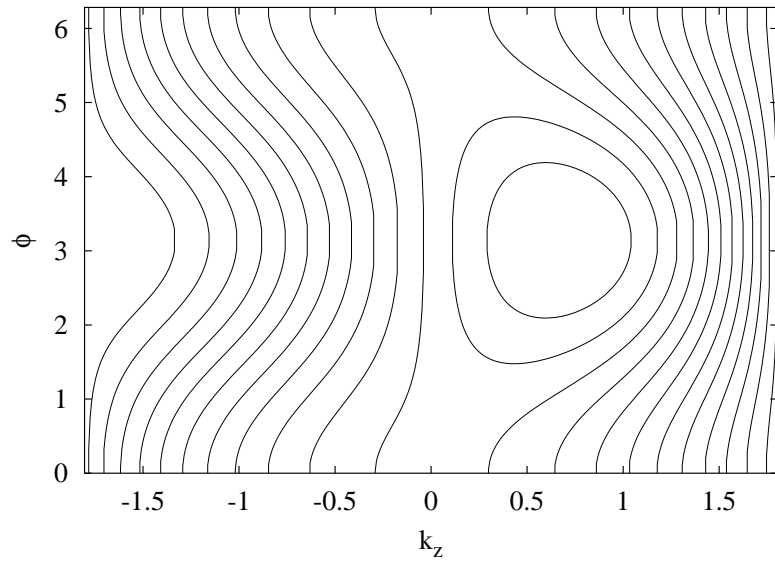


Figure 4.4: The phase space plot for different values of the integral of motion L , with $\epsilon=0.25$, $x_B = 1.2$ and $k_{S_z} = 0$.

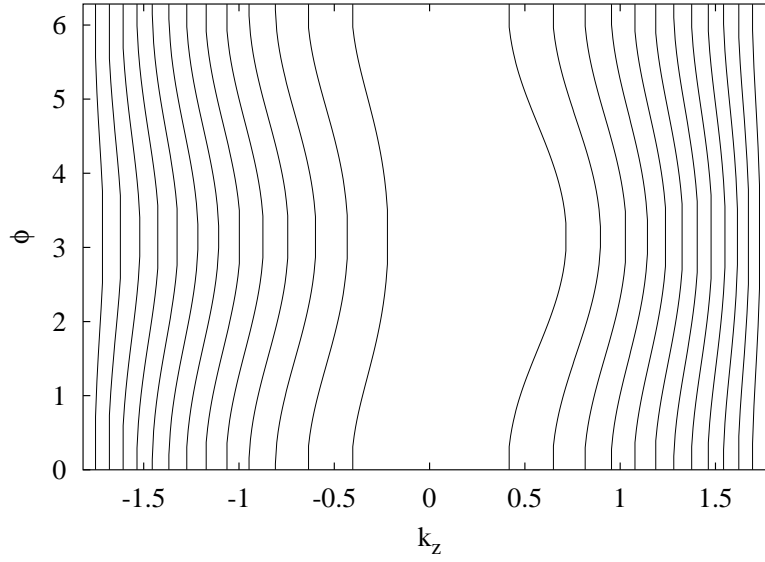


Figure 4.5: The phase space plot for different values of the integral of motion L , with $\epsilon=1.0$, $x_B = 1.2$ and $k_{S_z} = 0$.

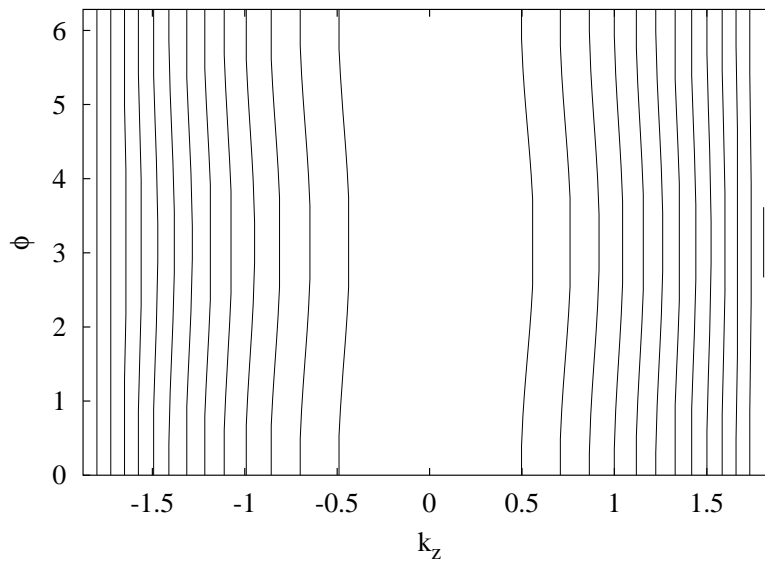


Figure 4.6: The phase space plot for different values of the integral of motion L , with $\epsilon=4.0$, $x_B = 1.2$ and $k_{S_z} = 0$.

For a given value of L , the (k_z, ϕ) phase space trajectory is determined by $\mathcal{L}(k_z, \phi) = L$. In Fig. 4.3-4.6 the possible trajectories are plotted for various values of the integral of motion L . From figure to figure, the value of the asymmetry ϵ changes. When $\epsilon \rightarrow 0$ it becomes an irrelevant parameter, see Eq. (4.54), and so Fig. 4.3 is a good representation for $\epsilon \lesssim 0.1$. When the asymmetry increases, the phase space plots change and for a large value of $\epsilon = 4.0$ the motion is reminiscent of a magnetic moment in constant magnetic field along the z -axis. This is to be expected since when $\epsilon \gg 1$ precession around the large constant term in $\langle \hat{S}_{L/Rz} \rangle$ dominates the motion.

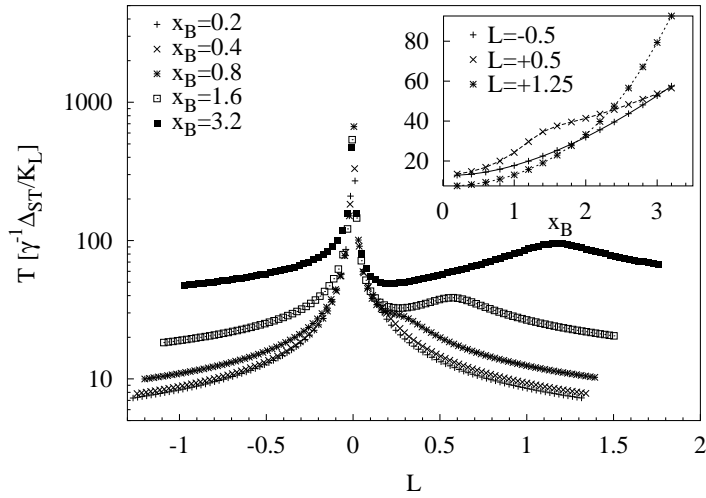


Figure 4.7: The period as a function the integral of motion L for for $\epsilon=0.1$ and various values of x_B .

Using Eqs. (4.42) and (4.43), which gives the ‘velocity’ at each point of the trajectory, the period can be determined using

$$T = 2 \int_{k_-}^{k_+} dx \left(\frac{dk_{Az}}{dt}(x) \right)^{-1}, \quad (4.56)$$

where k_- and k_+ are the turning points of the trajectory in question. A similar equation for $d\phi/dt$ is can also be used. The period is obtained by numerical integration of Eq. (4.56) with the turning points obtained from Eq. (4.49). In Fig. 4.7 the period is plotted as a function of the integral of motion L . The corresponding phase space trajectories are plotted in 4.3. The period diverges at $L = 0$ since these solutions involve $k_z \rightarrow 0$, where the velocity goes to zero. Away from $L = 0$, the T is in the range 10-100, measured in units of $\gamma^{-1} \Delta_{ST} / K_L$. The resulting numerical value of the period is $\approx 1 - 10$ second

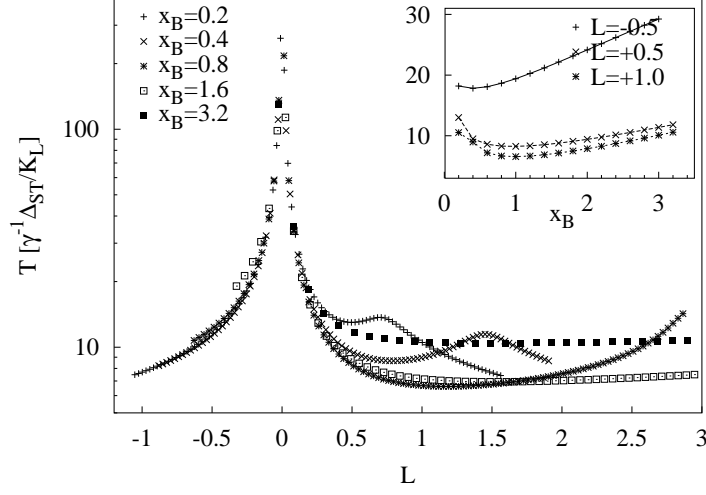


Figure 4.8: The period as a function the integral of motion L for for $\epsilon=1.0$ and various values of x_B .

for $\gamma^{-1}\Delta_{ST}/K_L \approx 0.01 - 0.1$ sec. Thus the period is quite long, approaching seconds and even above that.

Similar data for the period when $\epsilon = 1.0$ is shown in Fig. 4.8. Note that the period is decreased in comparison to the $\epsilon = 0.1$ case. We cannot *a priori* determine the value of the asymmetry since it is determined by sample quality and fabrication errors. The value of ϵ is extracted from experimental data through the magnetic field, or x_B , behavior of the period. The insets of Figs. 4.7 and 4.8 show the x_B dependence for some fixed values of L . For $\epsilon = 0.1$ there is a monotonic increase of T with x_B but for the the larger asymmetry $\epsilon = 1.0$ the behavior is non-monotonic with a minimum around $x_B \lesssim 1$. This reflects that the period for large asymmetry is

$$T(\epsilon \gg 1) \propto \frac{(x_B^2 + 1) + \text{const}}{x_B \epsilon}. \quad (4.57)$$

Note the $1/\epsilon$ dependence which reduces the period. For low asymmetry the period behaves as

$$T(\epsilon \ll 1) \propto (x_B^2 + 1) + \text{const}. \quad (4.58)$$

The different x_B dependence of the period observed in the experiment should indicate whether the asymmetry is large or small.

4.4.2 Numerical integration

The initial values of \mathbf{K}_α are unknown since they depend on the microscopic state of the nuclear system initially. The initial condition should be randomly chosen from a Gaussian ensemble [19]. Different realizations of initial conditions give different dynamics, but as long as they do not correspond to L too close to zero they give periods which are comparable. In Fig. 4.9 the current, see Eq. (4.21), is plotted for various initial conditions but fixed $\epsilon = 0.1$ and $x_B = 1.6$. The inset shows calculations where the semiclassical fields \mathbf{K}_α are split into N_b blocks, each with a different precession frequency due to the position dependent hyperfine coupling. These calculations show that even for many blocks the long period motion persists but there are additional fast oscillation on the timescale of γ^{-1} which we have averaged over before plotting them. Note that even including

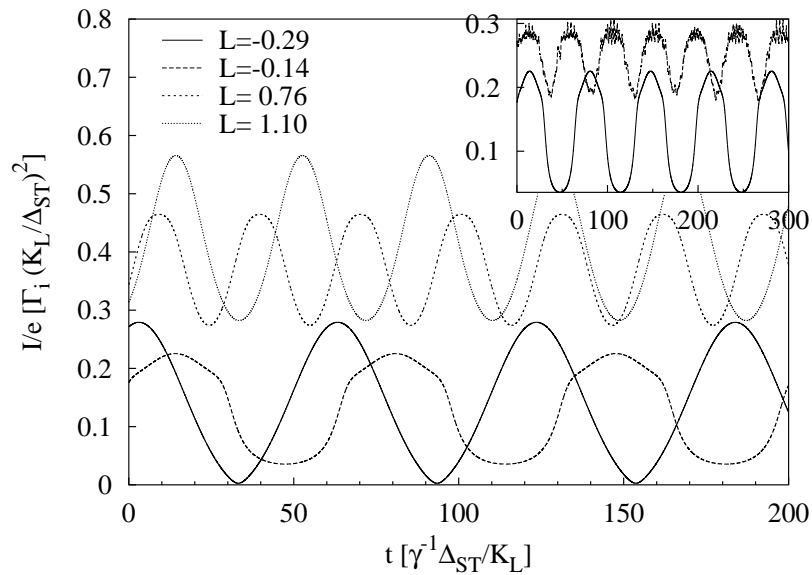


Figure 4.9: The current shown as a function of time for $\epsilon=0.1$, $x_B=1.6$, but for different initial conditions, i.e. different L . The inset current as a function of time for $L = -0.14$ and $N_b=1$ and 25, where N_b is the number of blocks.

the inhomogeneous coupling the coherent oscillations persist. The details of the dynamics change, i.e. fast oscillation appear, but the slow dynamics remain and, most importantly, no relaxation of the current is observed.

4.5 Conclusions

In conclusion, we have proposed a novel transport mechanism which leads to an oscillating current, whose period is proportional to $\gamma^{-1}\Delta_{ST}/K_L$. For low asymmetry and high magnetic fields x_B the period can become quite large. Some of our model parameters are not well known so the numerical value of the period is not quite certain, although it should lie in the range 0.1-10 sec. The asymmetry plays an important role in determining the dynamics of the system. Due to the different magnetic field dependence of the period depending on whether the asymmetry is large or small, it should be possible to determine from experimental data in which regime ϵ lies. For small ϵ the period increased monotonically with magnetic field. This seems to be consistent with the experimental data, which indicates that the asymmetry is not so large in the sample used. Indeed, this might be expected since the two dots are nominally identical [13]. Taking into account inhomogeneous hyperfine coupling does not destroy the long period oscillations although it introduces additional short period motion.

References

- [1] D. Paget and V. L. Berkovits, in *Optical Orientation*, edited by F. Meier and B. P. Zakharchenya (North-Holland, Amsterdam, 1984).
- [2] D. Paget, G. Lampel, B. Sapoval, and V. I. Safarov, *Phys. Rev. B* **15**, 5780 (1977).
- [3] G. Salis *et al.*, *Phys. Rev. Lett.* **86**, 2677 (2001).
- [4] G. Salis, D. D. Awschalom, Y. Ohno, and H. Ohno, *Phys. Rev. B* **64**, 195304 (2001).
- [5] K. R. Wald *et al.*, *Phys. Rev. Lett.* **73**, 1011 (1994).
- [6] J. H. Smet *et al.*, *Nature* **415**, 281 (2002).
- [7] R. K. Kawakami *et al.*, *Science* **294**, 131 (2001).
- [8] T. Machida, T. Yamazaki, K. Ikushima, and S. Komiyama, *App. Phys. Lett.* **82**, 409 (2003).
- [9] L. P. Kouwenhoven *et al.*, in *Mesoscopic Electron Transport, NATO Series*, edited by L. L. Sohn, L. P. Kouwenhoven, and G. Schoen (Kluwer, Dordrecht, 1997), Chap. Electron transport in quantum dots, p. 105.
- [10] L. P. Kouwenhoven, D. G. Austing, and S. Tarucha, *Rep. Prog. Phys.* **64**, 701 (2001).
- [11] S. DeFranceschi *et al.*, *Phys. Rev. Lett.* **86**, 878 (2001).
- [12] H. Matsuoka and S. Kimura, *Jpn. J. Appl. Phys.* **34**, 1326 (1995).

- [13] K. Ono and S. Tarucha, (unpublished).
- [14] K. Ono, D. G. Austing, Y. Tokura, and S. Tarucha, *Science* **297**, 1313 (2002).
- [15] D. Weinman, W. Häussler, and B. Kramer, *Phys. Rev. Lett.* **74**, 984 (1995).
- [16] M. Ciorga *et al.*, *App. Phys. Lett.* **80**, 2177 (2002).
- [17] I. A. Merkulov, A. L. Efros, and M. Rosen, *Phys. Rev. B* **65**, 205309 (2002).
- [18] M. I. D'yakonov and V. Y. Kachorovskii, *Sov. Phys. Semicond.* **20**, 110 (1986).
- [19] S. I. Erlingsson and Y. V. Nazarov, *Phys. Rev. B* **66**, 155327 (2002).
- [20] R. Sousa, X. Hu, and S. D. Sarma, *Phys. Rev. A* **64**, 43207 (2001).
- [21] S. I. Erlingsson and Y. V. Nazarov, (in preparation).

Chapter 5

Time-evolution of the effective nuclear magnetic field due to a localized electron spin

Sigurdur I. Erlingsson, Yuli V. Nazarov

An effective spin Hamiltonian is considered where the spatial dependence of the electron wavefunction results in an inhomogeneous hyperfine coupling of the electron spin to different nuclear spins. A semiclassical description of the nuclear spin system is introduced which also takes into account the inhomogeneous coupling. Using that the electron spin dynamics are much faster than for the nuclear spins, an approximate solution for dynamics of the nuclear system is obtained. From this solution certain electron spin correlation functions are calculated. Contrary to what one may guess, the dynamics are not chaotic and the correlation functions show no decay in time, only complicated oscillations. This may be attributed to the fact that the system has many integrals of motion and that it is close to exactly solvable.

5.1 Introduction

The coherent manipulation of localized spins in solid state systems is currently a very active field research. Studying such systems may lead to new insight regarding fundamental questions, e.g. the measurement problem in quantum mechanics and limitations on control of such systems due to environmental effects. There are also possible applications in which conventional electronics is used in combination with spin manipulation. This field of research is commonly referred to as spintronics. One of the most ambitious goals in this field of research is developing a quantum bit, or qubit. Such qubits would form the basic building blocks of the quantum computer. Building a qubit in solid state systems is advantageous since fabrication techniques are very advanced and scaling the number of qubits is straightforward, at least in theory. However, environmental effects are much stronger in comparison with systems based on NMR or trapped ions (which lack scalability). The qubit should be any (quasi) two level system in which the strength of the coupling to the environment can be sufficiently well controlled so that the residual environmental interactions are below a threshold set by the operating speed of the device [1–3]. The benefit of working with individual spins is that they are natural two level systems and the spin is less susceptible to environmental effects. There are two timescales, socalled T_1 and T_2 , which are used to characterize the quality of the qubit. These terms are borrowed from the NMR community which have been using them long before anyone thought of the qubit [4, 5]. The lifetime of a certain state of the qubit, or energy relaxation time, is determined by T_1 while T_2 gives the decoherence time.

Since the first proposal [6], the qubit candidate based on localized electron spins in quantum dots has been the subject of many theoretical and experimental studies. This system, and any other, has to fulfill some strict criteria to be a viable qubit, the most difficult to realize being long relaxation and decoherence times. There already have been quite a few studies of the relaxation time of electron spins in GaAs (which seems to be the most relevant material) quantum dots [7–11] for various different spin-flip mechanisms and they all give very long relaxation times. The operation of a qubit requires making a superposition of states that persists during the decoherence time. A few papers have addressed the question of the decoherence time of electron spin in GaAs quantum dots [12–17]. It was suggested in the literature that the most important source for decoherence of electron spins in GaAs quantum dots would be hyperfine coupling to the surrounding nuclei. In Ref. [12] the characteristic timescale for the decay of a specific correlation function was associated with the decoherence time of the electron spin. The decoherence in this case was due to the spatially dependent hyperfine coupling constant which caused small frequency changes through flip-flop processes involving spatially separated nuclei. A different approach was

used in Ref. [13] which focused on developing an effective magnetic field acting on the electron spin due to the total nuclear spin system. The authors were interested in ensemble averaged quantities and so they averaged over all possible initial configurations of the effective nuclear field.

In this work we will try to bridge between these two approaches, i.e. we will further develop the idea of the effective magnetic field due to the nuclear system acting on the electron spin in the quantum dot [10] including the effects of the spatially varying hyperfine coupling constant. The dynamics of the system will be represented by a set of equations of motion for the electron spin and the various subsystem of nuclei which are defined in such a way that the coupling to the electron spin is the same for all the nuclei within a subsystem. Due to the large difference of timescales for the electron and nuclear spin systems we are able to solve the problem in two steps. In the first step we establish that the nuclear system can be treated as an adiabatic effective nuclear magnetic field acting on the electron. The latter step involves the backaction of the electron spin which will determine the evolution of the nuclear spins.

5.2 Hyperfine interaction in quantum dots

The Hamiltonian describing the hyperfine coupling between conduction band electrons and the lattice nuclei in GaAs is of the well known form of the contact potential

$$H_{\text{HF}} = A\hat{\mathbf{S}} \cdot \sum_k \hat{\mathbf{I}}_k \delta(\mathbf{r} - \mathbf{R}_k). \quad (5.1)$$

In the GaAs conduction band (which is mainly composed of s -orbitals), the dipole-dipole part of the hyperfine interaction vanishes [18]. The quantum dots considered here are quite general, but we introduce some restrictions to simplify the model. First of all it is assumed that the number of electrons is fixed, preferably to one. From the experimental point of view this assumption is quite reasonable since having only a single electron in the dot has already been demonstrated [19, 20]. Also, by pinching off the connection to the leads the electron number should remain fixed over very long timescales. It can also be argued that our treatment applies for odd number of electron since the ground state should be a doublet. The second assumption is that the orbital level splitting is the largest energy scale of the system. In this case the hyperfine Hamiltonian can be projected to the lowest orbital level since contributions from higher orbitals are strongly suppressed due the large orbital energy separation. If the ground state orbital $\psi(\mathbf{r})$ of the the quantum dot is known, then an effective spin Hamiltonian can be written as

$$H_s = g\mu_B \mathbf{B} \cdot \hat{\mathbf{S}} + \gamma_{\text{GaAs}} \sum_k \mathbf{B} \cdot \hat{\mathbf{I}}_k + \sum_k A |\psi(\mathbf{R}_k)|^2 \hat{\mathbf{S}} \cdot \hat{\mathbf{I}}_k \quad (5.2)$$

where \mathbf{B} is the external applied field and the hyperfine interaction has been projected onto the lowest orbital.

5.3 Semiclassical dynamics

The fact that the single electron spin is coupled to a large number of nuclei but each nucleus is only coupled to the single electron spin hints at an asymmetry in the behavior of the electron and nuclear spins. Indeed the electron precesses in an effective nuclear magnetic field which is due to the whole nuclear spin system. This field is $\propto \sqrt{N_{\text{QD}}}$ times larger than the corresponding hyperfine field caused by the single electron spin in which the nuclear spins precess. Thus the dynamics of the electron are much faster than the dynamics of the nuclei. Also, the large number of nuclei involved makes it possible to treat the nuclear system in a semiclassical way [10, 13, 21]. In the following section we discuss the origin of the different dynamical timescales involved in the problem and we introduce a semiclassical approximation to the dynamics of the system.

The Hamiltonian in Eq. (5.1) describes the coupling of a single electron spin to many nuclear spins. The actual number is determined by the confinement of the electron, i.e. the number of nuclei the electron is coupled to is proportional to the volume that the electron occupies. In a typical quantum dot a single electron spin may be coupled to 10^6 nuclear spins. When the electrons interacts with so many (independent) nuclei it is possible to interpret the combined effect of the nuclei as an effective magnetic field .

The last term in Eq. (5.2) represents the coupling of the electron spin and the nuclear system through the hyperfine interaction. By introducing the operator of the nuclear magnetic field

$$\hat{\mathbf{K}} = \sum_k A |\psi_0(\mathbf{R}_k)|^2 \hat{\mathbf{I}}_k, \quad (5.3)$$

the hyperfine coupling can be written as

$$H_{\text{HF}} = \hat{\mathbf{S}} \cdot \hat{\mathbf{K}}. \quad (5.4)$$

Before proceeding further it is convenient to introduce a different way of writing Eq. (5.3). The wavefunction of the ground state orbital has some characteristic spatial extent which is determined by the confining potential. Without loss of generality it may be assumed that the lateral and transverse confining lengths are ℓ and z_0 respectively. The volume of the quantum dot is the defined as

$$V_{\text{QD}} = \pi z_0 \ell^2. \quad (5.5)$$

Let us define a dimensionless function

$$f(\mathbf{R}_k) = V_{\text{QD}} |\psi(\mathbf{R}_k)|^2. \quad (5.6)$$

Furthermore, denoting the maximum value of f with f_{Max} we introduce a dimensionless coupling constant

$$g_k = g(\mathbf{R}_k) = \frac{f(\mathbf{R}_k)}{f_{\text{Max}}}. \quad (5.7)$$

The hyperfine coupling constant expressed in terms of the concentration, C_n , of nuclei with spin I and a characteristic energy E_n is

$$A = \frac{E_n}{C_n I}. \quad (5.8)$$

The energy E_n is the maximum Zeeman splitting possible due to a fully polarized nuclear system, its value being $E_n \approx 0.135$ meV in GaAs [22, 23]. The nuclear system operator can then be written as

$$\hat{\mathbf{K}} = A \sum_k \frac{f(\mathbf{R}_k)}{V_{\text{QD}}} \hat{\mathbf{I}}_k \quad (5.9)$$

$$= \frac{A f_{\text{Max}}}{V_{\text{QD}}} \sum_k g_k \hat{\mathbf{I}}_k \quad (5.10)$$

$$= \frac{E_n f_{\text{Max}}}{N_{\text{QD}} I} \sum_k g_k \hat{\mathbf{I}}_k \quad (5.11)$$

where $N_{\text{QD}} = C_n V_{\text{QD}}$ is the effective number of nuclei in the dot. The operator defined in Eq. (5.11) represents combined contributions from many independent spins. For a typical unpolarized nuclear system the average squared modulus can be estimated as

$$\begin{aligned} \langle \hat{\mathbf{K}}^2 \rangle &= \frac{(E_n f_{\text{Max}})^2}{(N_{\text{QD}} I)^2} \sum_{kk'} g_k g_{k'} \langle \hat{\mathbf{I}}_k \cdot \hat{\mathbf{I}}_{k'} \rangle \\ &= \frac{(E_n f_{\text{Max}})^2}{N_{\text{QD}} I^2} \frac{1}{N_{\text{QD}}} \sum_k g_k^2 I(I+1) \\ &= \frac{E_n^2}{N_{\text{QD}}} \frac{I(I+1) f_{\text{Max}}^2 \overline{g^2}}{I^2}. \end{aligned} \quad (5.12)$$

where the average squared coupling strength is

$$\overline{g^2} = \frac{1}{N_{\text{QD}}} \sum_k g^2(\mathbf{R}_k). \quad (5.13)$$

It is important to note that $\sqrt{\langle \hat{\mathbf{K}}^2 \rangle} \propto E_n N_{\text{QD}}^{-1/2}$ and that this field acts on the electron spin even in the absence of polarization in the nuclear system. As was shown in Ref. [10] the typical fluctuations in the components of $\hat{\mathbf{K}}$ are

$$\Delta K^\alpha \Delta K^\beta \gtrsim \langle \hat{\mathbf{K}}^2 \rangle \frac{1}{N_{\text{QD}}^{1/2}}. \quad (5.14)$$

This means that as long as $N_{\text{QD}} \gg 1$ the operator in Eq. (5.11) can be replaced by a classical vector whose length is determined by Eq. (5.12). The actual value of \mathbf{K} is completely random since it is determined by unknown details of the nuclear system. The value of the effective nuclear field should be chosen from a Gaussian distribution [10, 13]

$$P(\mathbf{K}) = \left(\frac{1}{2\pi\sigma^2} \right)^{3/2} \exp\left(-\frac{\mathbf{K}^2}{2\sigma^2}\right), \quad (5.15)$$

where $\sigma^2 = \frac{1}{3}\langle \mathbf{K}^2 \rangle$ is the variance of the distribution.

Let us now turn to the dynamics of the combined electron and nuclear spins. The dynamics of both are determined by the Heisenberg equation of motion

$$\frac{d}{dt}\hat{\mathbf{S}} = \hat{\mathbf{K}} \times \hat{\mathbf{S}} + g\mu_B \mathbf{B} \times \hat{\mathbf{S}} \quad (5.16)$$

$$\frac{d}{dt}\hat{\mathbf{I}}_k = \frac{E_n f_{\text{Max}}}{N_{\text{QD}}} g_k \hat{\mathbf{S}} \times \hat{\mathbf{I}}_k + \gamma_{\text{GaAs}} \mathbf{B} \times \hat{\mathbf{I}}_k. \quad (5.17)$$

Multiplying Eq. (5.17) with g_k and summing over k gives the equation of motion for $\hat{\mathbf{K}}$

$$\frac{d}{dt}\hat{\mathbf{K}} = \frac{E_n f_{\text{Max}}}{N_{\text{QD}}} \hat{\mathbf{S}} \times \left(\sum_k g_k^2 \hat{\mathbf{I}}_k \right) + \gamma_{\text{GaAs}} B \mathbf{n}_B \times \hat{\mathbf{K}} \quad (5.18)$$

In contrast to the simple dynamics of the electron spin, the equation of motion for $\hat{\mathbf{K}}$ is quite complicated. The reason for the asymmetry in the form of Eqs. (5.16) and (5.18) is the position dependent coupling g_k . The quantity in the brackets on the rhs of Eq. (5.18) can not be expressed in terms of $\hat{\mathbf{K}}$. Only in the simple case of constant g_k it is possible to write a closed equation of motion for $\hat{\mathbf{K}}$ and $\hat{\mathbf{S}}$ [14].

Even though Eqs. (5.16) and (5.18) cannot in general be solved it is possible to extract general features of the dynamics. Assuming $\mathbf{B} = 0$, the electron spin will precess with frequency $\propto E_n N_{\text{QD}}^{-1/2}$ (since this is the magnitude of the effective nuclear magnetic field) and the nuclear system precesses with frequency $\propto E_n N_{\text{QD}}^{-1}$. The ratio of these two precession frequencies is $N_{\text{QD}}^{1/2} \gg 1$, which means that the electron spin effectively feels a quasi stationary nuclear system and in turn the nuclear system feels a time averaged electron spin.

To incorporate the (i) separation of timescales, (ii) the inhomogeneous coupling we introduce a scheme that separates the nuclear system into N_b subsystems, each being characterized by a fixed coupling g_b . The effective nuclear field of a given subsystem is

$$\hat{\mathbf{K}}_b = \frac{E_n f_{\text{Max}}}{N_{\text{QD}} I} g_b \sum_{k \in b} \hat{\mathbf{I}}_k \quad (5.19)$$

where the notation $k \in b$ is shorthand for all nuclei whose coupling is $g_k \in [g_b - \delta g/2, g_b + \delta g/2]$. As long as $N_b \ll N_{\text{QD}}$ each subsystem can be replaced by a classical variable. The initial condition for each block is chosen from a Gaussian distribution whose variance is

$$\langle \mathbf{K}_b^2 \rangle = \langle \mathbf{K}^2 \rangle \frac{g_b^2 V_b}{V_{\text{QD}} g^2}, \quad (5.20)$$

where V_b is the volume of the region which fulfills $g_k \in [g_b - \delta g/2, g_b + \delta g/2]$. The volume of the subsystem V_b is related to g_b via

$$V_b \equiv \left. \frac{dV}{dg} \right|_{g=g_b} \delta g, \quad (5.21)$$

where V is the volume of the region where $g \geq g_b$. The functional form of $g(\mathbf{r})$ is determined by the density $|\psi(\mathbf{r})|^2$. For example, using a parabolic confinement in the lateral direction and assuming a steplike density of the 2DEG in the transverse direction gives a coupling $g(\mathbf{r}) = \exp(-r_{\parallel}/\ell)^2$. The volume V is then given by

$$V(g) = z_0 \pi \ell^2 \ln(1/g), \quad (5.22)$$

which results in the following subsystem volume

$$V_b = V_{\text{QD}} \frac{\delta g}{g_b}. \quad (5.23)$$

Note that the value of the total effective field which the electron experiences does not depend on N_b .

Taking all this together we arrive at the following set of equations which determine the approximate dynamics of the nuclear system.

$$\frac{d\mathbf{K}_b}{dt} = \frac{E_n f_{\text{Max}}}{IN_{\text{QD}}} g_b \langle \mathbf{S} \rangle \times \mathbf{K}_b + \gamma_{\text{GaAs}} \mathbf{B} \times \mathbf{K}_b, \quad (5.24)$$

where the average electron spin $\langle \mathbf{S} \rangle$ is determined by the total effective nuclear field

$$\mathbf{K} = \sum_b \mathbf{K}_b. \quad (5.25)$$

Obviously separating the nuclear system into subsystem with a constant g_b is an approximation to the continuous coupling g_k . As the number of subsystems increases g_b will more closely represent g_k . However, for the the semiclassical approximation to be valid each subsystem must contain many nuclear spins. Thus, increasing N_b should better reproduce the actual system, as long as $N_b \ll N_{\text{QD}}$. The N_b differential equations, with the associated random initial conditions constitute a set of autonomous differential equations. Its solutions, for a given functional form $\langle \mathbf{S} \rangle = \mathbf{S}(\mathbf{K})$ completely determines the dynamics of the nuclear system. The solution of the average spin will be the discussed in the next section.

5.4 Adiabatic approximation for the electron spin

As we have shown in the previous section, the nuclear spin system may be treated as a slowly varying effective nuclear magnetic field acting on the electron spin. Assuming a constant external magnetic field along the z -axis, the Hamiltonian for the electron spin reads

$$H_e(t) = \Delta \hat{S}_z + \hat{\mathbf{S}} \cdot \mathbf{K}(t), \quad (5.26)$$

$\Delta = g\mu_B B$ being the Zeeman splitting due to the external field. Let us now introduce a general magnetic field

$$\mathbf{H}(t) = \Delta \mathbf{e}_z + \mathbf{K}(t), \quad (5.27)$$

to represent any slowly varying magnetic field. It is convenient to introduce the instantaneous eigenfunctions of the Hamiltonian, which are solutions of

$$H_e(t)|\mathbf{n}(t); \pm\rangle = E_{\pm}(t)|\mathbf{n}(t); \pm\rangle. \quad (5.28)$$

The eigenstates are labeled by $\mathbf{n}(t)$ to indicate that these eigenstates are either pointing ‘up’ (+) or ‘down’ (-) along the total magnetic field, whose direction is determined by the normal vector

$$\mathbf{n}(t) = \frac{\mathbf{H}(t)}{|\mathbf{H}(t)|}. \quad (5.29)$$

For spin 1/2 in an external field, the eigenenergies can be written as $E_{\pm}(t) = \pm\mathcal{E}(t)$, where

$$\mathcal{E}(t) = \frac{1}{2} \sqrt{H_x^2(t) + H_y^2(t) + H_z(t)^2} \quad (5.30)$$

and the corresponding eigenstates are written in the basis of the \hat{S}_z eigenvectors

$$|\mathbf{n}(t); +\rangle = \frac{1}{\sqrt{1 + |a(t)|^2}} (|\uparrow\rangle + a(t)|\downarrow\rangle) \quad (5.31)$$

$$|\mathbf{n}(t); -\rangle = \frac{1}{\sqrt{1 + |a(t)|^2}} (-a^*(t)|\uparrow\rangle + |\downarrow\rangle). \quad (5.32)$$

The time dependent mixing of spin components is Δ and \mathbf{K} is given by

$$a(t) = \frac{H^+(t)}{\sqrt{2}} \frac{(\sqrt{H_x^2(t) + H_y^2(t) + H_z(t)^2} - H_z(t))}{|H^+(t)|^2} \quad (5.33)$$

where

$$H^+(t) = \frac{H_x(t) + iH_y(t)}{\sqrt{2}} \quad (5.34)$$

The wavefunction may be expanded in basis of instantaneous eigenstates

$$|\psi(t)\rangle = \sum_{\sigma=\pm} c_{\sigma}(t) |\mathbf{n}(t); \sigma\rangle \quad (5.35)$$

where the expansion coefficients are

$$c_{\pm}(t) = c_{\pm}(t_0) \exp\left(\gamma_{\pm}(t) - \frac{i}{\hbar} \int_{t_0}^t d\tau E_{\pm}(\tau)\right) \quad (5.36)$$

The additional phase factor appearing in the previous equation is the usual adiabatic phase [24]

$$\gamma_{\pm}(t) = \int_{t_0}^t d\tau \langle \mathbf{n}(\tau); \pm | d/d\tau | \mathbf{n}(\tau); \pm \rangle. \quad (5.37)$$

Integrating by parts the rhs of the last equation and using the orthogonality of the instantaneous eigenstates, it can be shown that the phase γ_{\pm} is an imaginary number. Also, for a doublet $\gamma_{\pm} = \pm\gamma$.

Using the wave function in Eq. (5.35), the average electron spin is

$$\begin{aligned} \langle \hat{\mathbf{S}}(t) \rangle &\equiv \langle \psi(t) | \hat{\mathbf{S}} | \psi(t) \rangle \\ &= \sum_{\sigma=\pm} |c_{\sigma}(t_0)|^2 \langle \mathbf{n}(t); \sigma | \hat{\mathbf{S}} | \mathbf{n}(t); \sigma \rangle \\ &\quad + 2\Re \left\{ c_{+}^{*}(t_0) c_{-}(t_0) \exp\left(2\gamma(t) - \frac{i}{\hbar} \int_{t_0}^t d\tau 2E(\tau)\right) \right\}. \end{aligned} \quad (5.39)$$

The latter term in Eq. (5.39) oscillates with frequency $E(t)/\hbar \gg E_n N_{\text{QD}}^{-1}/\hbar$, so its average is zero on the timescales of the nuclear system. The average value of the electron spin entering Eq. (5.24) is

$$\langle \mathbf{S} \rangle = \sum_{\sigma=\pm} |c_{\sigma}(t_0)|^2 \langle \mathbf{n}(t); \sigma | \hat{\mathbf{S}} | \mathbf{n}(t); \sigma \rangle \quad (5.40)$$

$$= \frac{1}{2} \cos(\theta_0) \frac{\mathbf{H}}{|\mathbf{H}|}, \quad (5.41)$$

where θ_0 is the angle between the initial electron spin and \mathbf{n} , see Fig. 5.1 Dissipation will direct the spin opposite to instantaneous magnetic field. This is why we expect that at a timescale longer than that of dissipation the spin will be anti-parallel to instantaneous field and will follow this direction when this field slowly changes. To account for this we assume in further calculations that the spin is indeed antiparallel to instantaneous magnetic field.

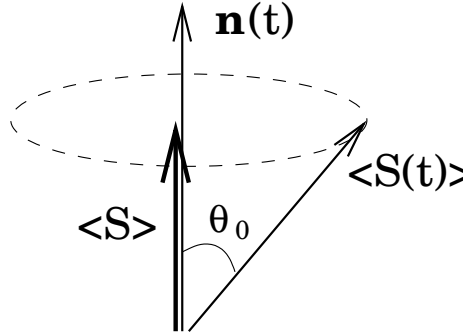


Figure 5.1: The time dependent electron spin $\langle \mathbf{S}(t) \rangle$ precesses rapidly around the total effective magnetic field, resulting in a slowly varying average spin $\langle \mathbf{S} \rangle$ that the nuclei see. The angle between the instantaneous electron spin and \mathbf{n} is θ_0

5.5 Correlation functions

A wide class of classical systems exhibits decaying correlation functions. This occurs in classically chaotic systems in which the motion is such that the memory about initial conditions is lost at some typical timescale [25]. Most of sufficiently complicated classical systems are eventually chaotic. One might expect that the set of equations Eq. (5.24) should describe chaotic dynamics and decay of correlation functions. We will see below that this is not the case.

A useful way to characterize the electron spin dynamics it is to introduce certain correlation functions. For an isolated quantum system these correlation function are expected to oscillate periodically, without any damping. Incorporating environmental effects usually shows up in modified behavior of the correlation functions. The expected behavior is that they should decay or be damped as a function of time. To investigate how the nuclear spin system acts as a spin bath (environment), we introduce the following correlation functions

$$G_{zz}(t, t_0) = \langle \uparrow | \hat{S}_z(t) \hat{S}_z(t_0) | \uparrow \rangle \quad (5.42)$$

$$G_{+-}(t, t_0) = \langle \uparrow | \hat{S}^+(t) \hat{S}^-(t_0) | \uparrow \rangle, \quad (5.43)$$

where the time evolution of the operators is

$$\hat{o}(t) = U^{-1}(t, t_0) \hat{o} U(t, t_0), \quad (5.44)$$

and U is the Schroedinger time propagator $|\psi(t)\rangle = U(t, t_0)|\psi(t_0)\rangle$.

Since we are focusing on the slow dynamics it is useful to write these correlation functions for long timescales. In the adiabatic approximation the corre-

lation functions may be written as

$$G_{zz}(t, t_0) = \frac{1}{4} \left(\frac{1 - |a(t)|^2}{1 + |a(t)|^2} \right) \left(\frac{1 - |a(t_0)|^2}{1 + |a(t_0)|^2} \right) \quad (5.45)$$

$$G_{+-}(t, t_0) = 2 \left(\frac{a(t)}{1 + |a(t)|^2} \right) \left(\frac{a^*(t_0)}{1 + |a(t_0)|^2} \right). \quad (5.46)$$

Furthermore, it is possible to define a new correlation function

$$G(t, t_0) = G_{zz}(t, t_0) + \frac{1}{2}(G_{+-}(t, t_0) + G_{-+}(t, t_0)) \quad (5.47)$$

$$= \langle \downarrow | \hat{\mathbf{S}}(t) \cdot \hat{\mathbf{S}}(t_0) | \uparrow \rangle \quad (5.48)$$

The most interesting regime corresponds to weak external magnetic fields. In this case there is no preferred direction and the dynamics show the richest behavior. In that limit the correlation functions take the simplified form

$$G_{zz}(t, t_0) = \frac{K_z(t)K_z(t_0)}{4K(t)K(t_0)} \quad (5.49)$$

$$G_{+-}(t, t_0) = \frac{K^+(t)K^-(t_0)}{4K(t)K(t_0)} \quad (5.50)$$

$$G(t, t_0) = \frac{\mathbf{K}(t) \cdot \mathbf{K}(t_0)}{4K(t)K(t_0)} \quad (5.51)$$

From these equations it is evident that the electron spin correlation function is determined by the nuclear system variables.

For completeness we also give the results for the opposite limit. For large external magnetic fields the correlation functions reflect that the dynamics is mainly a precession around the external field. The correlation function are

$$G_{zz}(t, t_0) = \frac{1}{4} \left(1 - \frac{K_x(t)^2 + K_y(t)^2 + K_x(t_0)^2 + K_y(t_0)^2}{2\Delta^2} \right) \quad (5.52)$$

$$G_{+-}(t, t_0) = \frac{1}{4} \left(\frac{K^+(t)K^-(t_0)}{\Delta^2} \right). \quad (5.53)$$

5.6 Nuclear subsystem dynamics

The dynamics of the combined electron and nuclear system is given by Eqs. (5.24) and (5.39). The large separation of timescales allows the electron spin to be calculated separately, resulting in an average spin that depends on \mathbf{K} . In the absence of an external magnetic field the average electron takes the simple form given in Eq. (5.39) and the equations of motion for the \mathbf{K}_b 's become

$$\frac{d}{dt} \mathbf{K}_b = \gamma g_b \frac{\sum_b \mathbf{K}_b}{|\sum_b \mathbf{K}_b|} \times \mathbf{K}_b. \quad (5.54)$$

Here we introduce the characteristic precession frequency γ of the nuclear system

$$\gamma = \frac{E_n f_{\text{Max}} \cos \theta_0}{2N_{\text{QD}} I}. \quad (5.55)$$

The order of magnitude of γ is determined by E_n/N_{QD} . In GaAs $\gamma \approx 10^{-7}$ meV $\approx 10^5$ Hz for quantum dots containing $N_{\text{QD}} \approx 10^6$ nuclei. From these equations quite a few integrals of motion can be constructed

$$0 = \frac{d}{dt} |\mathbf{K}_b|^2 \quad (5.56)$$

$$0 = \frac{d}{dt} \left| \sum_b \mathbf{K}_b \right|^2 \quad (5.57)$$

$$0 = \frac{d}{dt} \mathbf{I} = \frac{d}{dt} \left(\sum_b \frac{\mathbf{K}_b}{g_b} \right) \quad (5.58)$$

$$0 = \frac{d}{dt} \left(\mathbf{I} \cdot \left(\sum_b \frac{\mathbf{K}_b}{g_b^2} \right) \right). \quad (5.59)$$

Only in the case of 2 or 3 subsystems are these integrals of motion helpful in obtaining exact solutions.

The preceding integrals of motion are generally not integrals of motion of the original Hamiltonian. However, the integral of motion in Eq. (5.58) is closely related to an exact integral of motion of the original Hamiltonian, i.e. the total spin of the electron and nuclear system. The total spin of the whole system is an integral of motion:

$$\frac{d}{dt} \hat{\mathbf{J}} = \frac{d}{dt} \left(\hat{\mathbf{S}} + \sum_k \hat{\mathbf{I}}_k \right) = 0. \quad (5.60)$$

The exact value is set by the microscopic initial state of the nuclei and as long as $N_{\text{QD}} \gg 1$ we have

$$\hat{\mathbf{I}} \equiv \sum_k \hat{\mathbf{I}}_k = \hat{\mathbf{J}} - \hat{\mathbf{S}} \approx \hat{\mathbf{J}}. \quad (5.61)$$

Thus, the total spin of the nuclear system is an approximate constant of motion, which is reflected by the integral of motion in Eq. (5.58). It should be mentioned that the dipole-dipole interaction between the nuclei change the total spin but only on very long timescales of around milliseconds [13].

The correlation functions are obtained by integrating numerically Eq. (5.24) using the 4th order Runge Kutta method. The $K_b(t)$'s are used to calculate $a(t)$ that enter Eq. (5.45) and (5.46). The calculations were done at $\mathbf{B} = 0$, and $N_b = 8, 32, 128$ and 256. For each number of subsystems N_b the calculations were repeated for various initial conditions, but no averaging is performed. The results of these calculations for $G_{zz}(t)$ are presented in Figs. 5.2-5.5.

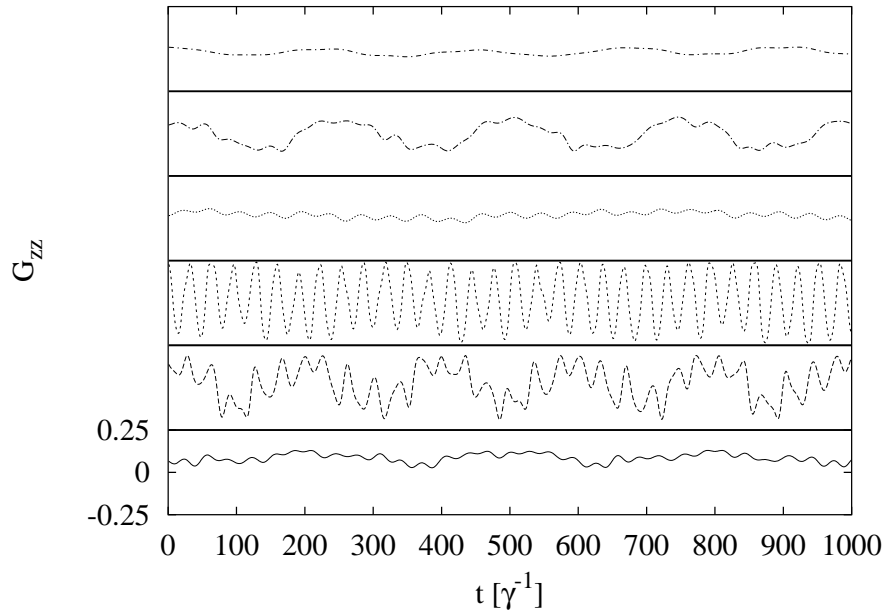


Figure 5.2: Numerical calculations of the correlation function $G_{zz}(t)$ for $N_b = 8$ and various randomly chosen initial conditions. The curves are offset for clarity and the vertical range is the same for all curves, i.e. -0.25 to 0.25

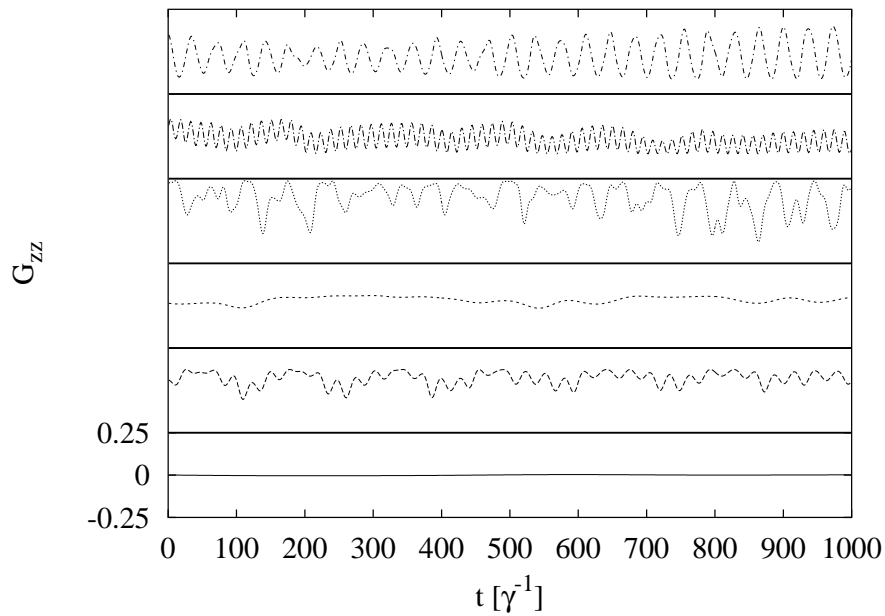


Figure 5.3: Numerical calculations of the correlation function $G_{zz}(t)$ for $N_b = 32$ and various randomly chosen initial conditions. The curves are offset for clarity and the vertical range is the same for all curves, i.e. -0.25 to 0.25

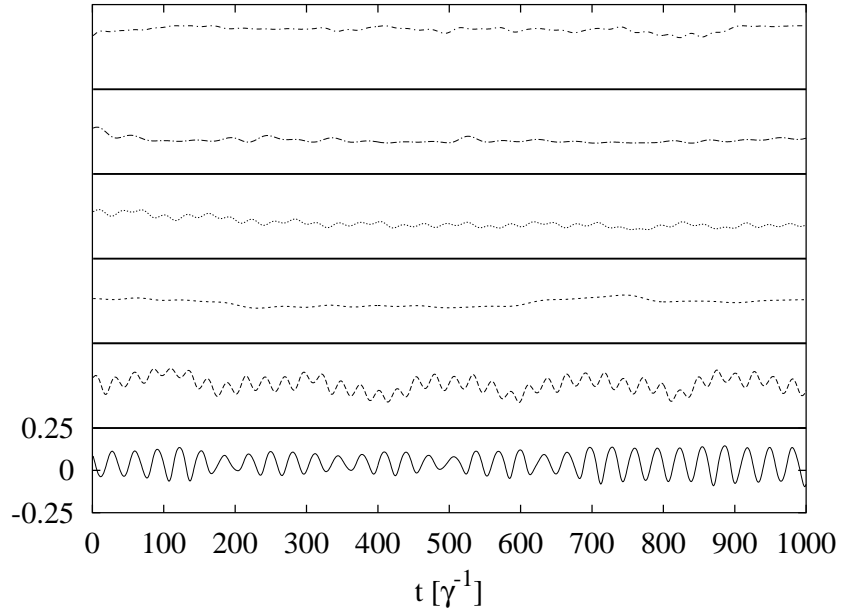


Figure 5.4: Numerical calculations of the correlation function $G_{zz}(t)$ for $N_b = 128$ and various randomly chosen initial conditions. The curves are offset for clarity and the vertical range is the same for all curves, i.e. -0.25 to 0.25

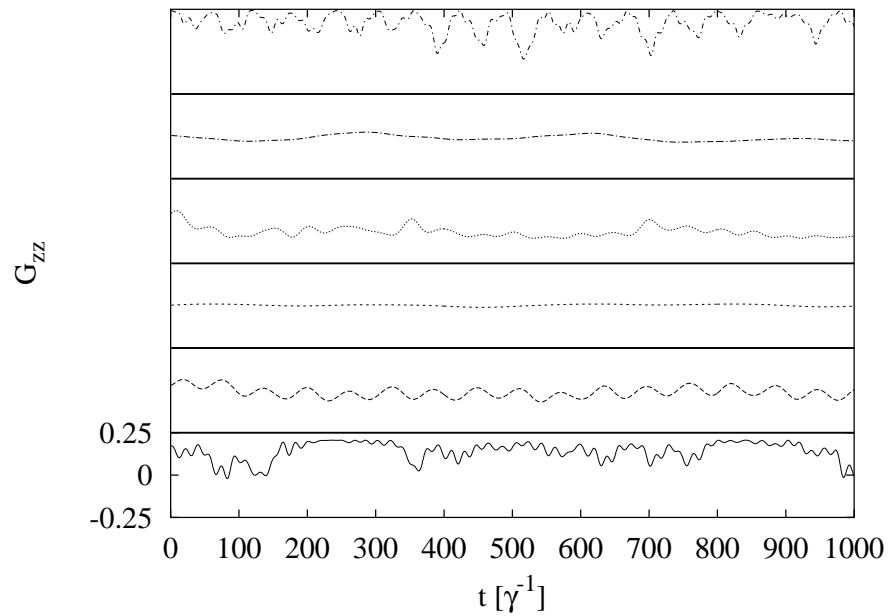


Figure 5.5: Numerical calculations of the correlation function $G_{zz}(t)$ for $N_b = 128$ and various randomly chosen initial conditions. The curves are offset for clarity and the vertical range is the same for all curves, i.e. -0.25 to 0.25

The common feature of all curves, for all values of N_b , is that they do not decay with time. This behaviour persists to even higher times, not shown here. Even though more complicated behaviour is observed for large N_b , the characteristic frequencies of the correlation function oscillations do not show any obvious dependence on the number of subsystems used, as long as $N_b \gg 1$.

5.7 Conclusion

Although a more detailed study of the dynamics is needed, it is evident from the numerical calculations that the correlation functions of the electron spins do not show any decay in time. In the limit of low external magnetic field, the dynamics of the system can be quite complicated depending on the initial state of the subsystems and their number N_b . The timescale of the slow electron evolution is determined by γ^{-1} even though the details depend on the initial conditions and the number of subsystems. At high applied magnetic fields the behaviour of the correlation functions is constrained by the external field, see Eqs. (5.52) and (5.53)

Since the system has many integrals of motion, it may be close to exactly solvable and thus one expects periodic oscillations and no decay [26]. The observed behaviour of the system may be explained in this way, i.e. the oscillations of the correlation function reflect that the system lies somewhere on the boundary on being exactly solvable. These features will probably vanish if further terms into the Hamiltonian in Eq. (5.2) are included. The most natural term would be the dipole-dipole interaction between the nuclei which would kill most of the integrals of motion. It is important to recognize that the timescale related to the dipole-dipole interaction is very long, of the order 10^{-3} s, and the relaxation time would reflect that.

In connection to coherently controlling the spin, the motion of the electron spin in the effective nuclear magnetic field will cause ‘errors’. Even though in this model nuclear spins do not decohere the electron spin, they lead to a complicated (unknown) evolution that is difficult to predict. Consequently, an electron spin initially in $|\uparrow\rangle$ can be found in the opposite spin state on a timescale $\propto \gamma^{-1}$. Thus, the hyperfine coupling to the nuclear system does not lead to decoherence in this model but it can strongly affect the dynamics of the electron spin.

References

- [1] Y. Nakamura, Y. A. Pashkin, and J. S. Tsai, *Nature* **398**, 786 (1999).
- [2] J. E. Mooij *et al.*, *Science* **285**, 1036 (1999).

- [3] B. E. Kane, *Nature* **393**, 133 (1998).
- [4] C. P. Slichter, *Principles of Magnetic Resonance*, 3rd ed. (Springer-Verlag, Berlin, 1990).
- [5] A. Abragam, *Principles of Nuclear Magnetism* (Oxford University Press, New York, 1961).
- [6] D. Loss and D. P. DiVincenzo, *Phys. Rev. A* **57**, 120 (1998).
- [7] A. V. Khaetskii and Y. V. Nazarov, *Phys. Rev. B* **61**, 12639 (2000).
- [8] A. V. Khaetskii and Y. V. Nazarov, *Phys. Rev. B* **64**, 125316 (2001).
- [9] S. I. Erlingsson, Y. V. Nazarov, and V. I. Fal'ko, *Phys. Rev. B* **64**, 195306 (2001).
- [10] S. I. Erlingsson and Y. V. Nazarov, *Phys. Rev. B* **66**, 155327 (2002).
- [11] L. M. Woods, T. L. Reinecke, and Y. Lyanda-Geller, *Phys. Rev. B* **66**, 161318(R) (2002).
- [12] A. V. Khaetskii, D. Loss, and L. Glazman, *Phys. Rev. Lett.* **88**, 186802 (2002).
- [13] I. A. Merkulov, A. L. Efros, and M. Rosen, *Phys. Rev. B* **65**, 205309 (2002).
- [14] Y. G. Seminov and K. W. Kim, *Phys. Rev. B* **67**, 73301 (2003).
- [15] R. de Sousa and S. Das Sarma, *Phys. Rev. B* **67**, 033301 (2003).
- [16] S. Saykin and V. Privman, *Nano Lett.* **2**, 651 (2002).
- [17] J. Schliemann, A. V. Khaetskii, and D. Loss, *Phys. Rev. B* **66**, 245303 (2002).
- [18] S. W. Brown, T. A. Kennedy, and D. Gammon, *Solid State Nucl. Magn. Reson.* **11**, 49 (1998).
- [19] S. Tarucha *et al.*, *Phys. Rev. Lett.* **77**, 3613 (1996).
- [20] J. M. Elzerman *et al.*, *Phys. Rev. B* **67**, 161308 (2003).
- [21] M. I. D'yakonov and V. Y. Kachorovskii, *Sov. Phys. Semicond.* **20**, 110 (1986).
- [22] D. Paget, G. Lampel, B. Sapoval, and V. I. Safarov, *Phys. Rev. B* **15**, 5780 (1977).
- [23] M. Dohers *et al.*, *Phys. Rev. Lett.* **61**, 1650 (1988).
- [24] A. Messiah, *Quantum Mechanics* (North-Holland Publishing Co., Amsterdam, 1962), Vol. 2.
- [25] A. M. O. deAlmeida, *Hamiltonian systems: chaos and quantization* (Cambridge University Press, Cambridge, 1988).
- [26] J. Schliemann, private communication.

Appendix A

Thermal average over nuclear spin pairs

Even though we do not average over the classical field \mathbf{K}_l , which is fixed, there are still fluctuations in the nuclear system. Each pair of nuclei can fluctuate, without affecting the classical field. One should think of these fluctuations as small deviations around a given value of \mathbf{K}_l , i.e. we (thermally) average over the pairs for a fixed value of the classical field. When the thermal average over a pair of free nuclei is performed the following nuclear correlation function appears in Eq. (3.21)

$$\begin{aligned} G_{\text{corr}} &= (S_{+-}^{\alpha})^* S_{+-}^{\beta} \langle \delta I_k^{\alpha} \delta I_{k'}^{\beta} \rangle_T \\ &= (S_{+-}^{\alpha})^* S_{+-}^{\beta} \langle \delta \hat{I}^{\alpha} \delta \hat{I}^{\beta} \rangle_T \delta_{k,k'}, \end{aligned} \quad (\text{A.1})$$

where $\delta \hat{I}^{\alpha} = \hat{I}^{\alpha} - \langle I^{\alpha} \rangle_T$ and the electron spin matrix elements are $S_{+-}^{\alpha} = \langle \mathbf{n}_+ | S^{\alpha} | \mathbf{n}_- \rangle$. The Kronecker delta reflects that there are no correlations between two different nuclei and we have dropped the k subscript in $\langle \delta \hat{I}^{\alpha} \delta \hat{I}^{\beta} \rangle_T$ since the nuclei is assumed to be identical. By defining the symmetric correlator

$$g^{\alpha\beta} = \frac{1}{2} \langle \delta \hat{I}^{\alpha} \delta \hat{I}^{\beta} + \delta \hat{I}^{\beta} \delta \hat{I}^{\alpha} \rangle_T \quad (\text{A.2})$$

we get the following

$$G_{\text{corr}} = (S_{+-}^{\alpha})^* S_{+-}^{\beta} (g^{\alpha\beta} + i/2 \epsilon^{\alpha\beta\gamma} \langle \hat{I}^{\gamma} \rangle_T). \quad (\text{A.3})$$

In an isotropic system, $\langle \hat{I} \rangle_T = 0$, the value of the correlation function is $G_{\text{corr}} = \frac{1}{2} \frac{1}{3} I(I+1)$.

Appendix B

Matrix elements for a parabolic quantum dot

Using the Darwin-Fock solutions and the Fang-Howard variational solution for the triangular quantum well we obtain the following equation for Eqs. (3.22)-(3.25)

$$\begin{aligned}
 a_{ll'}\gamma_{ll'} &= \delta_{M,M'} \frac{A^2 C n}{V_{\text{QD}} \zeta} \frac{(eh_{14}\ell)^2 \Delta^3}{8\pi\rho c^5 \hbar^4} \frac{\Gamma(n+n'+|M|+1) 2^{-3(n+n'+|M|)}}{n!n'!(n+|M|)!(n'+|M|)!} \\
 &\times (n(\Delta)+1) \sum_{\nu} \frac{c^5}{c_{\nu}^5} \left(\frac{\Delta}{\hbar c_{\nu} \ell^{-1}} \right)^{2(n+n'+|M|-1)} \\
 &\times \int_0^{\pi} d(\cos\theta) A_{\nu}(\theta) \frac{(\sin\theta)^{2(n+n'+|M|)} \exp\left(-\frac{1}{2} \left(\frac{\Delta \sin\theta}{\hbar c_{\nu} \ell^{-1}} \right)^2\right)}{\left(1 + \left(\frac{\Delta \cos\theta}{3\hbar c_{\nu} z_0^{-1}} \right)^2\right)^3}
 \end{aligned} \tag{B.1}$$

where $\zeta^{-1} = z_0 \int dz |\chi(z)|^4$ and $c^{-5} = c_l^{-5} + c_t^{-5}$ is the effective sound velocity of the phonons. The anisotropy functions are

$$A_t(\theta) = \frac{\sin^2\theta(8\cos^4\theta + \sin^4\theta)}{4} \tag{B.2}$$

$$A_l(\theta) = \frac{9\cos^2\theta\sin^4\theta}{2}. \tag{B.3}$$

The equation for $\tilde{a}_{ll'}\tilde{\gamma}_{ll'}$ is identical except for a different Kronecker delta function $\delta_{M,-M'}$. The integral needs in general to be evaluated numerically but when $\Delta \ll \hbar c_{\nu} \ell^{-1}$ the exponential term and the denominator become unity and the resulting integral is simple to calculate.

Summary

Nuclear Spins in Quantum Dots

The main theme of this thesis is the hyperfine interaction between the many lattice nuclear spins and electron spins localized in GaAs quantum dots. This interaction is an intrinsic property of the material. Despite the fact that this interaction is rather weak, it can, as shown in this thesis, strongly influence the dynamics of electron spins in quantum dots. In chapter 1 some basic features of quantum dots are described and the most important sources for the mixing of spin components in GaAs, i.e. the hyperfine and spin-orbit interaction, are introduced and discussed.

The hyperfine mediated transition rate from a triplet state to the ground state singlet is considered in chapter 2. The transition involves changing both the orbital and spin degree of freedom so the phonon scattering alone cannot facilitate the transition. Also, the hyperfine interaction alone can not cause the transition because the nuclear spin system cannot absorb the energy released by the singlet-to-triplet transition. Thus, both a source of inelastic scattering and the hyperfine interaction are required for the transition. The resulting transition involves virtual excited states. Assuming a small exchange splitting a simple expression for the transition rate is obtained that involves only the first excited singlet state.

The subject of chapter 3 is the hyperfine mediated transitions between Zeeman split doublet components of the ground state orbital of a single-electron quantum dot. The spin-flip mechanism is the same as for the singlet-triplet case, i.e. the transition goes via higher orbital virtual states and involves both the hyperfine interaction and phonon scattering. A closer look is taken at the relevant electron-phonon coupling mechanism: The piezoelectric phonons. In addition, a semiclassical picture of the nuclear system is formulated. The great number of nuclei in the quantum dot makes it possible to consider them as an effective nuclear magnetic field acting on the electron spin. The transition amplitude between the doublet components due to the hyperfine interaction remains finite even if the external magnetic field goes to zero. This is in contrast to spin-orbit interaction where the transition amplitude vanishes at zero field.

Thus, at sufficiently low magnetic field the hyperfine related spin-flip rate will dominate the spin-orbit one. The rates obtained in chapters 2 and 3 are usually much smaller than non-spin-flip transition rates in quantum dots.

Transport through a GaAs double quantum dot in the so-called spin-blockade regime is the subject of chapter 4. The current is blocked due to the absence of transitions between singlet and triplet states within the quantum dots. Motivated by a recent experiment, we consider the influence of the hyperfine interaction on transport in the spin-blockade regime. A small transport current will flow if the singlet and triplet states are mixed. In our model the mixing is induced by the different effective nuclear magnetic fields acting the electron spins in the two dots. Not only does the nuclear system affect the electron spins and lift the spin-blockade, there is also a back-action on the nuclear system that is determined by the average electron spin in the two dots. The nuclear system precesses around the average electron spin, leading to a time dependent transport current whose characteristics are in qualitative agreement with the experimental observations.

In the last chapter the dynamics induced by the hyperfine coupling of the electron and nuclear spins in a quantum dot are studied. An effective spin Hamiltonian is considered where the spatial dependence of the electron wavefunction results in an inhomogeneous hyperfine coupling of the electron spin to different nuclear spins. Generally, it is not possible to solve this Hamiltonian except in the special case of homogeneous coupling. To obtain an approximate solution, we split the nuclear system into N_b subsystems where all nuclei within a given subsystem have equal coupling to the electron spin. An important feature of the original Hamiltonian is the separation of the timescales, i.e. the electron spin dynamics are much faster than that of the nuclear spins. This allows us to use the adiabatic approximation when calculating the average electron spin which each nuclear spin sees. In this way the electron spin is removed from the problem leaving $3N_b$ coupled differential equations. These are solved numerically and the results used to calculate certain electron spin correlation functions. Contrary to what one may guess, the dynamics are not chaotic and the correlation functions show no decay in time, only complicated oscillations. This may be attributed to the fact that the system has many integrals of motion and that it is close to exactly solvable. This behavior persists even for $N_b \gg 1$, which is the limit in which our approximation becomes more accurate.

Sigurdur I. Erlingsson, Delft 2003

Samenvatting

Nucleaire Spins in Quantum Dots

Het hoofdthema van dit proefschrift is de hyperfijninteractie tussen de spins van de vele nucleï in het kristalrooster en de spins van gelokaliseerde elektronen in GaAs quantum dots. Deze interactie is een intrinsieke eigenschap van het materiaal. Ondanks het feit dat deze interactie vrij zwak is, kan ze, zoals aangetoond in dit proefschrift, de dynamica van elektronspins in quantum dots sterk beïnvloeden. In hoofdstuk 1 worden enkele basiseigenschappen van quantum dots beschreven en worden de belangrijkste bronnen voor de vermenging van de spin componenten in GaAs, dwz. de hyperfijninteractie en de spin-baan interactie, geïntroduceerd en besproken.

De door de hyperfijninteractie gemedieerde overgang van een triplet toestand naar de singlet grondtoestand wordt beschouwd in hoofdstuk 2. De overgang gaat gepaard met een verandering van zowel de baan- als de spinvrijheidsgraad waardoor met fononen verstrooiing alleen de overgang niet bewerkstelligd kan worden. Ook de hyperfijninteractie kan de overgang niet alleen veroorzaken omdat het nucleaire spinsysteem de energie die vrijkomt bij de triplet-naar-singlet overgang niet kan opnemen. Dus, zowel een bron van inelastische verstrooiing als de hyperfijninteractie zijn nodig voor de overgang. De resulterende overgang gaat gepaard met virtuele aangeslagen toestanden. Onder de aanname van een kleine zgn. 'exchange' splitsing is een simpele uitdrukking verkregen voor de snelheid van de overgang, waarbij alleen de eerste aangeslagen singlet toestand betrokken is.

Het onderwerp van hoofdstuk 3 is de door hyperfijninteractie gemedieerde overgang tussen Zeeman-gesplitste doubletcomponenten van de laagste orbitaal van een één-elektron quantum dot. Het spin-flip mechanisme is hetzelfde als in het geval van de singlet-tripletcomponenten, dwz. de overgang gaat via hogere virtuele orbitaaltoestanden and gaat samen met zowel de hyperfijninteractie als fononen verstrooiing. De relevante elektron-fonon koppeling is nader bekeken: de piezo-elektrische fononen. Bovendien is een semi-klassiek beeld van het nucleaire systeem geformuleerd. Het grote aantal nucleï in de quantum dot maakt het mogelijk om deze te beschouwen als een effectief nucleair magnetisch veld

dat op de elektronspin werkt. De overgangsamplitude tussen de doubletcomponenten ten gevolge van de hyperfijninteractie blijft eindig, zelfs als het externe mangelveld naar nul gaat. Dit is in tegenstelling tot de overgang ten gevolge van spin-baan interactie, waarvan de overgangsamplitude verdwijnt bij nul veld. Bij magnetische velden die laag genoeg zijn zal de hyperfijn-gerelateerde spin-flip snelheid dus domineren over de spin-baangerelateerde. De snelheden verkregen in hoofdstuk 2 en 3 zijn gewoonlijk veel lager dan de snelheden in quantum dots voor overgangen zonder spin-flip.

Transport door een GaAs dubbele quantum dot in het zogenaamde spinblokkade regime is het onderwerp van hoofdstuk 4. De stroom is geblokkeerd door de afwezigheid van overgangen tussen singlet en triplettoestanden in de quantum dots. Gemotiveerd door een recent experiment beschouwen we de invloed van de hyperfijninteractie op het transport in het spinblokkade regime. Een kleine stroom zal lopen als de singlet en triplet toestanden vermengd worden. In ons model wordt de vermenging veroorzaakt door de verschillende effectieve nucleaire magneetvelden die op de spins in de twee dots werken. Niet alleen beïnvloedt het nucleaire systeem de elektronspins en heft het de spinblokkade op, er is ook een terugwerking op het nucleaire systeem dat wordt bepaald door de gemiddelde elektronspin in de twee dots. Het nucleaire systeem precedeert om de elektronspin, wat leidt tot een tijdsafhankelijke stroom waarvan de karakteristieke kwalitatief overeenkomen met de experimentele waarnemingen

In het laatste hoofdstuk wordt de dynamica bestudeerd die wordt geïnduceerd door de hyperfijnkoppeling van de elektronspins en de nucleaire spins. Een effectieve spin Hamiltoniaan wordt beschouwd waar de plaatsafhankelijkheid van de golf functie van het elektron resulteert in een inhomogene hyperfijnkoppeling van de elektronspin naar de verschillende nuclei. Het is niet mogelijk om deze Hamiltoniaan op te lossen, behalve in het speciale geval van een homogene koppeling. Om een benadering van de oplossing te verkrijgen splitsen we het nucleaire systeem in N_b subsystemen, waarbij alle nuclei in een gegeven subsysteem gelijke koppeling hebben naar de elektronspin. Een belangrijke eigenschap van de originele Hamiltoniaan is de scheiding van de tijdsschalen, i.e. de dynamica van de elektronspin is veel sneller dan die van de nucleaire spins. Hierdoor mogen we de adiabatische benadering toepassen bij het berekenen van de gemiddelde elektronspin die door elke nucleaire spin wordt gezien. Op deze manier wordt de elektronspin uit het probleem verwijderd en blijven er $3N_b$ gekoppelde differentiaalvergelijkingen over. Deze zijn numeriek opgelost en de resultaten zijn gebruikt om bepaalde elektron correlatiefuncties te berekenen. In tegenstelling tot wat men zou denken is de dynamica niet chaotisch en laten de correlatiefuncties geen verval zien in de tijd, enkel ingewikkelde oscillaties. Dit zou kunnen worden toegeschreven aan het feit dat het systeem vele bewegingsintegralen heeft en dat het bijna exact oplosbaar is. Dit gedrag houdt aan

voor $N_b \gg 1$, de limiet waarin onze benadering nauwkeuriger wordt.

Sigurdur I. Erlingsson, Delft 2003

Curriculum Vitae

Sigurdur I. Erlingsson

- 25 August 1972 Born in Reykjavik, Iceland
- 1988-1993: High School/Gymnasium education
Hafnarfirdi, Iceland
- 1990-1991: Exchange student in Charleston, South Carolina, USA.
- 1993-1999: M.Sc. physics from the University of Iceland under
the supervision of Prof. Vidar Gudmundsson
Title: *Finite size effects in the far-infrared absorption of a confined 2DEG*
- 1999-2003: PhD physics from the Delft University of Technology under
the supervision of Prof. Yuli V. Nazarov
Title: *Nuclear Spins in Quantum Dots*

List of publications

1. *Nucleus-mediated spin-flip transitions in GaAs quantum dots*
S.I. Erlingsson, Yu. V. Nazarov and V. I. Fal'ko, *PRB* **64**, 195306 (2001)
2. *Hyperfine-mediated spin-flip transitions in GaAs quantum dots*
S.I. Erlingsson, Yu. V. Nazarov and V. I. Fal'ko, *Physica E* **12**, 823 (2002)
3. *Hyperfine-mediated transitions between a Zeeman split doublet in GaAs quantum dots: the role of the internal field*
S.I. Erlingsson and Yu. V. Nazarov, *PRB* **66**, 155327 (2002)
4. *Hyperfine-mediated transitions between a Zeeman split doublet in GaAs quantum dots: the role of the internal field*
S.I. Erlingsson and Yu. V. Nazarov, *J. Supercond.*, **16**, 293 (2003)
5. *Coherent oscillations of current due to nuclear spins*
S.I. Erlingsson and Yu. V. Nazarov, submitted to PRL
6. *Time-evolution of the effective nuclear magnetic field due to a localized electron spin*
S.I. Erlingsson and Yu. V. Nazarov, in preparation